NTNU – Trondheim
Norwegian University of
Science and Technology

Hybrid testing of deep water moored structures

Fredrik Storflor Moen

Marine Technology
Submission date: June 2014
Supervisor: Carl Martin Larsen, IMT

Norwegian University of Science and Technology
Department of Marine Technology

NTNU Trondheim
Norwegian university of science and technology
Department of marinetechnology

MASTER THESIS, SPRING 2014

for

Stud.tech.

FREDRIK STORFLOR MOEN

Hybrid testing of deep water moored structures

(Hybrid testing av fortøyde dyptvannsplattformer)

.

The main reason for use of model tests in the design of floating production units is the need for reliable prediction of motions caused by the combined actions of waves, wind, and current. Since wind and higher order wave effects give load frequencies in the same regime as in-plane motion eigenfrequencies, damping and all nonlinear effects should be adequately represented in the model. Mooring lines and risers give a significant contribution to damping, non-linear restoring forces and even inertia forces. These elements must hence be included in model tests.

The model scale for hull and waves should preferably not be smaller than 1:40. A test facility with 10 meters water depth will hence have a full scale depth limitation of 400 meters, while water depth for offshore drilling has passed 3000 meters. In order to have a reasonable scale for the floater hull on this water depth, the mooring and riser system must be truncated. The challenge is hence to make a truncated model that has identical static and dynamic properties as for the real system.

The idea to be investigated in this project is to design a test arrangement using a control system that can introduce correct resulting forces and moments on the floating platform. The forces from mooring lines and risers must be found from real time computations using non-linear finite element models for all slender members. This multidiscipline project requires contributions from hydrodynamics, structural dynamics, automatic control and data processing and communication.

The MSc project will be carried out in close cooperation with MARINTEK.

The work may be defined in activities as follows

1. Literature study that should cover all aspects of hybrid testing, but concentrate on system architecture. The content of the pre-project from fall 2013 may be referred to.

2. Define all details in simplified physical and numerical models that contain essential features of a hybrid test setup including the control loop.

3. Build the model and demonstrate essential features by using the model for varying examples.

The work may show to be more extensive than anticipated. Some topics may therefore be left out after discussion with the supervisor without any negative influence on the grading.

The candidate should in her/his report give a personal contribution to the solution of the problem formulated in this text. All assumptions and conclusions must be supported by mathematical models

and/or references to physical effects in a logical manner. The candidate should apply all available sources to find relevant literature and information on the actual problem.

The report should be well organised and give a clear presentation of the work and all conclusions. It is important that the text is well written and that tables and figures are used to sup-port the verbal presentation. The report should be complete, but still as short as possible.

The final report must contain this text, an acknowledgement, summary, main body, conclusions and suggestions for further work, symbol list, references and appendices. All figures, tables and equations must be identified by numbers. References should be given by author name and year in the text, and presented alphabetically by name in the reference list. The re-port must be submitted in two copies unless otherwise has been agreed with the supervisor.

From the report it should be possible to identify the work carried out by the candidate and what has been found in the available literature. It is important to give references to the original source for theories and experimental results. The report should be delivered according to instructions from the faculty, and - if needed – additional material (binder, DVD/CD/memory stick) should be delivered to the supervisor.

Supervisor: Carl M. Larsen
Contact person at Marintek Thomas Sauder

Deadline: 10 June 2014

Carl M. Larsen
Supervisor

Abstract

This thesis presents a design concept for deep water model testing of moored floating offshore structures in ocean basin, and presents a single degree of freedom (SDOF) test setup for this purpose. Conventional methods has limitations in the ocean basin with regards to depth and scaling. The model scale should therefor not be larger than 1:40. A test facility with 10 meters depth will not be able to have full scale depth larger than 400 meter. Ultra small scaling smaller than 1:150 should also not be preferred, which leads to a full scale depth of 1500 m in ocean basin. Conventional methods has its limits in prediction of responses caused by environmental loads. For floaters the wind and higher order wave effects excite loads in range of the eigen frequencies of the structure for the in-plane motion. These resonant responses are more important for deeper water. Damping, restoring forces and all nonlinear effects should be adequately represented in the model test. Mooring lines and riser are important for damping and the nonlinear restoring, thus these factors must be included in the model tests.

This thesis focus on building a test setup , which can be used for deep water moored structures model testing, using both control systems and traditional systems. The aim is to have the correct restoring stiffness, mooring line dynamic, forces and moments on the model. The resulting forces are calculated with real-time software using a non-linear finite element model (FEM) in time domain. Real-time testing puts demands on communication and numerical solver efficiency and speed, thus it is important in order to not introduce any time delays that may cause uncertainties.

The test method presented is a simplified SDOF motion for a floater in surge. The test setup will use a linear spring with similar natural period in surge for the floating vessel, and actuator forcing will substitute the nonlin-

ear spring stiffness for the restoring characteristics, based on displacement of the floater in real-time analysis. This method will use less possible forcing from the actuator by choosing line stiffness close to the model scale restoring characteristic. A literature study on this subject based on earthquake civil engineering results in active hybrid testing methods, show promising results for this concept applied on structural engineering problems. Traditional model testing methods use results from model tests and extrapolate to full scale after the model tests have been conducted. This method is not able not predict all effects and uncertainties are introduced.

Results from a SDOF setup using actuators with a non-linear software, show suitable results for the concept further development, and use of actuators for representing deep water mooring lines. However limitations on the simplified model introduced more damping on the model than a model in ocean basin. The design of the systems communication between FEM analysis tool and controller for actuators is suitable for real-time hybrid model testing (RTHMT), time delays is small. The presented test setup can easily be implemented to testing of a model of water, and the concept can be used for other translations as well.

Sammendrag

Det er utfordringer knyttet til skalering og testing av dypvannskonstruksjoner. Aktiv hybridtesting forsøker å løse dette. Et designkonsept for dypt vanns modelltesting av fortøyde dypvannsplattformer er utviklet. Konseptet er tilpasset modelltesting i et havbasseng. Det presenterte systemet er forenklet til en frihetsgrad. Konvensjonelle testmetoder har begrensninger i et havbasseng med hensyn til dybde og skalering.

Havbassenget har begrensninger med tanke på dypvanns forankrede konstruksjoner og maksimal test dybde er 1500m, for en modelskala på 1:150. Konvensjonelle metoder har begrenser med tanke på prediksjon av respons som skyldes miljøbelastninger. For flytere vil vinden og høyere ordens bølgeeffekter eksiterer miljøkrefter i området for egen frekvenser for konstruksjonen i horisontal planets bevegelser.

Bevegelser nær resonansfrekvens er viktige for testing på dypt vann. Demping, fjærkrefter og alle ikke-lineære effekter bør være representert i en modelltest. Ankerliner og stigerør bidrar til demping og ikke-lineære fjærkrefter, og bør tas hensyn til i modellforsøkene.

Oppgaven fokuserer på å bygge et testoppsett, som kan brukes av fortøyde dypvannsplattformer i modelltesting, ved hjelp av både kontrollsystemer og tradisjonelle systemer. Målet er å påføre de riktige fjærkreftene, anker line dynamikk, krefter og momenter på modellen. De resulterende krefter er beregnet med en sanntidsprogramvare ved hjelp av en ikke-lineær elementmodellen i tidsdomenet. Sanntids testing setter krav til kommunikasjon og numerisk løser hastighet, og dermed er det viktig for ikke å unngå tidsforsinkelser. Tidsforsinkelser kan føre til usikkerhet i resultatene.

Testmetoden som presenteres er en forenklet en frihetsgrad system for en fly-

ter i jag. Testoppsettet erm modellert med en lineær fjær forsøkt modellert med lik egenperiode i jag for flyteren. Aktuatoren erstatter den ikke-lineære fjærstivheten i jag, basert på forskyvning av flyteren i sanntids tidsdomene analyse. Denne metoden vil anvende minst mulig pådrag fra aktuatoren ved å velge fjærstivhet til fjærene i systemet nær modellskala ankerline karakteristikk. Resultater innen eksperiment på bygning som er utsatt for jordskjelv, viser til lovende resultater for aktiv hybrid testing. Tradisjonelle modell testmetoder bruker resultatene fra modellforsøk og ekstrapolerer til full skala dyp etter modellforsøkene er utført. Denne metoden er ikke i stand til ikke å forutse alle effekter og usikkerheter er innført.

Resultater fra testoppsettet viser gode resultater siden den målte tidsforsinkelsen i styringssystemet og RIFLEX er liten, og vil i liten grad påvirke det flytende systemet. Konseptet er egnet for videre utvikling og bruk av aktuatorer for å representere ankerliner til dypvannsplattformer. Det ble funnet en svakthet ved at oppsettet ikke klarer å etterligne realistiske resultater på grunn av dempning. Dempingen i test oppsettet er høyere enn en tilsvarende modell i havbassenget. Utformingen av systemene, kommunikasjon mellom elementmetode programvare og kontroller for motorene er vist egnet for sanntids aktiv hybridmodell testing. Forsinkelsene som ble målt er små, og vil i liten grad påvirke resultatene. Testoppsettet kan enkelt overføres til et forsøk i vann, og lignende test oppsett for translasjoner i andre retninger kan benyttes.

Acknowledgement

The work has been carried out under supervision of Professor Carl Martin Larsen at the Department of Marine Technology, Norwegian University of Science and Technology (NTNU). The work has also been carried out by collaboration with The Norwegian Marine Technology Research Institute (MARINTEK) and with especially help from Thomas Sauder. I want to thank Thomas Sauder and Professor Carl Martin Larsen for guidance and suggestions that has been most appreciated, and the present work has not been possible without these. Also want to thank Frank Anderson at MARINTEK for help for control algorithm and cybernetic guidance on test setup.

Without MARINTEK investments in laboratory equipment and guidance in this thesis it would have not been possible.

Lastly, I would like to thank the fellow students in my office, for the discussion and for providing feedback on the report.

Tyholt, June 8, 2014

Fredrik Storflor Moen

Contents

List of Figures

List of Tables

Nomenclature

Abbreviations

General rules

- Only the most used symbols are listed in following section.
- Meaning of symbols is given when introduced in thesis.
- Vectors are presented by bold-face letters.

ADS	Automation Device Specification
AHMT	Active Hybrid Model Testing
AMOS	Center for Autonomous Marine Operations and Systems
ATLAS	Active Truncated Line Anchoring Simulator
COG	Center of Gravity
DOF	Degree of Freedom
EMT	Extended model testing
EtherCat	Ethernet for Control Automation Technology
FEM	Finite Element Method
FPSO	Floating Production Storage and Offloading
GBS	Gravity Based structures
HIL	Hardware in the loop
HMPE	High Modulus Polyethylene
HLA	High Level Architecture
LF	Low Frequency

LSRT3	L-Stable Real-Time 3rd order
Marin	Maritime Research Institute Netherlands
PHMT	Passive Hybrid Testing Method
PID	Proportional Integral Derivative Controller
PLC	Programmable Logic Controller
QTM	Qualisys Track Manager
RTHMT	Real-time Hybrid Model Testing
RK3	Runge Kutta 3rd order
SIMA	Simulation workbench for marine applications
SDOF	Single Degree of Freedom
ST	Structured Text
TDP	Touch Down Point
TLP	Tension Leg Platform
TwinCat	The windows control and automation technology
UDP	User Datagram Protocol
ULS	Ultimate Limit State
WF	Wave Frequency

Greek Letters

λ	Scaling Factor

Roman Letters

F_N	Froude Number
K_v	Feedback Velocity
K_P	Proportional Gain
c	Damping
k	Stiffness
x	Displacement

Matrices

M	Mass matrix
C	Damping matrix
K	Stiffness matrix

Vectors

F	Force Vector
u	Displacement vector
$\dot{u}$	Velocity vector
$\ddot{u}$	Acceleration vector

Chapter 1

Introduction

Model testing is considered the most reliable way of testing a floaters operational limits and features. Numerical software for time domain analysis has its limits, and model testing is the still most reliable way of testing offshore structures. In model testing a similar model as the full scale model is made by Froude scaling in most tests. The model must be scaled according to the limitation for the basin. These limitation are results of many factors such as an exceedingly large scale will disturb the wave field with reflecting waves from model. Other factors could be from scaling effects, or if sea states with high current are tested (this will limit the scale). These are just some of the limitations in scaling. The model scale for hull and waves should be preferably not be smaller than 1:40. The ocean basin will hence have a full scale depth limitation of 400 m in this scale. While water depth for drilling rigs has passed 3000 m.

1.1 Motivation

Hydrodynamic verification of deep water systems (1000 meter and deeper) is a new field of development in the last 10 years. There exist a variety of methods and procedures for verification of deep water systems. For deep-water moored structures there are many test methods available. The main types can be grouped as:

- Ultra small scale model testing
- Deep water pits for tension leg platform (TLP) and risers
- Combined model test and simulations, passive hybrid model testing
- Large scale (outdoor) model an field tests
- Real-time hybrid model testing (RTHMT)

Some ocean basins have the possibility of testing TLP with normal scaling, but then deep pits is used and allow testing to depths more than 2000 m.

Ultra small testing use scales larger than 1:100. Tests from the Verideep project at MARINTEK (Lie *et al.*, 2000) verified that ultra scale could be feasible for certain global responses. It has been demonstrated that model scales down to 1:150- 1:170 can in certain cases be used in verification of floater motion and mooring line tensions, at least for FPSO (Floating Production Storage and Offloading) and semi-submersible (Lie *et al.*, 2000). This method has issues with limitations such as slamming and correct mooring line forces.

Deep water pits can, for deep water moored floaters, give correct riser forces and tension leg forces, but mooring lines will not be correct due to shallower depth for mooring lines.

Large scale outdoor testing provides no control of the environmental forces and repeatability of test will be difficult. Thus large scale model testing has been rarely used.

The truncated model testing method also called passive hybrid model testing (PHMT) is used at present at MARINTEK for deep water moored structures. This method will have correct stiffness in the horizontal plane for the floater such that the motion will be the same, but extrapolation to full depth will

use numerical software and there is risk of higher order effects not being accounted for (Garlid, 2010). The RTHMT can use exciting laboratory facility and uses numerical software, which has been in use for a long time and is generally accepted in the industry. The RTHMT has similarities to the PHTM . In RTHMT only the mooring and riser will be numerically analyzed. Thus the uncertainties in capturing the higher order effects are reduced. The setup method imposes new challenges and is multidisciplinary since it will requires active control actuators, real-time data communication, fast calculation and accurate results. Time delay and accurate forces imposed at the model are important in this method.

1.2 Previous related work

The RTHMT has been studied for many decades in the earthquake engineering industry, however for the hydrodynamic problems the Offshore Basin of the Maritime Research Institute Netherlands (MARIN) in Netherlands have proposed active truncated line anchoring simulator (ATLAS) for decomposing mooring systems (Buchner *et al.*, 1999). This method decompose the mooring line at the ocean basin sea floor and introduce actuators at the bottom for representing full depth dynamics.

Recent activity at NTNU has involved two master theses, one in the cybernetic part and one other in the use of RIFLEX and data communication in 2011. The new research center AMOS (Center for Autonomous Marin Operations and Systems) has hybrid testing as one of their research activities. At MARINTEK this field is prioritized. MARINTEK USA had a project in this area on decomposed RTHMT, and at MARINTEK in Norway EMT (Extended model testing) have been the main activity. EMT are described in section 3.5. The main study in this thesis is related to the design of a simplified RTHMT of model. Little previous work has been done in this field, or at least published, when relating to hydrodynamic testing of models.

In design of actuators and cybernetic controlling there is particular one article which is relevant (Chabaud & Skjetne, 2013) which presents design rules to build the RTHMT.

Seismic civil engineering have since the 70's used RTHMT for buildings ex-

posed to earthquake, the test was conducted to only a small but complex part of a large structure. Time delays, numerical computations and compensations methods has been developed in this field, but using same procedures in hydrodynamics RTHMT will need modifications and different architecture. In seismic RTHMT the numerical differential equation is stiff and dampening of high natural frequencies. Other fields of RTHMT could be valuable, is offshore wind turbines. Which is a new field with challenges introducing correct wind and wave loads at same time. Launching full scale models need validation and reliable result from model test. A wind turbine is strongly coupled between wind and wave loads. In model tests of wind turbines the loads should be separated, and the wind loads can be actuated by a RTHMT. This is the topic of Valentin Chabaud PhD thesis.

Chabaud thesis will study a coupled pitch-surge motion of a TLP floater of 5 MW wind turbine. The problem is a 2D structure, which in horizontal plane is strongly coupled with horizontal translations and rotations. In this project numerical methods are studied and the use of L-Stable Real-Time 3rd order (LSRT3) with respect to Runge Kutta 3rd order (RK3) is to be assessed. The LSRT3 is widely used in earthquake engineering (Bursi *et al.*, 2011) and is recognized. Other methods such as Newmark β has also been used in earthquake engineering RTHMT, but LSRT3 is recommended (Bursi *et al.*, 2011).

1.2.1 Earthquake engineering & structural dynamics

The idea of RTHMT was first introduced by M. Hakuno in 1969 in a SDOF structure by using electromagnetic actuators in real time, and an analog computer to solve the equation of motion. Hakuno's experiment used real-time hybrid testing for evaluating the dynamic responses of structural systems under seismic loading. In this test a complex substructure that is difficult to simulate dynamic behavior, was used in the experiments. The surrounding structure is simulated numerically, and actuators are imposed to the structure to represent the surrounding structure. This substructure can be chosen to conduct RTHMT due to damage is expected, or difficult to model numerically. The structure is divided into two parts, the real model and the numerical model. This is similar for the RTHMT for deep water moored structures where the floater is the real model, and mooring line is the nu-

merical structure.

RTHMT in earthquake engineering has been of much interest for many decade. The first three modes in a substructure tested in (Carrion & Billie F. Spencer, 2007) was 0.57, 2.75 and 5.91 Hz, which is not far from the natural frequency in surge for a comparison example in this project. RTHMT with combined fast hardware and software, high-performance hydraulic components showed that the system is capable of performing high speed computations and also high loading rates required for fast RTHMT for a earthquake test of a structure. The time delays discovered are mainly lag associated with the dynamics of actuator while delays related to communication and controller are generally small for the RTHMT test (Carrion & Billie F. Spencer, 2007). This was not expected, and will be studied further for the RTHMT proposed in this project. Many techniques to compensate for these time delays has been developed for this issue in this area of RTHMT.

1.2.2 Real-time hybrid simulator

The most important activity at NTNU for this project is the master thesis written by Stian Garlid (Garlid, 2010). There are mentioned few words regarding architecture of a RTHMT. One concepts is the ATLAS system at Marin in Netherlands. This setup is very similar as the setup Cao Yusong at MARINTEK USA proposed (Cao & Tahchiev, 2013). This setup involves a truncated mooring line and a actuator at the ocean basin bottom. Few details regarding this setup is mention, except one very general article with few details (Buchner *et al.*, 1999). In Garlid's thesis a hexapod system is presented briefly. Use of hexapod is widely used at MARINTEK in the towing tank and actuator dynamics and control algorithms are developed. This method has some advantages due to the actuators, which are not placed below surface. The hexapod can control position or force in six DOFs (Degrees of freedom) for the test model. This setup can both impose compressive and tension forces to the model. The hexapod is large and has a large mass, it's many arms and complex geometry makes the control algorithms difficult, and the hexapod will be fixed to the model and will interfere with the motions of the model .

Another setup architecture in (Garlid, 2010) actuate the model with use of motors and winches at mooring line ends. The actuators only change

the tension in the mooring lines and not any directional forces. This thesis is also done in cooperation with Kristan Dahls thesis (Dahl, 2010) which looks into cybernetic part of Stian Garlid's system. Their work is divided into to part. First part focuses on the communication to and from RIFLEX, including a vessel simulator instead of physical model. Second part focuses on actuation of forces onto a moving object. This includes setting up a feedback system. The RTHMT setup for the test of the communication was purely a computer simulation. A simulator in RIFLEX replaced the model in ocean basin. This simulator used a barge at 1000 m depth with two mooring lines. The simulator sent the position signal using user datagram protocol (UDP). Communication with RIFLEX used the High Level Architecture (HLA) . The system was simulated at different time step and the effect of numerical damping was examined. When comparing result and the vessel simulator there was observed a phase lag between the reference force and simulated force. The phase lag was 4-5 time steps. The time steps used was 0.01, 0.015 and 0.02 seconds. Some of the phase lag was introduced due to the JAVA-code used in communication between input and output from in RIFLEX. As a conclusion the simulation indicates the use of RIFLEX in real time analysis. It showed that it can be feasible if the mooring lines are calibrated, and false time lag is removed.

1.3 Main contributions

We summarize what we consider the main contributions of the present work as follows:

- The RTHMT method have been presented and a system implementing this configuration using SDOF motion and using electric drives to actuate the mooring line forces obtained from RIFLEX have been presented.
- A communication setup that can communicate real-time with RIFLEX using HLA and JAVA program for writing and reading data in HLA have been made for communication between HLA and the windows control and automation technology (TwinCat) program for drive control.

1.4 Structure of the present thesis

The structure of the presented thesis is as follows:

In chapter 2 the mathematical formulations which the dynamic analysis is based upon is presented. Theory related to model testing and mooring lines used in the design of RTHMT test setup is presented.

In chapter 3 the RTHMT theory is discussed based upon todays deep water model test. Limitation of the PHTMT discussed and basics for RTHMT.

In chapter 4 the model used for FEM and time domain analysis is presented. A convergence analysis is performed for a mooring line.

In chapter 5 the design and complete model of the build RTHMT test setup is presented with use in combination of time domain analysis in RIFLEX. The modifications needed to be made is also presented.

In chapter 6 the controller systems for the drives and the program for running RTHMT is presented.

In chapter 7 other applications of RTHMT than only station keeping is presented.

In chapter 8 the results from RTHMT is discussed and presented.

In chapter 9 the concluding remarks is presented and a summary with recommendation to further work is presented in chapter 10.

Chapter 2

Theory

In this chapter the mathematical formulations which is used in the time domain analysis is presented. Relevant theory for design of the RTHMT is presented and is discussed later in thesis. Some basic concept is also presented and further discussed later.

2.1 Coordinate systems

In the RIFLEX model the earth fixed coordinate system is north-east system centered on the floater coordinates. The heading is denoted in clockwise direction based on the earth fixed system. The body fixed coordinate system is centered on the floater COG. The body fixed coordinate system uses right handed coordinates system. This system is denoted (X_b, Y_b, Z_b) with the vertical axis pointing upwards and the X_bY_b-plane is the still water line, when the floater is at rest, with X_b pointing in the floater west. At rest the body-fixed and earth-fixed coordinate system coincident with the floater COG.

2.2 Wave dynamics

The hydrodynamic forces in first order wave theory are proportional to the wave amplitude. When waves are considered at an object, higher order forces will occur. Both wind and wave forces will give sum-, mean, and difference frequency forces. Especially the difference frequency forces are important for moored structures since they can introduce resonance oscillations in surge and sway. For low frequency motion (LF) the damping is small for moored structures and large motions can occur.

Wave frequency (WF) force are harmonic forces that oscillate in the same frequency as the incident waves. LF force are higher order forces generated when multiple waves are acting on an object with different frequencies in each wave component. The higher order wave forces is represented by the quadratic term of the Bernoulli equation 2.1 (Faltinsen, 1989).

$$p + \rho g z + \rho \frac{\partial \phi}{\partial t} + \frac{\rho}{2} \mathbf{V} \cdot \mathbf{V} = C \tag{2.1}$$

2.2.1 Regular waves

From linear potential theory, regular waves can be written as:

$$\zeta(x,t) = \zeta_a \sin(\omega_n t - kx) \tag{2.2}$$

Equation 2.2 can also be transformed into waves moving in arbitrary directions.

2.2.2 Irregular waves

Irregular sea state can be approximated by summation of multiple harmonic waves as shown in equation 2.3

$$\zeta(x,t) = \sum_{n=1}^{N} \zeta_{An} \cos(\omega_n t - k_n x + \epsilon_n) \tag{2.3}$$

Where ϵ_n is the random phase angle between 0 and 2π. $\zeta(x,t)$ is the wave amplitude, k is the wave number and ω_n is the angular frequency. By looking into the area within a small frequency interval $\Delta\omega$ is equal to the energy of all wave components within this interval:

$$\frac{1}{2}\zeta_{An}^2 = S(\omega_n)\Delta\omega \tag{2.4}$$

Relation between wave amplitude and wave spectrum can be written as:

$$\zeta(x,t) = \sum_{n=1}^{N} \sqrt{2S(\omega_n)\Delta\omega sin(\omega_n t - k_n x + \epsilon_n)} \tag{2.5}$$

2.3 Mooring and Responses

2.3.1 Mooring lines

Mooring lines are usually constructed of multiple segments. These segments varies along the mooring line. At sea surface lighter cable is used, and heavy cable is used at mid section and the lower parts. The light segment of the mooring line is used for reducing the weight in water for the upper part. The lower part consist often of chain. This is because the anchor must have horizontal force and no vertical force. Horizontal force is achieved when the lower part is heavy enough. The weight of the chain will take up all vertical

forces. Chain is also useful since the mooring line interact with sea bottom. Synthetic ropes can't interact with the seafloor, becuase sand particles can get inside the rope and destroy fibers. The mid part often consist of synthetic fiber or a light segment. Mooring lines must restore the vessels horizontal motions and keep it at same position according to operational requirements. The mooring lines are exposed to environmental loads. Current forces will introduce drag on the mooring lines and can give dynamic amplification (Faltinsen, 1989). Incident wave excitation of the floater will force the floater to oscillate. Mooring lines will then also be excited and try to restore the oscillations, the mooring lines will change geometry due to oscillations. This will introduce large velocities of the flow around the mooring line, and the drag force will be a varying non-linear drag force, which can be calculated by equation 2.6.

$$dF = \pi \frac{D^2}{2} C_M a_1 + \frac{\rho}{2} C_D D|u|u \tag{2.6}$$

where D is the diameter of the mooring line, C_M is the mass coefficient, C_D is the drag coefficient, u is the velocity for the flow going through the line and a_1 is the horizontal acceleration of the mooring line. This drag force will damp the floaters motions.

The stiffness from the mooring lines can be divided into elastic stiffness and geometric stiffness. The elastic stiffness is given by the elasticity of the mooring lines and the geometric stiffness is calculated by the change of the geometry of the mooring lines. Together these two contributions are often called effective stiffness. Geometric stiffness is non-linear and is important to model correctly in mooring lines analysis.

2.3.2 Mooring types

There is a variety of mooring types and materials used for deep water floaters seakeeping, but most common is the catenary and taut mooring system. The deepest conventional moored deep water offshore drilling rig using anchors, is at a depth of 3,165 m in 2013. The differences between taut and catenary system is described in table 2.1 and figure 2.1. Introducing synthetic rope in

the mooring system will increase the nonlinear effects which is more complicated to model in model tests. In increasing water depth, synthetic rope will be advantageous since it have higher strength to weight ratio than traditional chain and wire. Thus synthetic rope have a very different behavior compared to traditional chain and wire. The axial stiffness characteristics are nonlinear and vary with time and loading history. The synthetic fiber material used is polyamide (Nylon), polyester aramid and high modulus polyethylene (HMPE). The HMPE have high creep rate. Creep is the strain increase in rope length under sustained tension or cyclic loading. The synthetic fiber ropes are constructed from materials that has visco-elastic properties. These fibers does not obey Hooke's law perfectly and have viscoelastic properties.

The visco-elastic properties can be described to have following properties:

- Hysteresis effect in the stress-strain curve.
- Creep
- Stress relaxation

This effect is not similar with the traditional chain and wire. Behavior of this materials is assumed to be linear elastic.

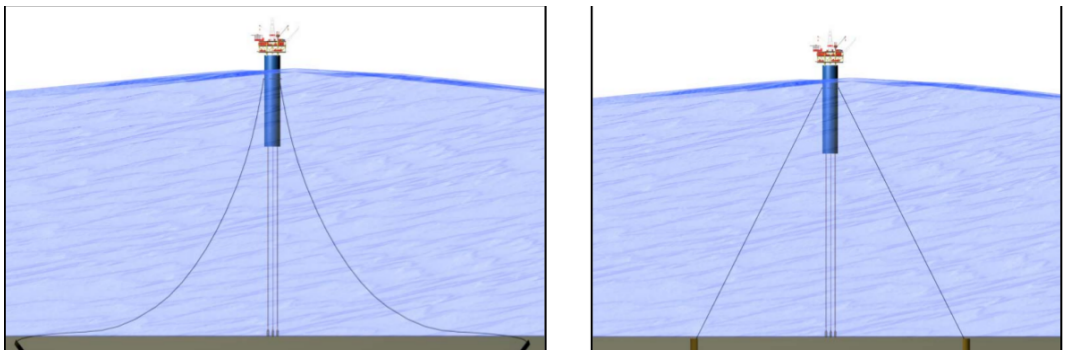

Figure 2.1: Catenary vs Taut mooring system (Halkyard, 2013).

[1]Length of mooring line between anchor and floater.

Table 2.1: Catenary vs Taut mooring system (Halkyard, 2013)

	Catenary Mooring	Taut Mooring
Restoring force	Line weight	Line stretch
Line length[1]	2-3 times water depth	1.3-1.5 Times water depth
Offset controll	Pretension	Line stiffness and pretension
Anchor type	Drag anchor	Vertical loaded anchor
Deepwater impact	Efficiency of wire chain system reduced, vertical load increases	Efficiency of taut wire system improves, Light weight, low modulus synthetic ropes very efficient.

2.3.3 Mooring line stiffness

For calculating the mooring line characteristic, the catenary equations are used to calculate a nonlinear mooring line characteristic, but there are more nonlinear effects in mooring lines.

There are mainly four nonlinear effect in the mooring lines:

- Geometric nonlinear effect due to large change of mooring line shape.
- Interaction with seafloor which cause friction. With also changing geometry the exposed line with seafloor changes.
- Non-linear elastic behavior, only for synthetic ropes.
- Non-linear effect due to generalized Morison formulation

2.3.4 Mean drift and slow drift forces

Mean drift and slow drift forces are nonlinear effect due to the hydrodynamic effects. For floaters such as semi-submersible the hydrostatic restoring for heave, roll and pitch are small and then the the natural frequencies are small. The large amplitudes responses will occur despite low energy in spectrum in this frequency range. Large amplitudes from slowly-varying excitations can occur. The slowly-varying excitations comes from nonlinear wave structure interaction and wind loads. The slow drift force comes from

2nd order hydrodynamic pressure due to the first order wave, interaction between first order motion and first order wave and the 2nd order potential due to slowly force on the free-surface and the body. An incident wave can be expressed by equation 2.7, and contain two wave components with different frequencies.

$$\eta = A_1 \cos(\omega_1 t - k_1 x) + A_2 \cos(\omega_2 t - k_2 x) \tag{2.7}$$

These two progressive waves in deep water will have following potential due to the incident wave given in 2.7.

$$\Phi(x, z, t) = -\frac{gA_1}{\omega_1} e^{k_1 z} \sin(\omega_1 t - k_1 x) - \frac{gA_2}{\omega_2} e^{k_2 z} \sin \omega_2 t - k_2 x \tag{2.8}$$

When looking into the second order pressure term associated to the squared velocity. This will lead to a difference frequency and sum frequency load effect on the floater. The second order pressure components is given in equation 2.11.

$$(\frac{\partial \phi_1}{\partial x})^2 = \frac{(A_1^2 + A_2^2)}{2} \tag{2.9}$$

$$+ \frac{A_1^2 \cos[2(\omega_1 t + \epsilon_1)]}{2} + A_1 A_2 \cos[(\omega_1 + \omega_2)t + \epsilon_1 + \epsilon_2] \tag{2.10}$$

$$+ A_1 A_2 \cos[(\omega_1 - \omega_2)t + \epsilon_1 - \epsilon_2] \tag{2.11}$$

The first term in equation 2.11 is the mean drift term, second term is the sum-frequency terms and last term is the difference frequency term, which cause the resonant motion.

For RTHMT LF motions is important since the LF motions is more difficult to predict than WF both in model test and full scale. RIFLEX analysis need complicated numerical tuning in order to get LF responses as model tests. LF motion is difficult to predict in RIFLEX since higher order effect will occur

and effects with higher order than 2nd order, and numerical model should be validated with full scale or model test. LF motion responses have the largest amplitudes compared to WF motions. As deeper water is introduced the LF motions also will govern more as will be discussed in section 2.7. For RTHMT actuators and data communication WF motions will put largest demands on time delay and computation time. WF motion for large λ will lead to higher frequencies for motions, phase lag will be important to check for not introducing inaccuracy. For RTHMT WF motion will have highest demand regarding time delay and actuator response.

2.4 Froude scaling

In model test of floaters scaling is based on Froude scaling law, because gravity waves are of interest. It is also possible to use Reynold scaling, but then gravity waves should not governing the model test results. Reynolds scaling is important when inertia and viscous forces are governing. When viscous forces and wind are important Reynolds scaling is better suited. In Froude scaling the viscous forces needed to be corrected, normally referred to as scaling effects (DNV, 2010b). Froude scaling requires dynamic similarity between model and full scale as seen in equation 2.12. Wind turbine testing will be a conflict since the turbine it self would be preferred to use Reynold scaling, but the floating strucutre should be Froude scaled.

$$\frac{U_m^2}{\sqrt{gL_m}} = \frac{U_F^2}{\sqrt{gL_F}} = F_N \tag{2.12}$$

In table 2.2 important relations between model scale and full scale are given according to Froude scaling.

The ratio between inertia forces and gravity forces need to be the same for model scale and full scale in Froude scaling. Correct Froude number will ensure that the surface waves that are gravity driven are correctly scaled. For deep water moored structures model tests Froude scaling is used. For more slender structures where viscous forces dominated, Reynold should be used. For a model test it will be a compromise. If Froude scaling is used there

Table 2.2: Model to prototype multiplier for the variables commonly used in mechanics under Froude scaling(Chakrabarti, 1994)

Variable	Unit	Scale factor	Remarks
Length	L	λ	Any characteristic dimension of object
Area	L^2	λ^2	Surface area or projected area on a plane
Volume	L^3	λ^3	For any point of the object
Moment of inertia mass	ML^2	λ^5	Taken about a fixed point
Time	T	$\lambda^{\frac{1}{2}}$	Same reference point (e.g., starting time) is considered as zero time)
Displacement	L	λ	Position at rest is considered as zero
Velocity	LT^{-1}	$\lambda^{\frac{1}{2}}$	Rate of change of displacement
Acceleration	LT^{-2}	1	Rate of change of velocity
Natural period	T	$\lambda^{\frac{1}{2}}$	Period at which inertia force = restoring force
Force	MLT^{-2}	λ^3	Action of one body on another to change or tend to change the state of motion of the body acted on.

will be scale effects due to the difference Reynold's number in full scale and model scale. Drag coefficients dependencies for different Reynolds number are shown in figure 2.2. The figure show relationship for drag coefficient and Reynolds number. The multiple curves show differences of roughness, but this effect is not of interest since the dependencies for drag coefficient over Reynolds number is the same. Results are from a cylinder with different Reynolds number. From this graph it is possible to see the scaling effect from Froude scale when comparing drag from model scale and full scale.

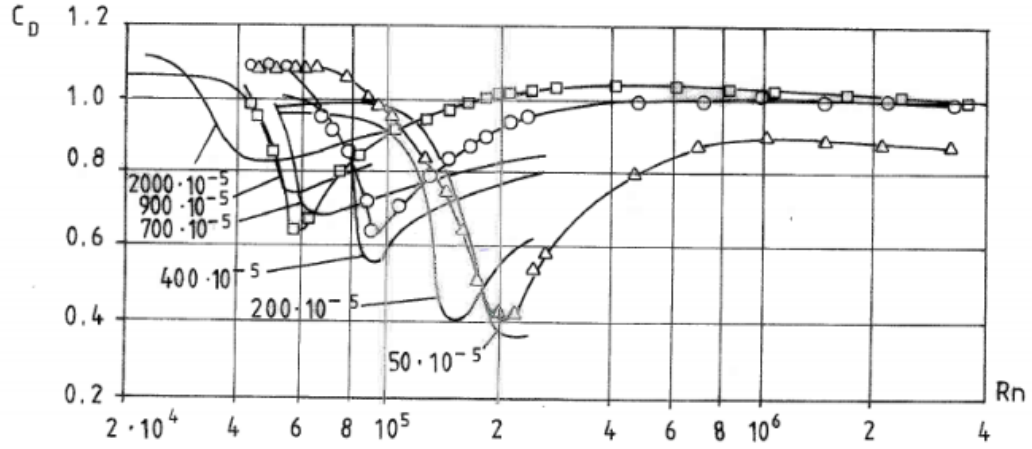

Figure 2.2: Drag coefficient in different Reynolds regimes (Greco, 2012).

In model scale the Reynold number will be smaller than full scale, leading to an increase in drag, because of different flow separation, surface friction and spray. Scale effects such as current and drag of circular cylinders with separation is usually large, but all together on the complete model the scale effect may not be significant compared to other hydrodynamic forces. Many components will be without scale effects due to Froude scaling. Some main environmental loads and its scale effects are described in table 2.3.

Table 2.3: Main components and scale effects (Lehn, 2012)

Force	Description	Scaling remarks
$F_{wave,load}$	First order wave force	Froude scaling, no scale effects
F_{drift}	Sum and difference frequency wave force	Froude scaling, no scale effects
F_{wind}	Wind force	Force is scaled, no scale effects
$F_{current}$	Current forces	Large scale effects, if separation is well defined small effects
$F_{mooring,riser}$	Mooring and riser forces	Diameter reduced to compensate
$F_{viscousdrift}$	Viscous drift force	Significant for floaters in large waves
F_{VL}	Morrison type wave force due to wave particle motion	Surface roughness is more significant in oscillatory flow than steady current

2.5 Time Domain analysis

Model test and RTHMT will be analyzed in time domain. Use of time domain analysis is useful when hydrodynamic load effects can not be linearized and not included in the frequency domain approach. While highly non-linear loads can only be accounted for in the time-domain analysis. In time domain analysis higher order load effects can be captured. In time domain statistical calculation can be done without making assumptions regarding distributions of the responses. For solving the equations of motion in time domain numerical methods need to be used. A differential equation of dynamic system is given in 2.13. Effects which can not be accounted for in frequency domain are effect such as transient slamming loads, LF motion, high frequency motion such as ringing, coupled riser, mooring and floater response. Ringing is not a concern in RTHMT for deep water moored structures, because the natural periods is much higher. Ringing is the main concern for bottom fixed structures such as gravity-based structures (GBS) and wind turbines. RTHMT is still very interesting for TLP model test, but complexity and maintaining

correct stiffness to test dynamic responses such as ringing with truncation or other test methods is difficult. In time domain extreme loads are often of interest. Such effects need long time duration and are time consuming. This can be solve with selective modeling where the model is redefined and simplified.

In frequency domain analysis irregular sea loads can be obtained by superposing regular wave loads components. In frequency domain transients are neglected and only steady state is assumed. Then the dynamic response and loads are oscillating with same frequency as the incident waves.

2.5.1 Numerical methods

Newmark-β is a stepwise method of numerical integration used to solved differential equations. The differential equations for a system with n DOF, for example a floater in ocean basin ca be written as follows:

$$\mathbf{M} = \begin{bmatrix} m_{1,1} & m_{1,2} & \cdots & m_{1,n} \\ \vdots & \vdots & \ddots & \vdots \\ m_{m,1} & m_{m,2} & \cdots & m_{m,n} \end{bmatrix}$$

$$\mathbf{C} = \begin{bmatrix} c_{1,1} & c_{1,2} & \cdots & c_{1,n} \\ \vdots & \vdots & \ddots & \vdots \\ c_{m,1} & c_{m,2} & \cdots & c_{m,n} \end{bmatrix}$$

$$\mathbf{K} = \begin{bmatrix} k_{1,1} & k_{1,2} & \cdots & k_{1,n} \\ \vdots & \vdots & \ddots & \vdots \\ k_{m,1} & k_{m,2} & \cdots & k_{m,n} \end{bmatrix}$$

The dynamic equation can then be written as given in equation 2.13 for an n DOF system.

$$\mathbf{M}\ddot{u} + \mathbf{C}\ddot{u} + \mathbf{K}u = F(t) \tag{2.13}$$

The Newmark β method general step by step integrations equation is given in equation 2.14.

$$\begin{aligned} \dot{u_{k+1}} &= \dot{u_k} + (1-\gamma)h\ddot{u_k} + \gamma h\ddot{u_k} \\ u_{k+1} &= u_k + h\dot{u_k} + (\frac{1}{2} - \beta)h^2\ddot{u_k} + \beta h^2\ddot{u_k} \end{aligned} \tag{2.14}$$

The value of γ determine the numerical damping.

- $\gamma > \frac{1}{2}$ positive damping
- $\gamma < \frac{1}{2}$ negative damping
- $\gamma = \frac{1}{2}$ no damping

The parameter θ includes following methods:

- β =0 Central difference
- $\beta = \frac{1}{12}$ Fox-Goodwins method
- $\beta = \frac{1}{6}$ Wilson θ-method
- $\beta = \frac{1}{4}$ Constant average acceleration(Trapes method)

The equation 2.13 of motion is discretized by dividing the time interval at a uniform interval of Δt. The equation is then solved by using step by step time integration algorithm such as Newmark β or LSTR methods. For each time step the response of the system is obtain from model test and then the the discrete equation of motion for the moorings and risers are solved at the software resulting on a force resultant to be forced by using actuators. The numerical model to be integrated in real-time include the components

of test structure mass damping and numerical structure, and also additional components such as delay and lag should also be accounted for.

2.6 Damping

Many effects in damping are related to the Reynolds number, in Froude scaling the model scale and full scale will not have similar Reynolds number. This effect is accounted for. With RTHMT it is possible to also actuate damping contribution. Until now the stiffness characteristics has only been related to the actuating to the model. There is also possibility to introduce a damping model to the RTHMT. As mention above the slowly-varying drift force gives large loads, that are of interest, in model testing. This motions are resonant and the amplitude will be determine by the damping of motion. For this motion the damping is strongly related to fluid flow which again is related to Reynolds number. For mooring lines this effect can be determine. Damping coefficients can be found from software such as WAMIT, HARP or empirical estimates from experiments. During initial test in model scale test such as decay test and pullout tests is performed. During this test damping coefficients is possible to determine from experiment. This can be implemented in the RTHMT non-linear FEM time domain software which calculates the force resultant and corresponding direction to force the model. The mooring lines will represent the main damping for the slow-drift resonant motion. Use of synthetic ropes may reduce the dynamic effect of nonlinear loads and resulting slow-drift damping (Stansberg *et al.*, 2002). This is for a taut mooring system at deep water.

2.6.1 Damping model

The model will have a damping from water in RIFLEX. The hydrodynamical damping is used in RIFLEX and values used is given in B, but however the global structural damping is more concerning to model accurate. This damping model is related to the modal shapes of the model. The global Rayleigh damping matrix can be established as a linear combination of the

global tangential stiffness- and mass matrices given in equation 2.15.

$$C = \alpha_1 \mathbf{M} + \alpha_2 \mathbf{K} \tag{2.15}$$

α_1 and α_2 are mass- and stiffness proportional damping coefficients. If the distributed damping force is known as assumed in equation 2.15, the consistent damping matrix for a element can be determine same as the mass matrix. That is:

$$c_i = \int_{V_i} N^T c(x) N dV \tag{2.16}$$

Important property of the global Rayleigh damping is that the damping matrix in equation 2.15 is orthogonal with respect to the eigenvectors. The orthogonality can be used to express the linear damping for a linear dynamic system as a function of the damping coefficients. The damping ratio is given in equation 2.17.

$$\lambda_i = \frac{\bar{c}_i}{2\bar{m}_i\omega_i} = \frac{1}{2}(\frac{\alpha_1}{\omega_i} + \alpha_2\omega_i) \tag{2.17}$$

α_1 damp the lower modal shapes, and α_2 damp the higher model shapes.

2.7 Coupled analyses

"The main objective of a coupled analysis is to examine the influence of the floater mean position and dynamic responses due to slender structure effects such as damping, restoring and inertia forces"(Hansen *et al.*, 2004).

First general coupled analysis will be covered and then coupled analysis will be looked with an RTHMT perspective. For some of the floating systems installed/planned, coupled analyses is considered a must, both with respect

to safety and cost (Hansen *et al.*, 2004). As floaters are exposed to deep water the system introduce more non-linearities, and effects from riser and moorings will become increasingly more significant in calculating response of the floater. Coupled analysis can be then seen as the ultimate method with possibility to capture all important effects (Hansen *et al.*, 2004). Decoupled analysis will be an alternative if data from full scale, model test, or selected coupled analysis is based on the calculations. Coupled analysis can be expensive in computer time, but often selected modeling can improve the efficiency. Selected modeling is an analysis of a small part of the global system which capture important effects.

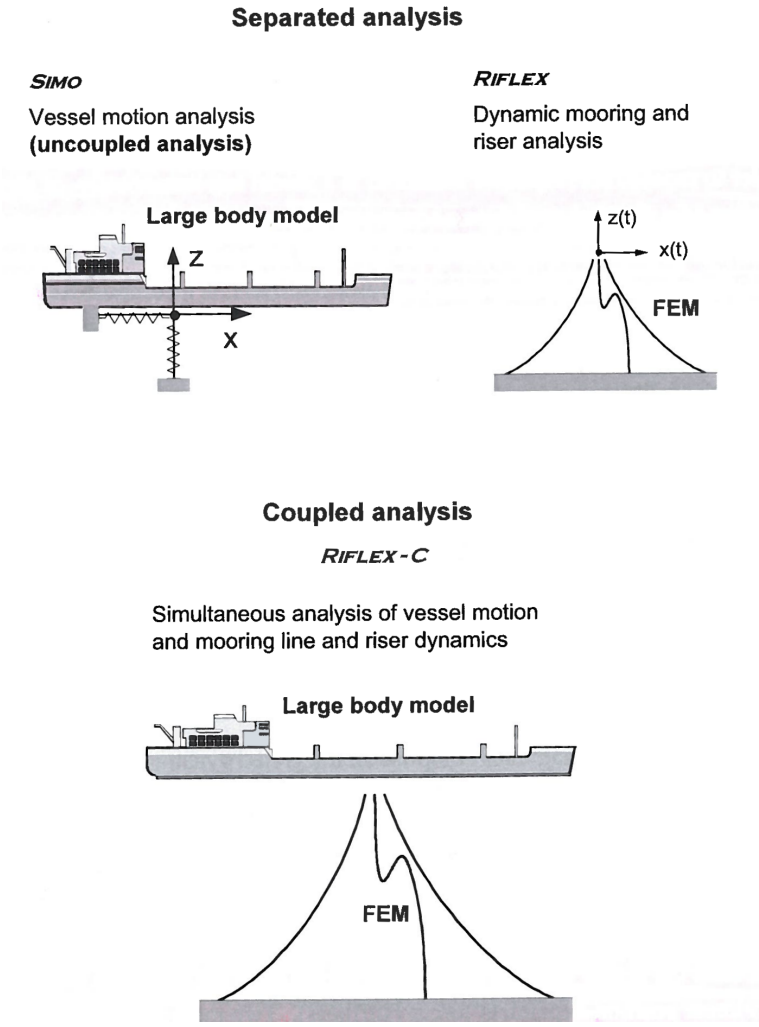

Figure 2.3: Illustration of traditional separated analysis and coupled analysis(Stansberg *et al.*, 1999)

Traditionally the vessel motions and load effect from the mooring lines and the riser are analyzed by a two-step procedure as shown in figure 2.3. In the separated two-step procedure the WF and LF motion response of the floater from mooring lines and risers are modeled as non-linear position dependent forces i.e stiffness.

Two simplifications are often introduced in this modeling (Ormberg *et al.*, 1998):

- 1) Damping forces are often neglected or simplified by a linear damping force acting on the floater.

- 2) The current forces on the mooring lines and risers are either neglected or implemented as an additional current force on the floater. This lead often to a inaccurate line tension.

These effects must be estimated and introduced as coefficients for the floater. For the dynamic responses for the mooring and risers the response is added as a top end excitation as mention above.

Main shortcoming for this approach are following (Ormberg *et al.*, 1998):

- The velocity-dependent forces damping on riser and moorings, are often very important for the calculating the LF motion response for the floater.

- Mean current loads on riser and moorings are often not accounted for. In deep water with strong current and many risers the interaction between the underwater elements current forces and LF motions of the floater is strong.

The shortcomings stated above will increase when the floater is introduced to deeper waters. In order to sufficiently account for the mean offset and LF motions a coupled analysis is preferred. It is also important to mention that when the water depth is increased the limitations of a laboratory model test is also introduced. Since the depth of the model basin is not deep enough, results from deep water moored floaters is more difficult. As a consequence of this, verification of floaters will be done more by simulations.

Coupled analysis is a time-domain analysis with use of non-linear finite element formulation. Coupled analysis is characterized by the response of the floater, riser and mooring lines will be calculated at same time and then

all interactions between the different systems will also be integrated in the analysis.

2.7.1 Coupling effects

As depth is increased, coupling between slender structures and floating structure become more important. Then dynamics is important and it should be solved simultaneously. The effect which should be examine is the coupling effects from slender structures, damping, restoring and inertia forces are governed by the following force contributions (DNV, 2010a):

- Static restoring force from the mooring and riser system as a function of floater offset.
- Current loading and its effects on the restoring force of the mooring and riser system.
- Sea floor friction (if mooring lines and/or risers have bottom contact).
- Damping from mooring and riser system due to dynamics, current, etc.
- Friction forces due to hull/riser contact.
- Additional inertia forces due to the mooring and riser system.

In a traditional mooring analysis, item 1) can be accurately accounted for. Items 2), 4) and 6) may be approximated. Generally, items 3) and 5) cannot be accounted for. A coupled analysis can include consistent treatment of all these effects. A correct damping is often critical in order to obtain realistic values of the floater and mooring response.

In comparison between coupled and separate approach. The coupled analysis gives more accurate estimates for the floater motions. If the coupled analysis is to be used then accurate mean offset and LF motion response and more accurate loads on the mooring in dynamics analysis is important. As mention above coupled analysis become more relevant with increasing depth due to the increase of mean offset and LF motions.

Chapter 3

Real-time hybrid model testing

3.1 Programs

3.1.1 RIFLEX

RIFLEX is a program used for static and dynamic analysis of slender marine structures. Hydrodynamic and structural analysis is performed in RIFLEX. The content from this section is taken from RIFLEX theory manual (Fylling & Sødahl, 1995). The general dynamic equilibrium equation solved for the finite element system model in Time domain is expressed following in RIFLEX:

$$\mathbf{R^I}(\mathbf{r}, \ddot{\mathbf{r}}, \mathbf{t}) + \mathbf{R^D}(\mathbf{r}, \dot{\mathbf{r}}, \mathbf{t}) + \mathbf{R^S}(\mathbf{r}, \mathbf{t}) = \mathbf{R^E}(\mathbf{r}, \dot{\mathbf{r}}, \mathbf{t}) \tag{3.1}$$

$\mathbf{R^I}$ - inertia force vector
$\mathbf{R^D}$ - damping force vector
$\mathbf{R^S}$ - internal structural reaction force vector
$\mathbf{R^E}$ - external force vector
$\mathbf{r}, \dot{\mathbf{r}}, \ddot{\mathbf{r}}$ - structural displacement, velocity and acceleration vectors

Equation 3.1 is solved by step-by-step numerical time integration as mention in section 2.5.1. Equilibrium iteration is performed at each time step. A non-

linear analysis is used due to non-linear effects such as geometric stiffness, nonlinear material properties and bottom contact.

3.1.2 SIMA

SIMA is a graphical interface for use of modules such as RIFLEX or SIMO. In SIMA the HLA task is created and data traffic to HLA is chosen in SIMA for the RIFLEX model. The RIFLEX analysis is run from SIMA.

3.1.3 TwinCat

TwinCat is a real-time control software PLC and/or robotics runtime systems. In TwinCat the programming languages is C and C++, but for the PLC systems IEC 61131 standard, structured text (ST) is used. ST is simple programing languages, but however many built in functionality in TwinCat libraries can be used an increase flexibility and control systems in real-time. All connected EtherCat slaves is added in TwinCat, and controlling of this slaves can be done from PLC program in TwinCat.

3.2 General

The RTHMT uses both non-linear FEM numerical software and model test results simultaneously. The floater is scaled and design according to scaling laws and limitations in the laboratory in ocean basin, but the mooring system will be designed differently than traditional PHMT with truncation. In truncation, the truncated mooring lines represent all seakeeping for the floater. In RTHMT setup it will be used linear spring and not nonlinear as the truncated mooring lines used in PHMT for seakeeping. A figure of the system overview is shown in figure 3.1.

A actuator will actuate the nonlinear mooring line stiffness. The linear springs will be designed to give correct natural periods in the horizontal plane motions such as yaw, surge and sway. Same for the vertical plane motions periods such as heave, roll and pitch periods is the same. In addition to the linear spring the nonlinear spring stiffness will also be accounted for in

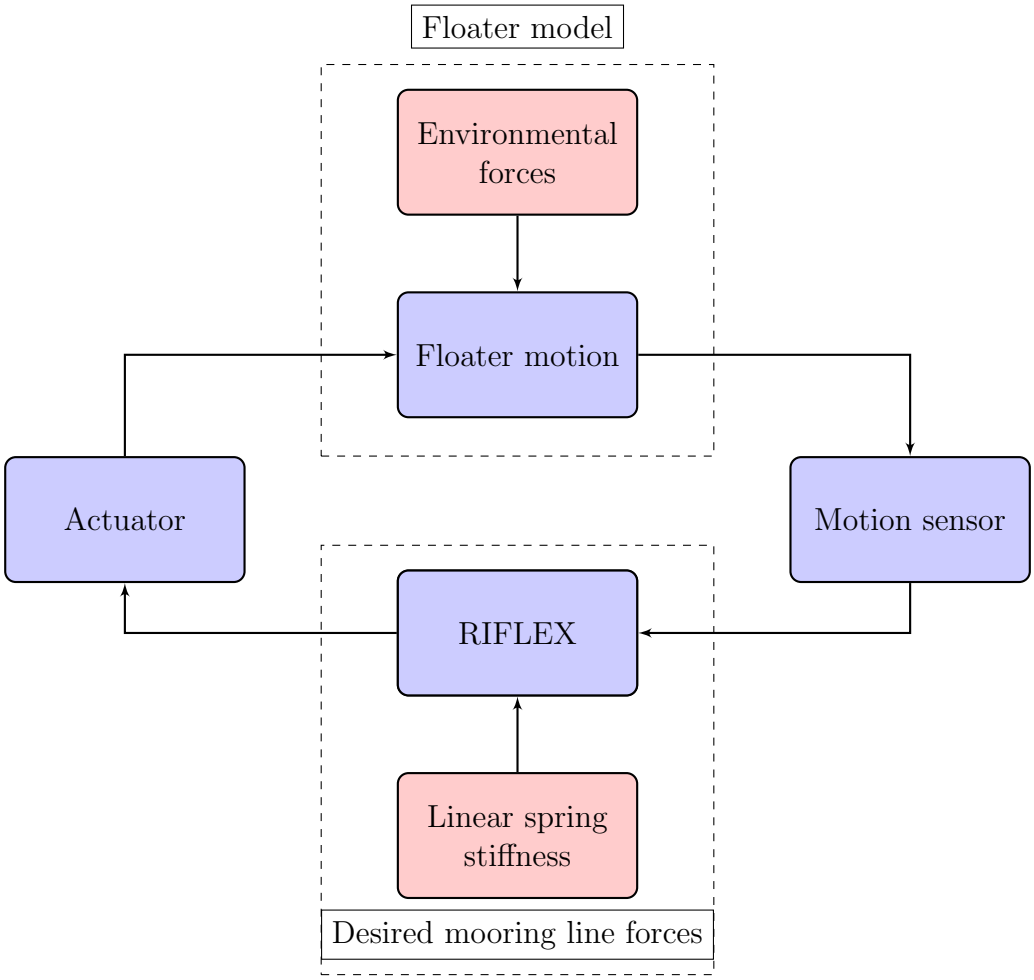

Figure 3.1: System overview

RTHMT. It will be a difference between the linear stiffness and the nonlinear stiffness for the floater. The different stiffness will be accounted for by using a actuator, which will force the floater with a force resultant calculated by real-time numerical software. The nonlinear stiffness will be represented by the actuator. The real-time numerical software will in real-time be given a position in 6 DOF for the floater at a given sample frequency. The position input to the floater will determine the nonlinear stiffness contribution for the floater during test based on the restoring characteristics.

In 10 recent years PHMT has been studied and developed at MARINTEK and verified. This method is also recognized in the industry for deep water model test. For 15 years ago Marin ocean basin in Netherlands started research on an active type truncated system call Active Truncated Line Anchoring Simulator (ATLAS) (Buchner *et al.*, 1999). No recent articles or research work on the ATLAS system at MARIN is found since 1999. RTHMT of deep water moored floaters has been mention in some PHMT papers and as an general overview in some articles, but most PHMT has been focus until now.

For RTHMT methods in the early phase semi-submersible or FPSO should be examine and tested with simple structure. TLP should not be implemented at this stage or other structures with low natural periods. FPSOs and semi-submersibles is useful since they have large natural periods, and TLP will have complicated stiffness and DOF's for the truncated depth.

3.3 Passive hybrid model testing

Almost all the truncated systems currently in use are of PHMT type (Stansberg *et al.*, 2002; Fryer *et al.*, 2001; Stansberg *et al.*, 2004; Baarholm *et al.*, n.d.). The PHMT are truncated and the depth beyond the ocean basin bottom is truncated and excluded. The truncated system must depending on the objectives of the model tests to have equivalent behavior with the full depth and the truncated depth.

The criteria of the behavior should include (Cao & Tahchiev, 2013).
1) Static stiffness

2) Dynamic responses (motion and loads)
3) Couplings of the mooring system with the floater and environmental conditions

In PHMT all these effect need many iterations of optimization of mooring lines, to account for all effects is difficult. Due to the overall global restoring force/moment characteristics, it may not be possible to maintain the similarity of the individual mooring lines and riser, not to mention the dynamic similarity. Loss of the geometry and dynamic similarity impose serious concern in the scaling result (Stansberg *et al.*, 2002; Stansberg *et al.*, 2004; Fryer *et al.*, 2001; Baarholm *et al.*, n.d.). Recently there have been many design improvement in the PHMT, but still there are some aspect needed as geometry similarity which are possible in RTHMT. So if the time-delays and its influence is accounted for in RTHMT the result will be more accurate. They will be more accurate since more criteria is meet as mention above, and more effects will be accounted for in the testing.

Model test in ocean basin laboratories has been recognized as being the most reliable tool to analyze moored offshore structures. However, as the exploitation of oil and gas goes to deeper water, model test are exposed to limitations regarding depth. Due to the limitations in the todays laboratories deep water moored model test must be truncated or tested by other methods where mooring lines dynamics is coupled with the environmental loads and other effect for the full depth is integrated in the analysis. Ultra small scale model tests has also been looked into, but aspect such as slamming and mooring line forces are hard to model correctly. Results from ultra scale testing and the limitations for MARINTEK ocean basin is presented in figure 3.2.

As the scale increased and above 1:150, the reduced repeatability of environmental modeling does not recommend smaller scale, but this is depending on the model test concept(Stansberg *et al.*, 1999). This is in agreement with the uncertainties which is mention in figure 3.3.

The damping from the drag of mooring lines will not be correctly scaled for ultra small models. Only advanced coupled numerical simulations is also an alternative, but due to the uncertainties of the modeling of the damping the results may not able to capture all higher order effects and impose uncertainties on the results (Stansberg *et al.*, 2004). Normally responses

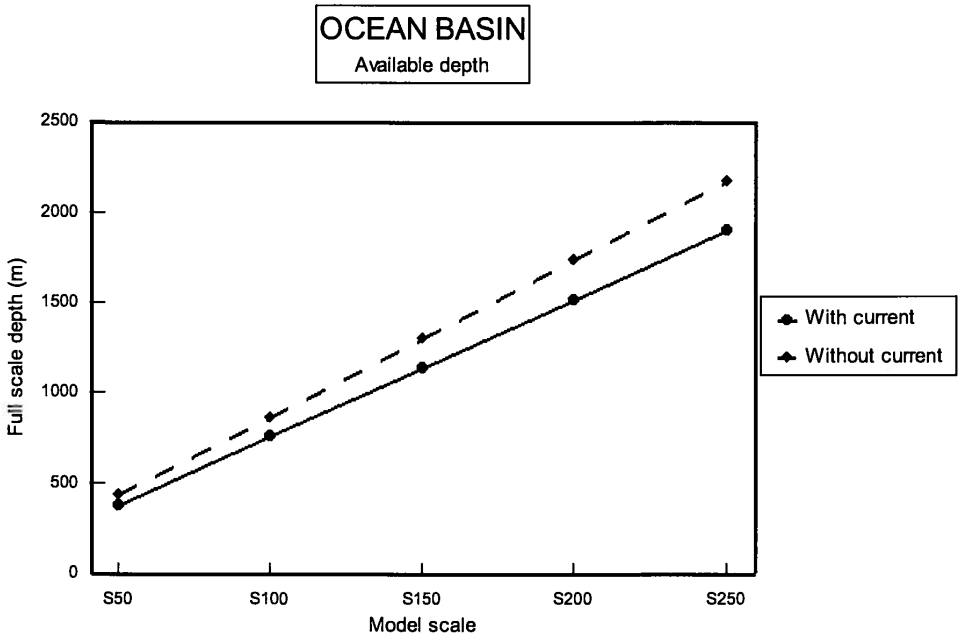

Figure 3.2: Maxiumum available basin depth as function of model scale for MARINTEK ocean basin (Stansberg *et al.*, 1999).

such as wave impact such as slamming, wave motions to find air gap, floater motions, mooring line tension, interaction between riser, mooring and hull, global loads and riser tension is of interest. Choice of deep water verification depend on the several factors and choice of type depend on the type of structure and the parameters to be studied.

3.4 Model test of deep-water moored structures

In chapter 3.2 the limitations of laboratories are mention and a way to cope with this is truncated model testing. Through extensive research programs at MARINTEK a PHMT verifications procedure has been developed, but still this method has limitations. From the Verideep project the numerical simulation need extensive tuning in order to predict accurate results in PHMT. This method also shows uncertainties in the LF motion response as expected

(Kendon *et al.*, n.d.).

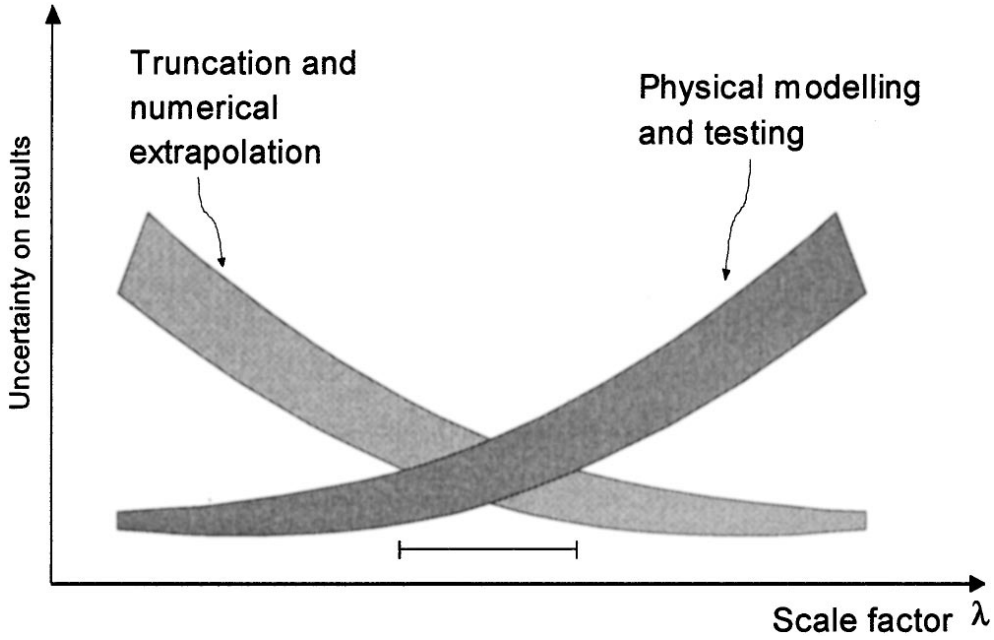

Figure 3.3: Illustration of balance between uncertainties related to truncation and scale factors(Stansberg *et al.*, 1999)

General increasing model scale will reduce uncertainties, but on the other hand laboratory basin limitation will be meet earlier at a larger scale. The balance between the uncertainties and scale factor related to truncation is shown in figure 3.3. With larger scale the system will need an increase in the truncation. The difficulties is to chose the proper scale in order to reduce the uncertainties.

For the truncated model test, it combines numerical simulations with model test. The truncations procedure is outline as below(Kendon *et al.*, n.d.):

1) Specification of full depth system and environment. 2) Truncation of the mooring and riser system to allow model testing at reasonable scales. 3) Model testing of the truncated system in irregular waves. Static excursion tests and decay tests are performed beforehand to ensure the model system is to specification. 4) Time domain simulations to reproduce the truncated model tests, where a numerical model of the vessel is calibrated against the model test results (so-called "model-the-model" calibration). 5) Time

domain simulations of the full depth system, where the tuned numerical model of the vessel from the truncated simulations is used in simulations with a full depth mooring and riser system.

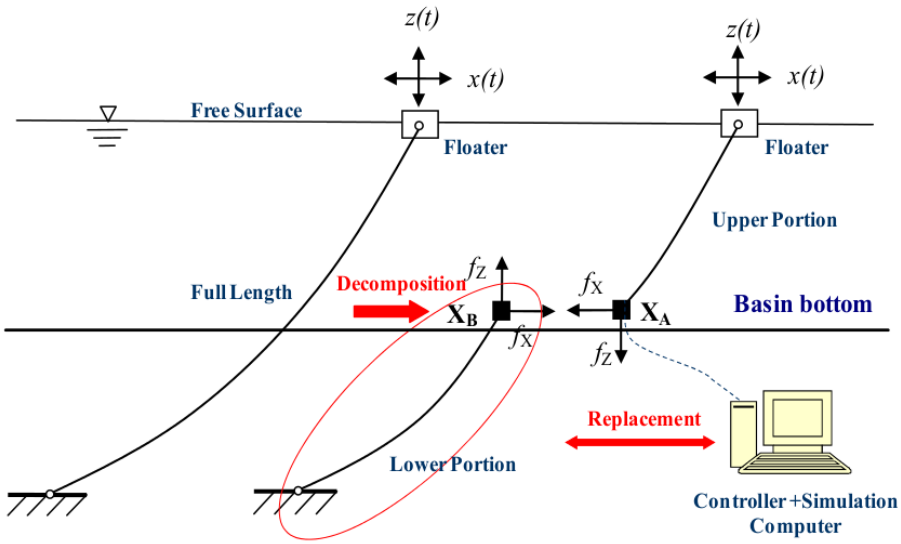

Figure 3.4: Sketch of the RTHMT decomposed mooring system(Cao & Tahchiev, 2013)

The decomposed active hybrid model proposed by (Cao & Tahchiev, 2013) is the most recent and the most relevant paper into the test method this project is focused on. Decomposed active hybrid testing method will have actuators at the end of the mooring lines at the TDP, instead of directly force the model as the proposed architecture in chapter 5. The decomposed mooring system is showed in figure 3.4. The actuators is placed at each mooring lines ends and need to have the ability to apply force in different directions. In the decomposed method proposed still PHMT approach is used in the design of the truncated mooring lines. The floater will in model scale be designed to have correct stiffness in horizontal plane, but the actuator will replace the extrapolation which in the PHMT approach was simulated after the model test. The actuator will be given a force resultant computed by a real-time simulation of the model. In this setup truncated mooring lines will be used. The complexity of using the truncated mooring system and forcing at each mooring line can be more difficult than needed. In order to apply correct force at each mooring line the mooring line used in model test which

is nonlinear, need to be taken into account. For correct forcing the numerical software and the mooring line in ocean basin should be taken into account. The truncated mooring lines is nonlinear with many different segments along the line, design to give correct stiffness in horizontal plane. Each mooring line need to have it's own numerical software results and controller for the actuator. The number of mooring lines can vary and if 16 mooring lines is used for example, it will be very complex.

The setup method, which is proposed in chapter 5, is more simplified since it will use linear springs and only actuate the non-linear contribution. The idea is to actuate as little as possible. With less possible external interference the results will be more accurate. For the decomposed mooring system it need as well to calculate the truncated nonlinear stiffness contribution when calculation of the force resultant which is determine in numerical software and will be applied at the end of the mooring line in the model. Decomposed mooring have a actuator at each mooring line which should work in two directions. This will be complex and computational expensive to calculate the force resultant and the force direction at each mooring line. The setup which is presented in this project has the advantage of minimizing the corrections and that the actuator is connected directly to the model. This simplifies the modeling and the calculations. The number of actuators will also be reduced at the method proposed in chapter 5, compared to decomposed system. For a RTHMT method proposed, the actuators should be able to actuate force/-moments in all 6 DOF. Then only 6 actuators could be needed only.

(Stansberg *et al.*, 1999) used hybrid verification and compared between simulation and model test at full depth at 365 m and same system truncated at 165 m depth. The simulation was carried out in RIFLEX program in coupled analysis in time domain. The results shown low mooring dynamics, but after the hydrodynamic floater model was calibrated with the truncated simulations, the simulations in full depth showed quite well corresponding between model test at full depth and simulation. In order to reduce uncertainties as shown in figure 3.3 in extrapolation of model test results to full depth.

The truncation system must try to fulfill following criteria:

- Same motions responses of the floater as with full depth.
- Truncated mooring system that has similarities with the physical properties of the full depth.

As mention in section 3.2 it is difficult to obtain accurate result from damping and stiffness. Important effects that should be prioritized in the truncated system within some important offset range is given in (Stansberg *et al.*, 1999) which is correct horizontal restoring characteristics, correct heel and moment imposed by mooring system, "representative" level of mooring line damping and "'representative" single line tension. The pitch moment is important for semi submersibles where coupling between surge and pitch is significant.

In order to design the truncated mooring lines the computer code MOORPOT-TRUNC (Fylling, 2005b) is used with MIMOSA (Kassen *et al.*, 2012) and optimization program NLPQL (Fylling, 2005a) for the truncated mooring lines.

As mention in section 2.3.4 the second order loads are important. These mean drift loads resulting from second order effect is important in design of mooring system. The natural period for surge, sway and yaw for moored structures is O(1-2 min). For floater with small water plane area the restoring terms in vertical motion is small, and leads to a large natural periods O(30s). The slowly-varying drift force can occur in the vertical plane and cause large amplitudes response for heave, roll and pitch. For the large natural periods with LF the wave radiation linear damping is small. Viscous damping and wave-drift damping is then important. Due to small damping, large amplitude in responses can occur near resonances. The main damping contributions for a moored structure is the wave-drift damping, viscous hull damping and viscous anchor-line damping. As described in (Greco, 2012) the slow-drift damping from mooring lines is important, in surge response within the wave period this damping is negligible, but in the small frequency range it is very important. For PHMT with truncated mooring this effect can not be accounted for correctly with the truncated mooring lines, but has to be implemented in the numerical simulations. The slowly-varying drift force can cause large responses and is a important effect and critical in design of mooring lines and risers. In RTHMT correct damping at correct Reynolds number in full scale is used in RIFLEX. In PHMT Froude scaling is used and Reynolds number in model scale is not the same as full scale.

3.5 Extended model testing

Until now MARINTEK has only perform extended model testing (EMT) which is used to check RIFLEX with model test and develop communication between RIFLEX and model testing in real-time. The same communication setup and TwinCat use as this methods was tested on an industry project in June in 2014 for EMT. Only concept of the EMT in June is presented, and no further results from RIFLEX model. In this model test setup a RIFLEX model in model scale have been modeled in RIFLEX. During initial test procedures such as pull-out and decay test, coefficients will be updated in the RIFLEX model as the results become available from model test. Drag on mooring lines need proper modeling, and is useful to iterate during initial testing procedures. With this setup the Quailsys tracking manager (QTM) position system sends the floaters positions to the SIMA model simultaneously. The QTM system is based on cameras, which read the position in 6 DOF based on light emitting nodes attached to the model. From the SIMA software there is no output which will be used in real-time. The EMT performed in June had to implement a filter on the 6 DOF position signal before it was sent to RIFLEX.

A simplified filter in TwinCat was developed to reduce noise and large residuals which sometimes lead to an error in RIFLEX analysis. This program reads only the position and compute analysis in time domain based on this input. This method was also tested with Åsgård semi-submersible model test earlier. Then a different communication setup was used. QTM position signal was sent on EtherCat to TwinCat for test performed in June, but during testing of Åsgard in 2012 similar setup as presented in (Garlid, 2010) was used with UDP communication. The on-line RIFLEX simulations were ran successfully during Åsgard model test campaign in the ocean basin (Sauder, 2011). In figure 3.5 a picture taken in the control room from ocean basin show a computer with a RIFLEX running with position fed real-time from model test QTM system and a camera view from the model in ocean basin.

In the EMT a HLA federation “fed” by model test was established. HLA is a way of communication used in simulation. HLA has different instances that participate in the simulation called federates. For the HLA federation built in EMT, one HLA federate contained a 25Hz for Åsgard EMT QTM position of the floater in the ocean basin which was measured. The whole

simulation itself is called the federation, and federate is the instances that participate in the simulation. HLA federation also involved RIFLEX simulations for two mooring lines, and SimVis for the visualization on the floater mooring lines. For all the federate used they need real-time communication between federates. All federates are connected to a Run time interface (RTI) which all data are being sent through, and not from one federate to another. RIFLEX needs position at each step to calculate response, and the SimVis need position at each time step from RIFLEX to visualization the model. SimVis is a module for visualization of the analysis in SIMA. This is not a active hybrid test methods since it doesn't have any forcing back to the model. This method is useful to identify and check the performance of the architecture and its components. RIFLEX was run with an frequency of 100Hz and the HLA federation was 25Hz for the Åsgard EMT. Positions signal had to be interpolated due to the differences in the sampling frequencies. Many tools were developed in order to perform the EMT and useful experience was highlighted. The EMT was a proof of concept for the architecture that were developed. In this test, behavior of riser which is not modeled correctly at TDP could be simulated and presented real time.

A simplified test setup for testing RIFLEX with position sensor has been developed at MARINTEK. This setup was used for EMT. Similar amplifier and logging system is used on this setup as on model test in ocean basin.This setup uses a simple position sensor with a steel wire on a winch. The resistance is measured and then distance measurement can be calculated. The sensor has a resolution of 100 Hz. The signal from the position sensor goes back to the amplifier (MX840). The amplifier is connected to a gateway (CX27) which uses EtherCat data communication to a computer which is EtherCat master, and the gateway is slave. The signal is then processed in TwinCAT software to actual distance measurements. A java code for using HLA in SIMA is used for communication from TwinCat to SIMA. This program is given in appendix D.2. An HLA federation is created in RIFLEX with different federates. One federate is mooring lines, and if the calculation time is slow different computers can communicate on HLA and have their own federates for mooring lines or risers, depending on calculation speed. The SIMA model is then displaced real-time by the displacement the position sensor measures. Similar model is developed for the test setup for RTHMT. Same setup is used, except a actuator is implemented. A flowchart of RTHMT data communication is in figure 5.3.

3.6 Computer technology

Since RTHMT was first presented for 20 years ago (Cao & Tahchiev, 2013). Great advances in computer technology has changed, the computational speed. In RTHMT computational speed is a success criteria and can not be possible without sufficient computational speed. Non-linear FEM used for mooring line dynamics has also been increased last decade. Now it is used in PHMT system, and results is recalculated to the full depth after the model tests. Currently MARINTEK uses RIFLEX to do the numerical extrapolation in their PHMT. In Riflex the time steps is corrected to the model scale in order to represent the physics correctly if not full scale is used.

3.7 Time delays

Since the time in model scale given as $\frac{1}{\sqrt{\lambda}}$, the time goes quicker in model scale. In the earthquake RTHMT they did not use time scaling. In earthquake engineering the time delay was significant represented by the actuator dynamics rater than the numerical and communication. The USED actuators for the test setup, The dynamics is not yet studied due to lack of documentation at this stage. Before RTHMT with the setup proposed in this chapter 5 the actuators must be calibrated and measured. For the actuator which represents the environmental loads on the model, very accurate tuning is not needed, as long as the exciting force is measured and correspond to the wanted environmental loads.For the other actuator which will actuate the mass with a calculated force, the dynamics need to be well studied. This will influence and give understanding on the response of the actuator. The calculation for the magnitude and the direction for the force that need to be actuated on the mass is very simple, in this setup and is not time consuming, also the data communication setup for this test is fast with EtherCat (Ethernet for Control Automation Technology). In seismic earthquake RTHMT the time delays was significant from the dynamics of the actuator and this was larger than the other contributions. With this is mind understanding of actuator dynamics should be addressed when time delay is analyzed.

3.7.1 EtherCat

EtherCat is a type of communication for sending data between sensors, actuators and to software doing simulations. Ethernet for Control Automation Technology is an open high performance Ethernet-based field bus system. For UDP or TCP/IP protocol telegram packages are sent and received. The UDP protocol was used in (Garlid, 2010) setup. For the EMT with Åsgard UDP was also used for communication, but for the test in June EtherCat was used for sending 6 DOF position signal. UDP is slower than EtherCat, since it will send packages and received them. The EtherCat send signal continuously. With EtherCat the Ethernet packages is no longer copied and processed. It is read while the telegram passes through. EtherCat is often called "processing on the fly". The amplifiers that will also be used have ability to use EtherCat for sending signals. All actuators used will have EtherCat communication setup.

Figure 3.5: Pictures of the EMT setup taken in control room (Sauder, 2011)

Chapter 4

RIFLEX model

In this chapter a RIFLEX model is presented for use of force results in the RTHMT in this thesis. A convergence analysis is performed and the model which is used is based on Åsgard semi-submersible platform. Simulation workbench for marine applications (SIMA) is used for time domain analysis. The model and results from the RIFLEX analysis is presented in this chapter.

Figure 4.1: Åsgard semisubmersible platform.

Figure 4.1 is the semi-submersible Åsgard B is equipped with 21 risers and 11 umbilicals/cables, and is held at location by a 16 line chain-polyester-chain spread mooring system. Åsgard B is the reference floater used in this thesis. Åsgard B is a gas and condensate processing platform. Main dimensions is given in table 4.1.

A model of a floating production unit with anchor line in model scale have been modeled in RIFLEX to get the force resultant from mooring lines. Statoil Åsgard platform was used with full mooring system to generate force history which will be used in the simplified RTHMT setup, but the scale need to be adjusted to an appropriate scale in order to be used on the simplified RTHMT setup. The model in RIFLEX is a six degree of freedom model. The model of Åsgard platform in SIMA is shown in figure 4.2. The platform is not the correct drawing of the real Åsgard platform, but the riser and

Table 4.1: Main dimensions Åsgard B.

Parameter	Unit	Value
Draught	m	25
Length Pontoons	m	102
Breadth Pontoons	m	96
Height of Pontoons	m	8.96
Corner Column Diameter	m	19.2
Inner Column Diameter	m	12

mooring lines is correct according to actual model. The first order wave response functions have been given and calculated by using the diffraction code in WAMIT, and was given. The second order wave excitation which is relevant for the difference frequencies in wave spectrum is calculated by using conservation of momentum in WAMIT. The model has 16 mooring lines and is divided in groups of 4. Riser system is also included. The mooring line marked red is the mooring line number 10 in figure 4.2. This line is used in the analysis in the convergence study. Marine growth is also included which increased weight and drag of mooring lines. The mooring lines are pretensioned according to given values in Appendix B.

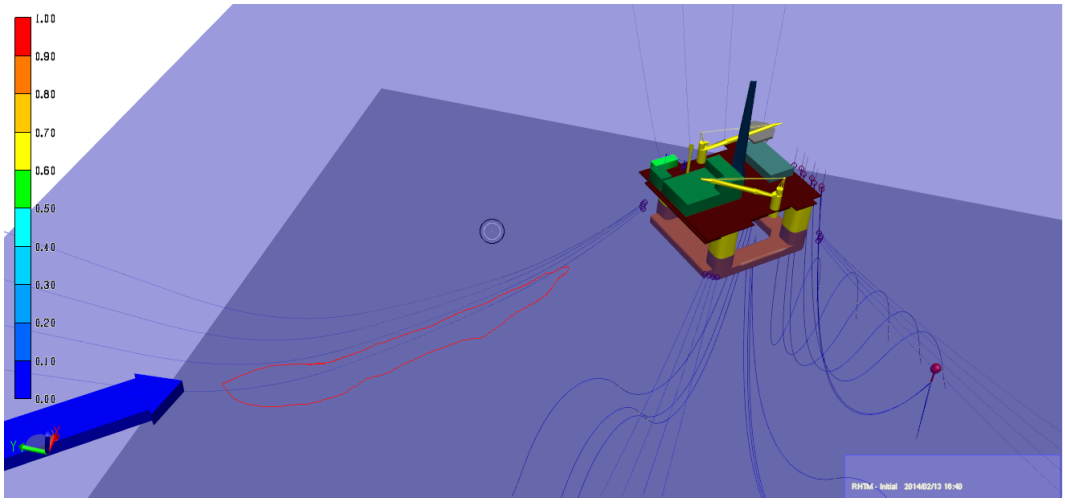

Figure 4.2: RIFLEXmodell of Åsgard semisubmersible

The environmental load is the same as ULS condition for Åsgard platform

Table 4.2: Enviromental condition for convergence study.

Direction	Wave spectrum	Hs[m]	Tp[s]	Current[m/s]
210°	Jonswap	14.7	17.2	1[1]

given in table 4.2, which is given in the metocean condition (Kendon, 2014).

4.1 Convergence study

In order to check this model feasibility for RTHMT, a convergence study has been performed. Different mesh densities along a mooring line will be tested in order to check for convergence of tension and angle.

Six different element configurations for mooring line number 10 in the RIFLEX model was tested. Details about elements along the mooring line is shown in table 4.3. In RTHMT FEM configuration along with numerical solvers is important. FEM convergence is important to get an accurate and representative solution, in RTHMT the time used to solve the model in time domain is a key success factor. Since the analysis must work faster than real-time. Convergence with lowest possible elements and still correct top tension and angle is important. In order to tune the model, a optimization process with respect to time and accuracy must be conducted.

Two particular segments of the mooring line are important. This is where mesh density should be large. Both sea floor and the wave zone should have many elements. The TDP (Touch down point) changes over time, and the contact friction and interaction with seafloor will vary along the bottom segment. In the wave zone, wave kinematic varies along the segment. RIFLEX assume linearly distributed loads along the element, and therefor many elements is needed at seafloor and surface. In the RIFLEX model, seafloor friction is also modeled.

For especially RTHMT fewest elements is preferred, but long segments will give higher contact strain energy. The results then for coarse models is then often generally conservative.

[1] At surfacelevel the velocity is 1 m/s, at 90 m depth 0.9 m/s and zero velocity at 100 depth.

Table 4.3: Mesh configuration for mooring lines

Sections	Length [m]	Case1	Case 2	Case 3	Case 4	Case5	Case6
1	700	300	150	30	15	3	1
2	1,5	10	5	1	1	1	1
3	300	300	150	30	15	3	1
4	1,5	10	5	1	1	1	1
5	180	300	150	30	15	3	1
6	1,5	10	5	1	1	1	1
7	120	300	150	30	15	3	1
8	1,5	10	5	1	1	1	1
9	52,45	100	50	10	5	1	1
10	1	10	5	1	1	1	1
Total Elements		1350	675	135	70	18	10

To check the convergence with different mesh densities, different meshes were tested. The mooring line is built up by 10 different segments with different cross section. All information regarding mooring line design is provided in Appendix B. Results in figure 4.3 showed little difference in the axial force for the mooring line between different mesh densities. This time series is for mooring line number 10, in RIFLEX. The differences is very small with less than 5% between the largest finest and coarses mesh.

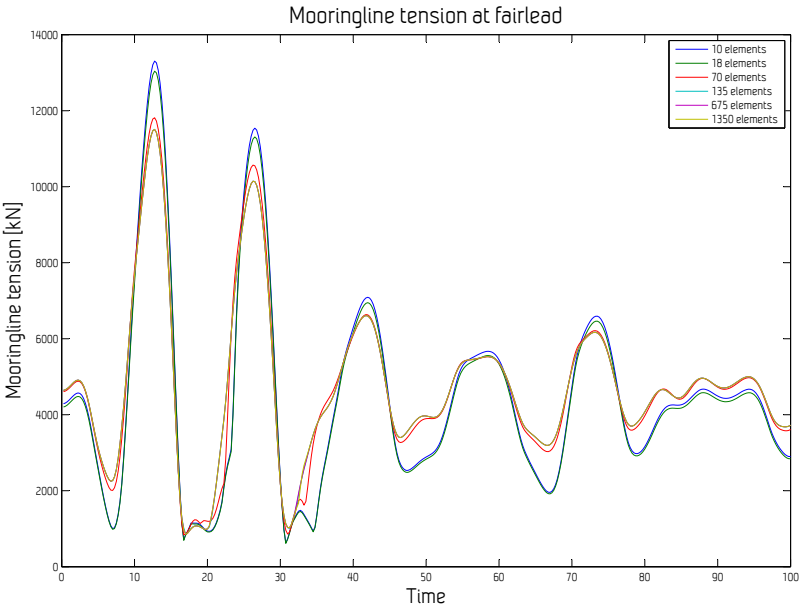

Figure 4.3: Axial force from different mesh densities

Figure 4.3 is a short part of a longer time domain analysis. It is easy to see the convergence of the different mesh densities. The coarse mesh has largest difference and points out, but however the mesh with 18 elements is very close but show lower tension than the mesh with 10 elements. For the three finest mesh the solution is almost same and difference between these meshes is small. A more narrow plot of the axial force at top node is shown in figure 4.4. As long as the mooring line has more than 70 elements the solutions have little difference in axial tension in the time series.

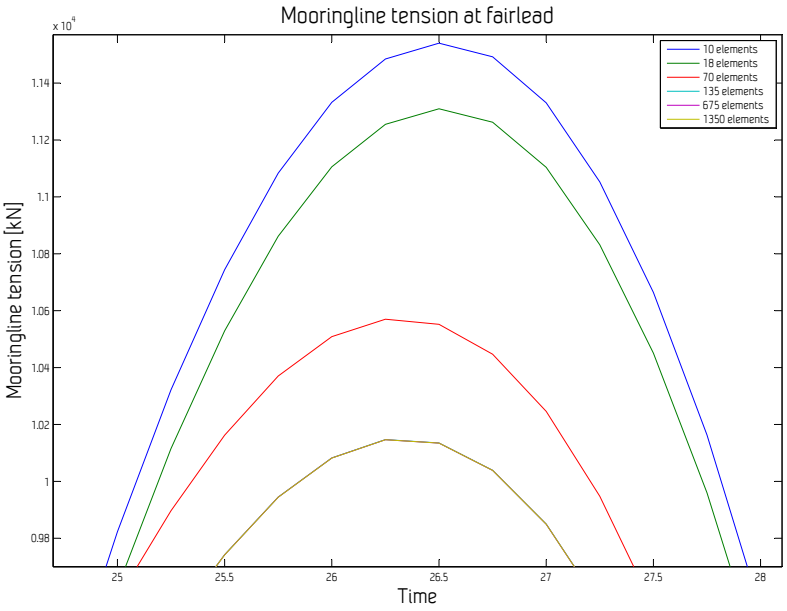

Figure 4.4: Magnified view of figure 4.3

The angle for mooring line at fairlead is also important and this will relate to force direction at top node. The angle is calculated with respect to body-fixed coordinate system and not earth-fixed for the floater. Both yaw and pitch angle for the mooring line at top node has been looked upon in this convergence analysis. The angle for the top element at mooring line 10 in pitch is shown in figure 4.5.

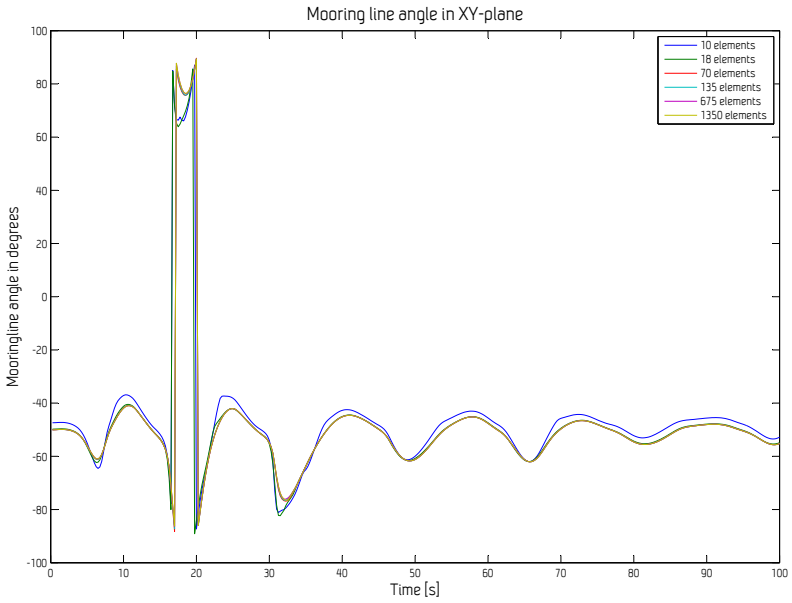

Figure 4.5: Time series with XZ-plane angle for top element

In figure 4.5 the "pitch" angle of the top element of the mooring line is plotted. There is a large peak, and this is due to a steep wave. The axial tension in figure 4.3 also has a peek. The different mesh types are very different at this peak and convergence is not as obvious as the rest of the time series. Since this model is in ULS (Ultimate limit state), the environment induces large waves and motions for the floater.

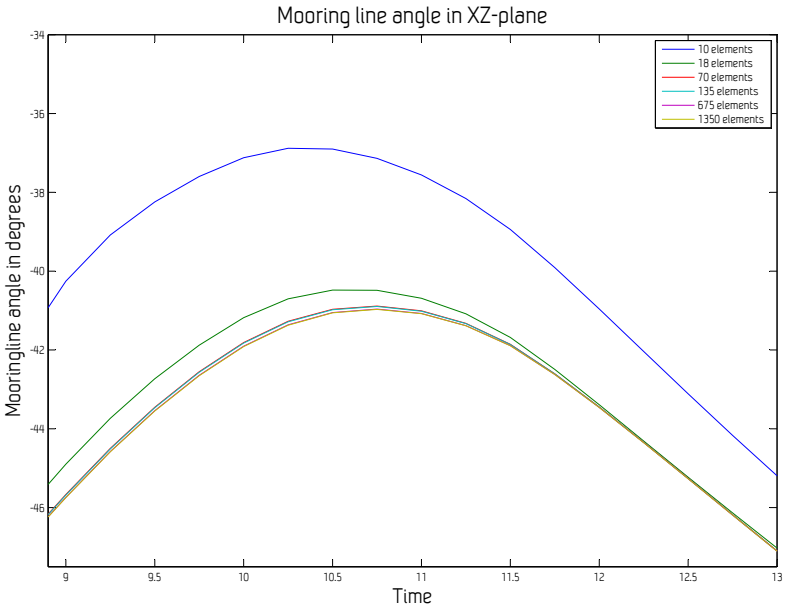

Figure 4.6: Detailed graph of figure 4.5 showing XZ-plane angle for top element

A more redefined figure of XZ-plane angle is shown in figure 4.6. In this figure the difference between the three finest meshes is hard to see. In this peak there is a phase difference between different mesh densities, but this phase shift was only seen on this peak. Coarses mesh has also largest difference in this plot.

Only for mooring line 10 the convergence analysis have been performed, and based on the results the floater will behave different globally if all lines had same element model at the same time. Therefore tests of all mooring lines was conducted with different mesh. This result show very little difference, between earlier results of convergence. Total number of elements on the finest mesh for the mooring lines is 21560. This number is without riser elements included, which is kept as originally modeled

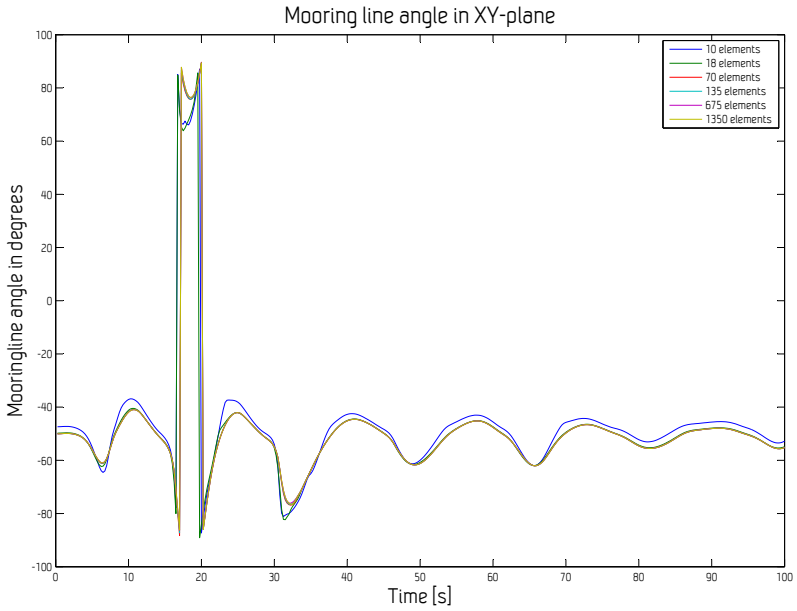

Figure 4.7: Time series with XY-plane angle for top element

The yaw angle of the mooring lines is shown in figure 4.7. The steep wave that was shown in figure 4.5 did not influence the yaw motions as significant as the pitch angle. In both graphs the response with different mesh have little phase difference.

A detail view of angle response in XY-plane at fairlead is shown in figure 4.8. A little phase difference occurred for the coarses mesh, but overall for the time series there is no phase difference except some local points on a peak and through. In this figure the trend of convergence is slower than for axial tension as earlier shown. The difference between the finer mesh is more significant, than what was observed in figure 4.4. The tension converge faster than the angle.

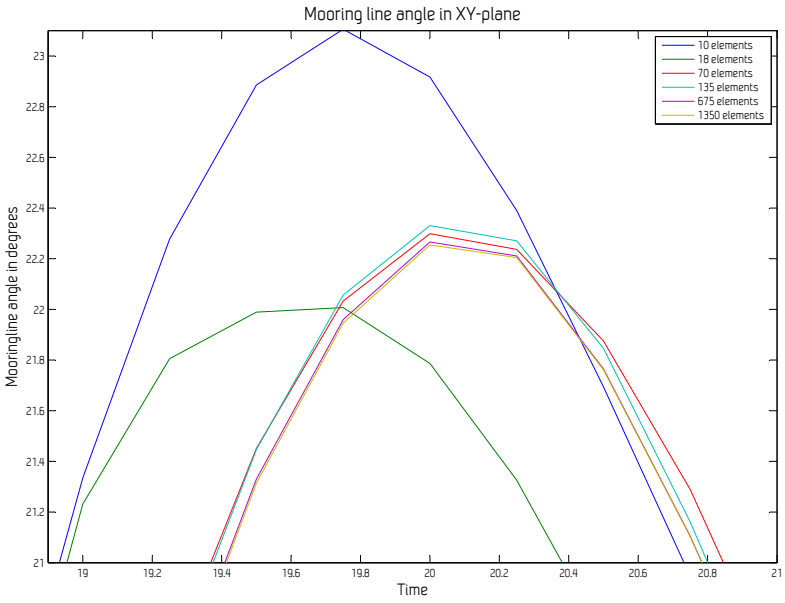

Figure 4.8: Detailed graph of figure 4.7 showing XY-plane angle for top element

In order to determine differences between different mesh densities a Weibull distribution based on axial tension time history have been calculated for each mesh and a graph of this is in figure 4.9.

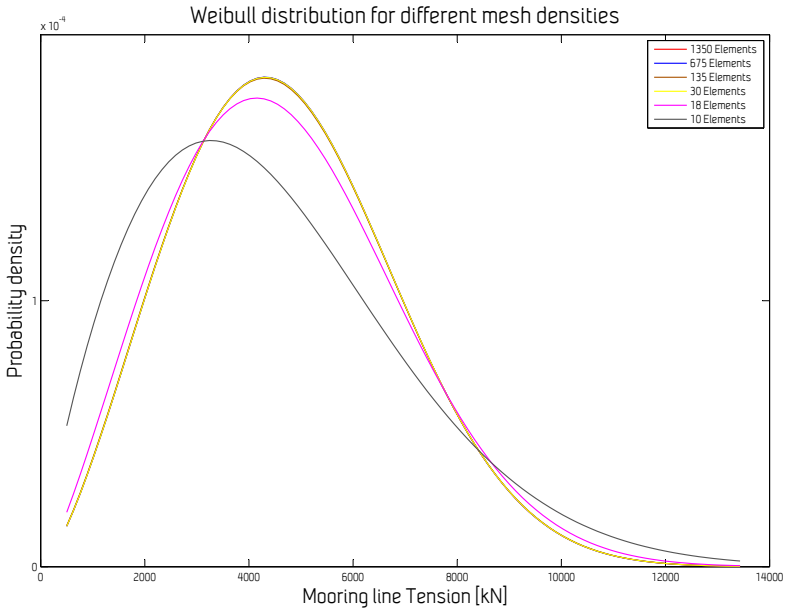

Figure 4.9: Weibull distribution for different axial tension mesh densities

As seen in figure 4.9 the distribution converge quickly. Difference between 70, 135, 675 and 1350 elements is small and difficult to see. The distributions more or less converges when the total no. of element reach 30 elements or more. In the calculation same element model for all mooring line has been used. There is also a change in skewness for the different mesh distributions. The coarse mesh have largest shift in skewness.

4.2 Calculation time

The element models in the convergence study is also used in this section for feasibility study of RTHMT with use of RIFLEX. Sampling frequency is important for feasibility studies, and a sampling rate of 32 Hz is chosen. In this same simulation, all displacements and forces are written to a binary file for the floater, this test is not with use of HLA, which will be used on

Table 4.4: Simulation time with different mesh size.

Processor	Intel Core Duo 2.5GHz, 64 bit
Memory	4 GB
Hard drive	Serial ATA

Table 4.5: Simulation time with different mesh size.

	Case1	Case 2	Case 3	Case 4	Case 5	Case 6
No. of elements	945	675	135	70	18	10
Time[s]	966.4	693.22	130.95	64.27	16.82	9.58

tests later in this thesis. The writing of displacements and forces to file is used for representing the HLA communication in real-time with actuators. In comparison of the calculation time in analysis computer characteristics should be kept in mind, and is given in table 4.4.

In simulation, model scale will be used and time will then be $\sqrt{\lambda}$ faster than full scale. λ is the scaling factor used according to Froude law. In table 4.5 results from time domain analysis of total simulation length of 100 seconds with different mesh densities. The model used has same element model for all mooring lines and in the table 4.3 the element number for each mooring line is presented, and the total number will be 12 times large for the mooring model. The simulation in RIFLEX uses full scale. The time will then be then often scaled with typically $\sqrt{\lambda} \approx 60 - 70$, but for this test $\lambda = 30$.

Same results as in table 4.5 is plotted as a function of number of elements in figure 4.10. The graph is based on 10 calculations with different element model on mooring lines. Simulation time as a function of number of elements show a linear relationship. The mooring line is modeled with one dimensional bar elements. If two-dimensional modeling is used less linear relationship is assumed. Results are promising and show possibilities of use of RIFLEX as non-linear FEM time domain analysis tool for a floater for mooring line dynamics with use of RTHMT.

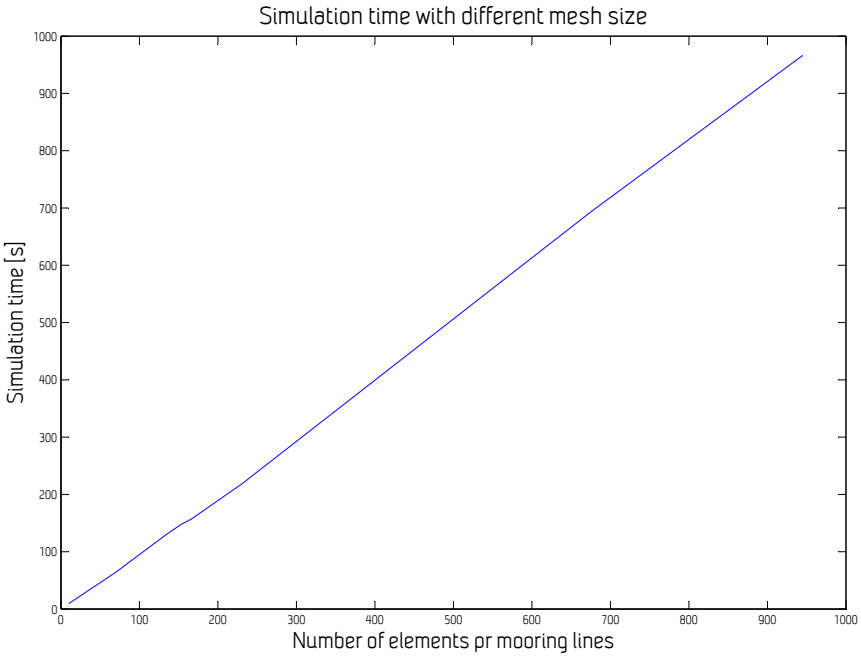

Figure 4.10: Simulation time as a function of nr of elements

In this chapter element model for Åsgard platform have been modeled and tested. Results as presented in figure 4.10 and figure 4.9 show suitability with real-time analysis based on the calculation time and convergence for the axial tension. The element model have also shown convergence to a fine element model, but calculation time is also important. Therefore case 2 from table 4.3 is chosen for use with RTHMT.

4.3 Simplified model used in RTHMT

RIFLEX is used for Åsgard platform to calculate the natural period. Surge degree of freedom will only be used in the simplified test setup. The natural period in surge is 126.5 seconds. A simple model of a semi-submersible platform is used in full scale. Same mooring line setup as the convergence

analysis in section 4.1, with modification, in order to reduce number of anchor lines and computer time. All connection plates is skipped in the mooring element model. The model is simplified in order to test the suitability for RTHMT. Only two mooring lines is used for the floater and not 16 as the full model. The heading angle of the waves is changed and the waves is same direction as the mooring lines. Only the surge motion is of interest in the analysis. This is because of a SDOF test arrangement was built. The model will mainly introduce heave, pitch and surge motion due to the waves. A HLA task containing the RIFLEX model and a SimVis model for visualization is published on HLA. The SimVis model was only modeled to see the responses initially and was not used during further testing due to this visualization model is computational effort, and slows down calculation time for the RIFLEX model. RIFLEX model have an acceleration factor on time in time domain analysis according to model scale. A even more simplified model was built in RIFLEX based on Åsgard full scale model. This model was built in model scale (1:40) in RIFLEX. By using model scale the sampling frequency from RIFLEX should be possible to set even higher. The tension of the mooring lines showed unrealistic values and high frequent response of tension variation during extended model testing occurred. The damping in the mooring line had been further increased and element number was increased higher, but still high frequent tension variation occurred. The simplified model was built with purpose of using lowest possible time step , but the model was to much simplified with minimum elements and too much simplification to get realistic results. The model was Froude scaled to with λ=60, but some extra modifications was needed for model it correct in model scale. For the rest of the thesis the Åsgard model at full scale in RIFLEX is used.

Chapter 5

Test setup

In this chapter the physical test setup for RTHMT is described. The control system and programming is later presented in chapter 6. The modeling of the RTHMT model is also described in this chapter. The data communication is presented for the test setup and procedures in testing.

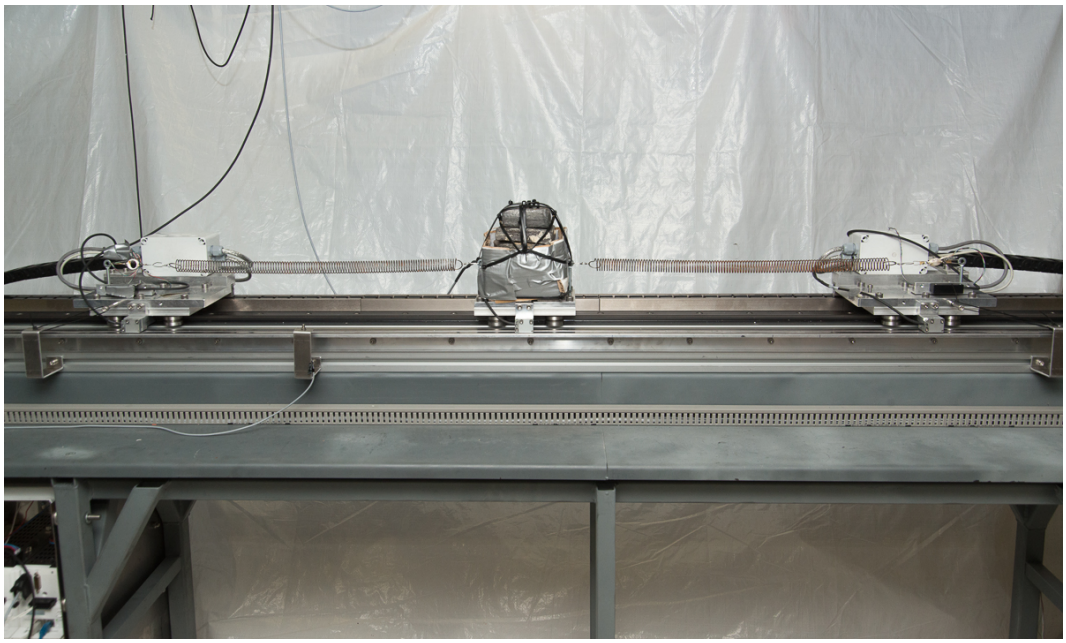

Figure 5.1: Overview of physical model.

The test setup is built up by a steel welded rig for carrying linear carriage system. The rig also have a built in a aluminum support for the encoder which read position for the carriage system. A dock for cabling is used for the moving parts, and a cabling bridge for all cables going to the electrical cabinet is used. The electric cabinet is built underneath the carriage system and is welded to the rig. In the electrical cabinet two Beckhoff AX5000 servo drives for controlling each drive is used.

A EtherCat Bus Coupler is used for reading input signals and sending output signals. Only position reading from the incremental position sensor is used with this terminal. The terminal is connected with EtherCat signal to a EtherCat master computer. For power supply a Siemens 24V power supply is used, delivering 24 V to the EtherCat Coupler and the two servo drives.

A Quantum MX840 amplifier with 8 channels for reading signals is also connected with separate power supply. The amplifier communicate with use of a gateway which use EtherCat. All EtherCat devices are connected in series. Only two cables are need for connecting the test setup externally. One for power supply and one ethernet cable. The rest is wired inside the electrical cabinet. Each of the carriage with drive have a Beckhoff AL3806 Ironless Linear Servomotor. Ironless drives are very useful since they will not cause cogging thrust, due to the magnetic forces between the permanent magnets and the ironcore inducing magnetic field.

The actuators for environmental loading and mooring line dynamics is driven by controlling voltage of a metal bar sliding into a passive magnet dock. A picture actuators is shown in 5.2. The metalbar is sliding frictionless between the magnet, the magnet needs to be placed at a wagon in order to have a precise movement in one degree of freedom for the magnet actuator. Friction will occur due to bearings on the linear carriage system. The drive is quite powerful and have a peak force of 1400 N, and a continuous force of 287 N. Along the carriage system, permanent magnets are placed on the side of the carriage system. This allow perfect docking for the ironcore plate from the actuator which is fixed on the carriage wagon. The carriage wagon have machined drilled aluminum top plate for supporting the drive, position encoder, electrical wire box, spring attachments and magnet end stopper steel plate.

The actuator will need accurate position and tuning to adjust the magnetic field to be correctly adjusted to passive magnets along the carriage system.

Figure 5.2: Linear magnetic actuators.

The position sensor for the actuator have system accuracy $\pm$ 40 μm and resolutions to 0.244 μm. The position encoders are of two types linear absolute and incremental. Both have a separate magnet tape for position reading. The drives is controlled with the incremental encoders. Drives should have been used with the absolute encoders, which is more accurate than the linear incremental encoder. However lack of support from the supplier, wrong assumptions of the firmware, which lead to wrong data telegram sent to servo drive are believed to be the problem for the absolute encoders.

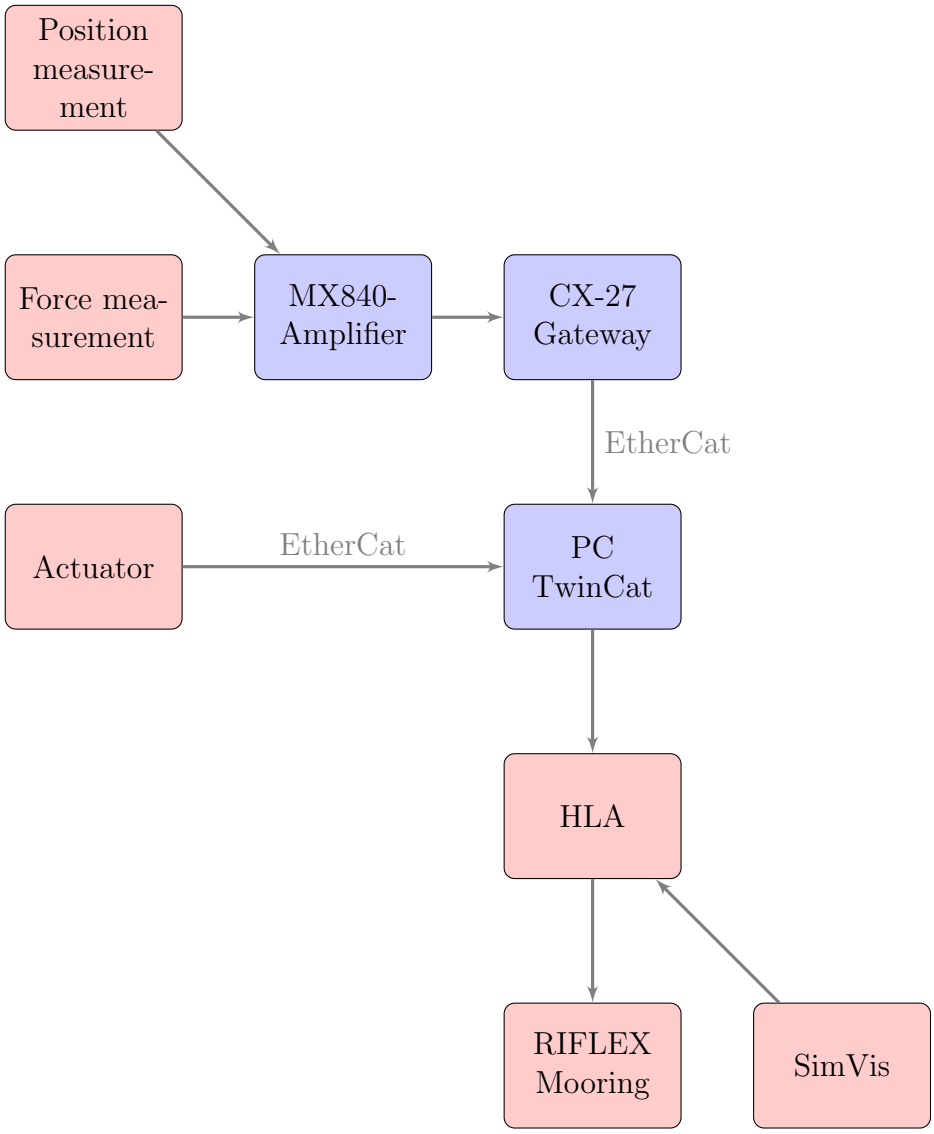

Figure 5.3: Flowchart of RTHMT test setup

5.1 RTHMT test setup

RIFLEX will not only read position signal as in EMT. It will also calculate a force and direction this displacement induces. This force will be sent on

HLA and then read in a java program. The java program send and receive data from RIFLEX. The java program mainly link HLA to TwinCat. The communication part with RIFLEX have been earlier developed by SIMA developers. The part of implementation RIFLEX to TwinCat for RTHMT have been developed by the author. Same data communication is used for EMT as for RTHMT, but RIFLEX is also sending data to TwinCat and not only reading information from TwinCat as for EMT. Same setup for RTHMT is used as figure 5.3, but HLA write and read information in RTHMT, and not only read as in EMT.

5.1.1 Data communication

RIFLEX communicate on HLA with TwinCat. From previous a Java program have been developed to test RTHMT with use of a simulation of the model instead of a actual model. This work was done in Stian Garlid's thesis (Garlid, 2010). For RTHMT use with both read and write in from HLA to TwinCat the program had to be further developed. There was no possibility of implementation of direct data communication from RIFLEX to TwinCat. The java program read and write to channels from TwinCat by finding the channel variable name in TwinCat. In the part of the program that connects HLA and TwinCat, Beckhoff packages is implemented for java in the original code developed by SIMA developers. For every time step, a variable is read from TwinCat and written to TwinCat. Same procedure is for RIFLEX using HLA. The time step for the java program is defined same as the one used in SIMA, but it have to be specified in java program. Previously, the ability to write values to TwinCat from RIFLEX was not possible. The java program is called HlaToTwinCat and can be found in Appendix D.2. Further description of the program is given in appendix D.2.

During the analysis, every time step values is written and read from RIFLEX and TwinCat. All this operations is performed in the doTimeStepWork method in the code. This method is started in every time step in the simulation. The time step is defined in SIMA and in java code. The code uses Java Client AdsToJava.dll to performe I/O operations. From RIFLEX the anchor line forces is decomposed and each component in each direction is calculated for each line. The forces at top node position is stored locally and called "oah_forces". "oah_forces" is a matrix containing one row per mooring

line and each column as the forces in each DOF. In this test setup only two mooring lines are used. The surge DOF force for the first two row is added together. Sum of the total mooring line force in surge direction is sent to PLC in TwinCat. All HLA related code is written by Frode Melling, and the TwinCat related code is written by the author.

5.1.2 Time delay

EtherCat signal is according to supplier of testing equipment able to do 1000 I/O in 30 μs This is far from the limitation used in this setup. In this arrangement four EtherCat drives is used, with roughly 40 variables using in I/O on 1 ms sampling rate. For the amplifier higher sampling rate is used, but still EtherCat has much more capacity in communication than what is used. EtherCat is therefor the last instance that slow the RTHMT. HLA communication and java program is rather more relevant for time delay. RIFLEX will be the instance in the control loop which represent most time delay as later discussed in chapter 8.

5.2 Modeling

To the extent possible the modeling of RTHMT is kept close to the actual model test in ocean basin. In all parts of the control loop this has been focus.

5.2.1 Environmental forcing

A ULS condition for Åsgard B is used for reference as the environmental impact load on the test setup. The model of this setup is built in SIMA, and a time history from SIMA will be used to generate force history for the actuator on the test setup. The environmental forcing will use a servo actuator with EtherCat. The scaling will need extra tuning than only using Froude scaling. According to Froude scaling the force will be scaled according to equation 5.1. A time series from SIMA is exported and the amplitude is scaled. Otherwise the period and frequency is the same as Froude scaling.

The time series is read by TwinCat and processed to a new position signal for the drive based on the spring characteristic to apply forcing.

$$F_S = F_M \lambda^3 \tag{5.1}$$

The exact value for λ should be around 30, amplitude will be tuned to match limitations on motion range for the drives. The magnetic actuator for the mooring line stiffness force will need more advanced controller systems, compared to the environmental loading actuator. The force will then be scaled by λ^3 to be correct in model scale.

5.2.2 Mooring stiffness force

There are two ways the mooring line top tension force can be calculated. The simple method is by using global restoring force characteristics for the model in surge, and then use only this data for the algorithm for the mooring line actuator for implementing non-linear stiffness. This will not take into account displacement time, which is important for accelerations induced. The more accurate method is by using RIFLEX in real-time with HLA communication to TwinCat. This method is more accurate since it will calculate the stiffness force and damping with environmental loading for the the complete mooring system. By only using line characteristic the test will be very simplified and inaccurate. In this thesis Åsgard B platform will have 6-DOF in RIFLEX. For simplicity surge motion only is looked upon in this thesis, coupling of actuators and 2-DOF or more will be to complex for this thesis. The RIFLEX model have 6-DOF, but due to symmetry in design and simplified mooring system the model can be seen as a SDOF. The motions is mainly surge, pitch and heave. With the mooring system and natural periods for Åsgard B in ULS the surge and sway is not so different form each other with only few seconds apart, for the natural period. This system can easily also be used for two-degree of freedom, but then the model must have other carriage system, and it may be useful to place the model in water.

As seen in table 5.1 determine spring stiffness and mass of the model need many consideration and will be a compromise. By only scaling full scale model there will be issues with mass and spring stiffness. The WF motions

Table 5.1: Froude scaling results.

λ	T_P	Mass [kg]	Stiffness [N/m]
30	60	3247	535.1
30	126	3247	121.1
60	60	406	133.5
60	126	406	30.3
100	60	88	48.1
100	126	88	10.9
150	60	26	21.4
150	126	26	4.8
180	60	15	14.8
180	126	15	3.4

is, as described in (Storflor, 2013), important requirement to handle without phase lag for the actuator for RTHMT. If this is possible, LF motions would not be a problem as long as the RIFLEX model is modeled with correct vessel coefficient for damping. The natural period in surge is reduced for not introducing too soft springs. The natural period is still be above the wave period. A spring less than 5 N/m will be very soft and will be difficult to build and implement. The carriage system is not built to have large mass and actuators will also have limitations. Therefore the mass will be around 15 kg for carriage system and natural period of Åsgard B will be adjusted.

5.2.3 Scaling of model for RTHMT

In initial design of this test setup Froude scaling was believed to be used. However limitations with mass of carriage according with spring stiffness needed a different method. As the design of the arrangement became more clear limitations and issues on scaling had to be solved. Then a modified scaling method is used, which is non-physical. This method is only for this specific test setup presented in this thesis.

- Excitation frequency
- Similar natural period
- Force range of actuators

- Displacement range of carriage system

- RIFLEX model restoring characteristics

The actuator need to be able to work in the same frequency range as in model scale or lower. Since Froude scaling will increase the frequency of excitation the actuators need to be able to work in this range without introducing noise or lag. Natural period is important to keep above WF for keeping similar dynamic with RIFLEX model. The mass and spring stiffness will also be adjusted to have correct similarities.

After further investigation and scaling of different springs, the specification from Froude scaling was not possible to achieve. Therefore much stiffer springs was used than what was calculated to be best according to scaling. RIFLEX model has also a spring stiffness which needs to be not so far from actual stiffness on test setup. Goal is to make the model most similar to its purpose in future.

Multiple iterations was performed and considerations as listed above was used in the process. A pair of 60 N/m springs was used in test setup. This springs had an displacement range from 0-0.7 m, which is according to carriage system range. Stiff springs is also applicable for reducing influence of coulomb friction on carriage system. Froude scaling of the restoring characteristics from RIFLEX model will not fit for this springs and test setup.

A displacement of $\pm$ 0.4 m, is the range of movement for the surge position in each direction of the test setup. The carriage system is 3 m long, but the actuators need also range for motion at each end. The springs was attached to the opposite end of the carriage system end for increasing elongation range of spring. This is also seen in picture 5.4.

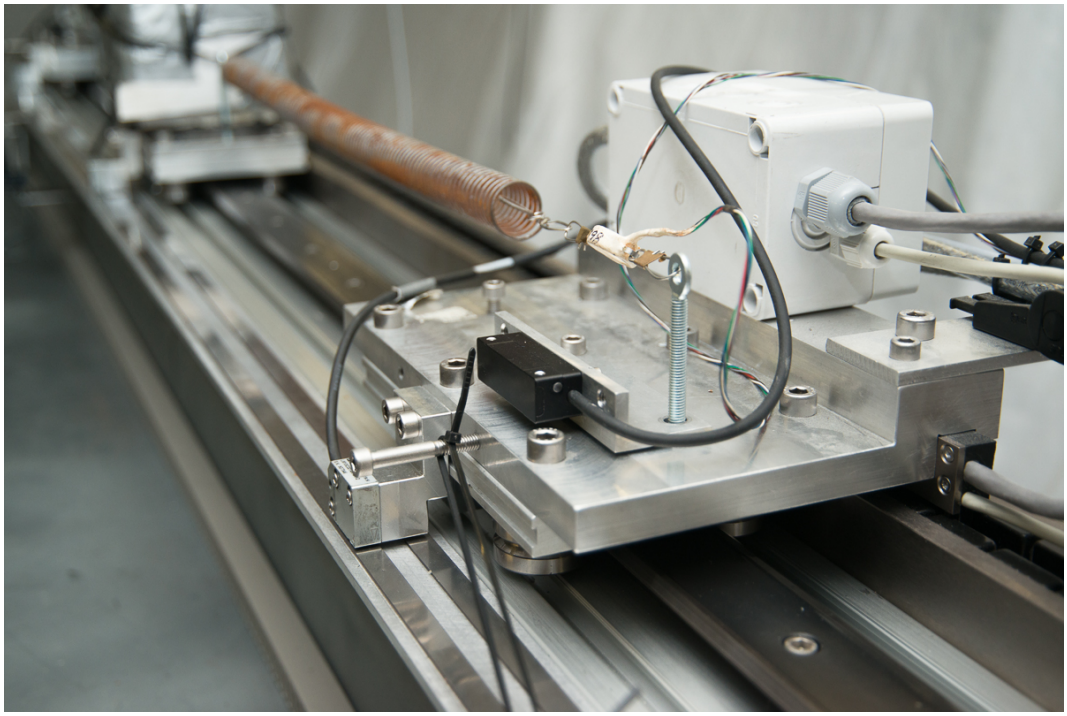

Figure 5.4: Spring attachment to the actuator with force ring.

The restoring characteristics are shown in figure 5.5. The displacement and restoring force is scaled with Froude laws, but different Froude scales is used for displacement and force. The scales used is respectively $\lambda = 30$ for displacement and $\lambda = 34$ for restoring force. However not the full displacement range is utilized due to limitation in range of displacement for the test arrangement. The range of displacement is 0-0.7 m. In full scale only small displacement will be applied with this scaling. The lower displacement range fits with the range available for the carriage system. The linear spring stiffness of the two springs attached to the model is also good fit for the RIFLEX model restoring characteristics. With small displacement, the actuators need to reduce the tension of the springs and at higher displacement, the tension is increased as seen in figure 5.5. The idea of less drive influence of the model is then achieved and this should be more accurate, when the drive have less influence of the system as possible.

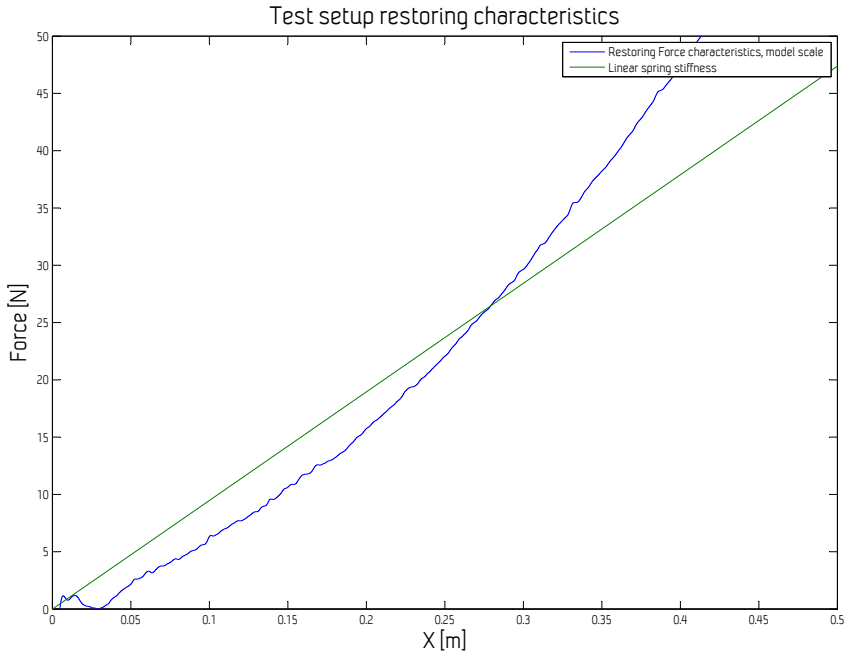

Figure 5.5: Restoring characteristics for the RTHMT system

5.2.4 Damping in linear carriage system

There will always be damping in a mechanical system. The damping force works against the motion and is in phase with the velocity. Linear damping is proportional with the velocity. Quadratic damping force is proportional to the square of the velocity. For dry friction, the damping is constant, and the damping force is independent of the velocity. Constant damping is also denoted Coulomb friction. In figure 5.6 the linear damping is a straight horizontal line. The quadratic damping is a straight line occurs as a increasing line as function of amplitude. The Coulomb damping will decrease as a function of amplitude.

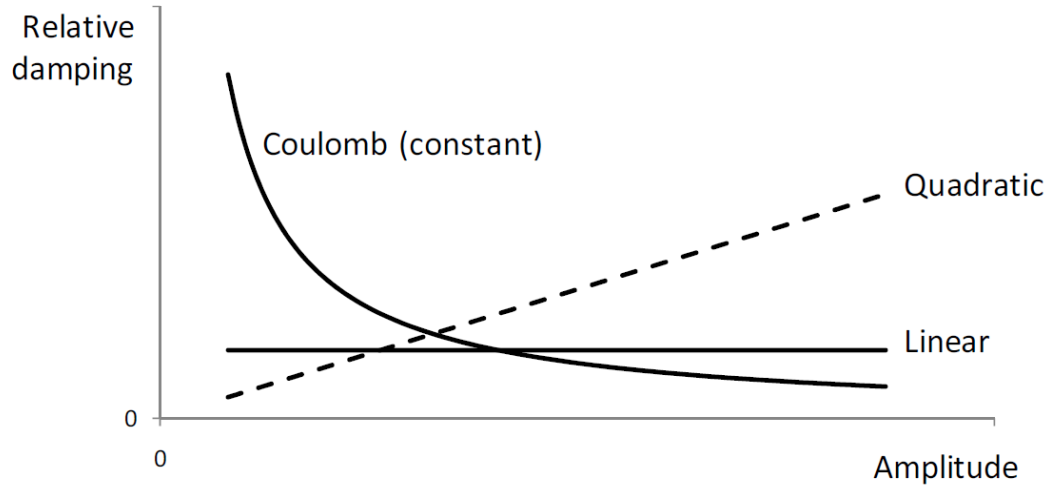

Figure 5.6: Relative damping for different damping models(Lehn, 2012).

The motion of the mass on the carriage is described as equation 5.2 with linear damping. The equation of motion with quadratic damping is described in equation 5.3 and for constant or Coulomb damping, the equation of motion is written as 5.4.

$$F(t) = m\ddot{u} + c\dot{u} + ku \tag{5.2}$$
$$F(t) = m\ddot{u} + c_1\dot{u}|\dot{u}| + ku \tag{5.3}$$
$$F(t) = m\ddot{u} + \mu N sign(\dot{u}) + ku \tag{5.4}$$

Compared to model in ocean basin some damping sources will not occur. Linear energy dissipation such as generation of surface waves will not occur, but linear energy dissipation such as friction in bearings will occur.

There is many methods for estimation of damping such as:

- Motion decay
- Half power bandwidth
- RAO and phase

- Forced oscillations
- Energy considerations
- Random decrement method

Motion decay method will be used for measuring damping in time domain. Motion decay is used for estimating of damping in model test in ocean basin. Half power bandwidth may be applicable if the relative damping level is less than 0.05.

In the test setup the actuator for mooring line will be the active damping, based on Riflex. Active damping refers to energy dissipation from the system by external means, such as controlled actuators in this test setup.

Cables for power supply and communication for both wagons will introduce damping. Cable bridge will have damping when the system is oscillating. If the cables is hang by wire in air, damping can be reduced. This method is similar as the cabling for ocean basin model test. The cable bridge will also introduce much bending due to sharp angles on cables which will damp the motion, and this will also give a small stiffness contribution, but however coulomb damping in the carriage system will governing. The actuators are controlled on position control. By controlling on position the damping and friction for the actuator will not be important.

5.2.5 Linear damping

The linear damping from equation 5.2 can be found by doing decay test and regression on the exponentially decay for the time series. A issue with this test is separate linear from constant damping. Since the system will have both linear and constant damping the decay test will not have complete linear or exponential decay. The decay will be a mix of both.

5.2.6 Coulomb Damping

As shown figure 5.6 Coulumb damping is a constant mechanical damping in which absorbs energy via sliding friction on the carriage system. The friction can be associated with two aspect the static and kinetic friction.

Static friction occurs when the sliding surface and the carriage wagon have no relative motion and the coefficient can be determine by equation 5.5.

$$F_S = \mu_s N \tag{5.5}$$

Kinetic friction occurs when the sliding surface and carriage wagon has relative motion against each other. Then the friction force can be determine by equation 5.6

$$F_K = \mu_K N \tag{5.6}$$

The Coulomb damping is non-linear, and it opposes the direction of motion of the system. To document the Coulomb damping. A test by logging of time series of pullout force was performed. The pullout force should be increased until the wagon is in motion. The kinetic friction force can be determine by constant velocity for the carriage wagon and repeating this in both direction, and sufficient runs until a mean friction force is observed.

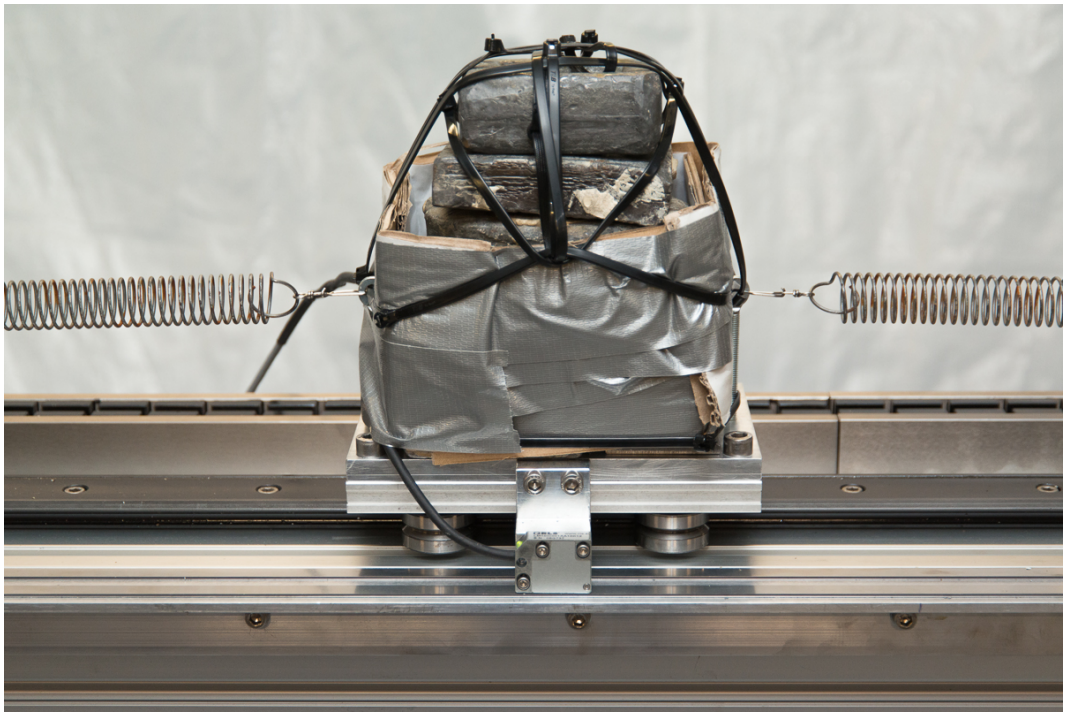

Figure 5.7: Picture of the carriage system with mass.

5.2.7 Sources of bearing damping

The roller bearing and carriage system for the test setup can be seen in figure 5.7. The roller bearings has four sources of damping. The lubrication film between the rolling bodies and contact surface on the housing. This is known as elastohydrodynamic (EHD) lubrication. This is a viscous damping contribution. Next source of damping is the bearing interface between the bearing rings, housing and shaft respectively. Damping due to squeezing lubricant in entry region where oil is entrained into the contact zone. Last damping source is the material damping due to deformation of the rolling elements and raceways often called Hertzian deformation.

5.2.8 Documentation of mooring line stiffness

By doing a pullout test with springs attached the restoring characteristics can be determine with RIFLEX connected and by turning off the environmental forcing. RIFLEX can calculate the restoring stiffness force by pullout the model in both directions. By logging the force rings for both linear springs and the force output from RIFLEX the mooring line characteristic can be determine and compared with the original mooring line characteristic from RIFLEX.

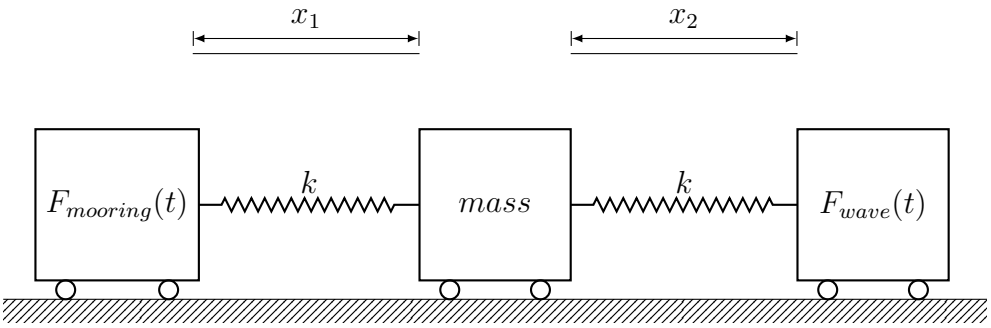

Figure 5.8: Drawing of test setup

5.2.9 Hydrodynamic loading

The hydrodynamic loads are not critical to be identically with the actual force in RIFLEX for the model. As long as the forces are logged from the excitation and the amplitude is within operational range for the model it is good enough. The excitation don't need to be identically as the loading would have occur in RIFLEX or in model test. In order to have almost identical forcing the regulator tuning for the control system needs to be adjusted to get correct loading. This can be very timing process and need more theoretical background from cybernetics. However a time series from RIFLEX is exported and used for loading to the model. The external hydrodynamic loading contains three components: Froude-Kriloff-, diffraction and drag force components.

5.2.10 Force from RIFLEX

The java program from RIFLEX write the forces on each anchor line which is read in a TwinCat variable. The decomposed horizontal component for the mooring lines tension is used. The horizontal component from two mooring lines tension is added together in the Java program and sent further to TwinCat as a programmable logic controller (PLC) value. This value is processed and scaled in TwinCat and then sent to actuator for forcing the carriage on the test setup. A java program is built in order to read axial force from RIFLEX and write it to TwinCat. TwinCat will read this value from RIFLEX and force the model based on this.

5.2.11 Tuning of model in RIFLEX

As described in 2.5.1 numerical time integration is is used for solving the differential equations numerically. There is introduced slightly numerical damping in the model. The integration and damping parameters is set to following: $\beta = 3.9$, $\gamma = 0.505$ and $\theta = 1$.

There is introduced Rayleigh damping on the model in RIFLEX. The noise in the RIFLEX signal was smoothed when the Rayleigh stiffness coefficient was used, this was mainly for the very simplified model used. The full scale model in RIFLEX used, don't have noise issues on the output signal. This coefficient is related to the higher order mode shapes. Still some irregularities is seen in the surge force from RIFLEX, but this is understood to be normal and will not cause problems in the control algorithm.

5.2.12 Filtering of force transducers

Due to high frequency oscillation with low damping in cross flow direction of the spring the sampling frequency and cut off frequency was reduced from initially 100Hz to 20Hz due to high oscillations on the signal, but mean of the signal was accurate without filtering.

5.2.13 Tuning of spring offset

At every startup, the spring offset should be tuned. In the laboratory the temperature can differ, and the material in the force transducers is temperature sensitive. Due to friction, the carriage system doesn't reach equilibrium at same position after a displacement. However, if the calculated force from the springs is checked with the force transducer each restart, the error is minimized. Due to friction this system will always have an uncertainty. Since the equilibrium position is not the same after every disturbance. The error on equilibrium position is roughly 1-2 cm based on 10 observation of decay tests. Before testing the test arrangement, all information on the position system is zeroed when the system activates. Absolute encoders would not have been zeroed during system activation.

Chapter 6

Control systems

In this chapter, the control system for RTHMT and theory behind force calculation and calculation done in PLC program, is presented. The motor control algorithm is discussed and time step optimization is performed.

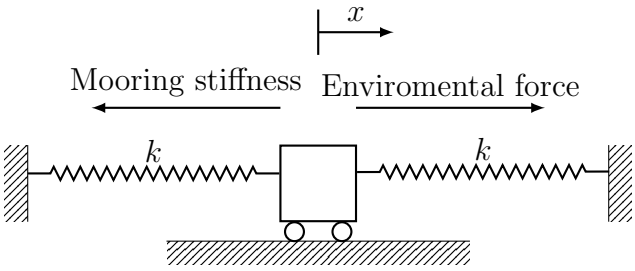

Figure 6.1: Simple drawing of test setup

In figure 5.3 a sketch of the test setup is shown with one harmonic forcing, and a replacement force for the mooring line dynamics given by RIFLEX.

TwinCat software will be used for controlling the actuator and logging of data. In TwinCat the HBM MX840 amplifier is connected and force measurement is logged. The amplifier have 8 channels. The position sensors for the carriage system is logged and used for real-time control of the actuator in TwinCat.

The actuators can be setup differently. The tasks is to actuate correct force on the wagon from RIFLEX. The test system is built as figure 5.8. This

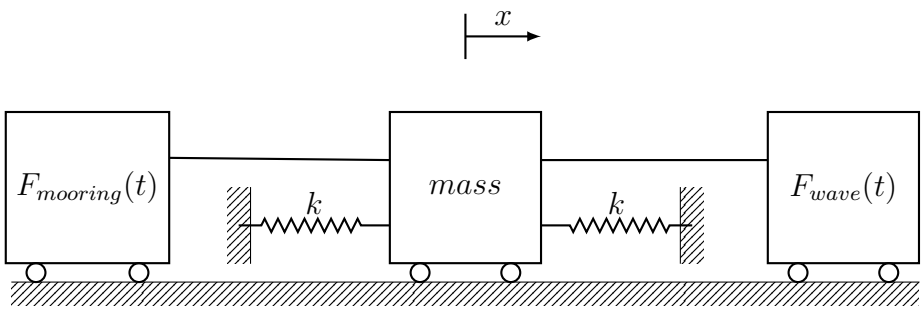

Figure 6.2: Drawing of test setup

method uses position control for actuators controlled and not force control. The system can also be forced controlled according to figure 6.2. Force controlled showed to be difficult with the software given from the supplier and supplier would not recommend this method. This is due to lack of functions in TwinCat for this use. This was not know at the time the equipment was bought. The concept is to model a mass in SDOF as seen in figure 6.1, and use drives on position control.

The challenges with this setup is to control forcing correctly. The magnet actuator have a mass and can not be fixed to the wagon in middle. This challenge is coped with the setup in figure 5.8 a picture of the actual model is shown in figure 6.3. The control algorithm to get the correct force from RIFLEX is based on measuring displacement for the actuator wagon which is connected with a spring and the wagon with the mass. Measuring distance between the actuator wagon and mass wagon is important. The middle wagon and the actuating wagon is connected with a spring. By position control, by using this spring distance measurement, correct force can be actuated according to analysis results. Both actuators will have a same the procedure. The actuators specifications regarding responsiveness and speed should be able to cope with this setup.

Test of selected springs have been performed and a spring stiffness on 60.9 N/m is used in further tests. The spring have range from 17-70 cm. In this range the stiffness is linear, and the spring will not yield or be deformed. Both springs are similar.

Input for the actuators will be the absolute distance given x_1 and x_2 in figure 5.8. This distance will determine the position change that will give the new

desired position to have the wanted forcing on the model.

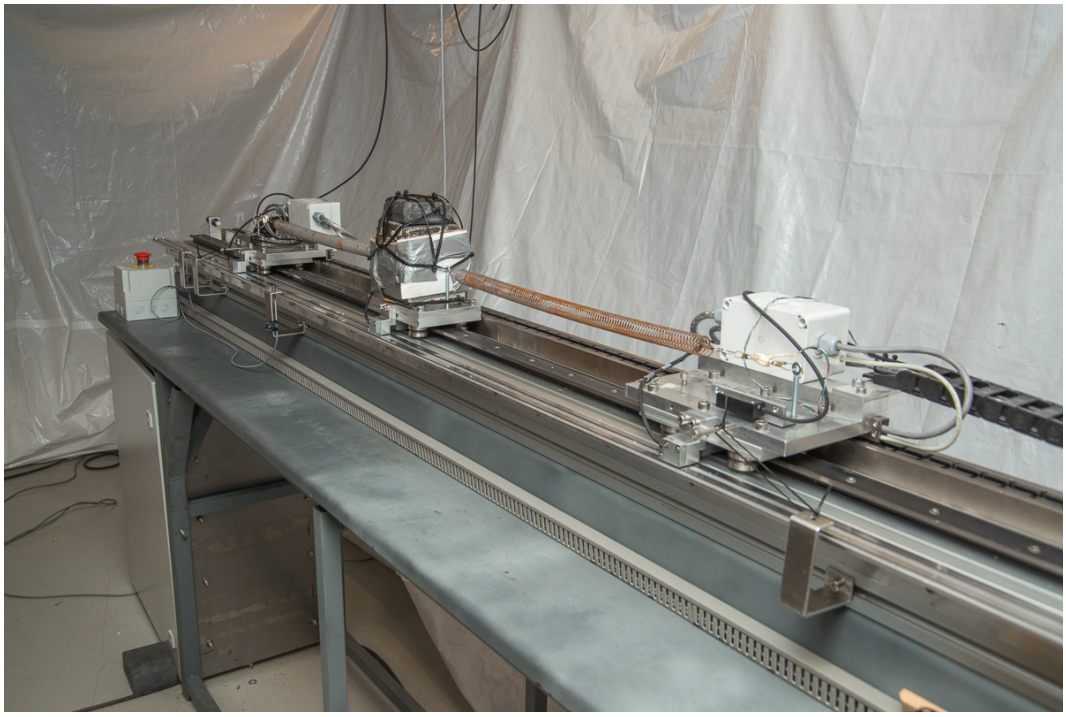

Figure 6.3: Picture of test arrangement

6.1 Programming

The program controller algorithm for the drives and instrumentation is written in structured text (ST). In TwinCat it is possible to write in CFC (Continuous function chart),FBD (Function block diagram), and ST. The TwinCat program codes is given in appendix C.

6.1.1 First test program for actuators

The first test program tested for the actuator is a defined sine curve which calculate the position for the actuator for each time step.

Function block is a built position generator position that can differ between sine-, ramp-, or sawtooth curve position signal to the actuator. A built in function for motion is used and linked to the wave generation with a boolean variable for enabling next position generation. The drive is linked to an axis. The axis uses a incremental position sensor to measure the position of the actuator. In TwinCat the FBD for motion command is linked to the drive commands position control. I next section disadvantages with this program will be discussed.

6.1.2 Motion control for actuators

The motion function with function block diagram sends a new position to the actuator at every time step, but after each move is finished the actuator position function send a verification of the move motion command to the wave generator function. The wave generator must therefor wait until the move is finished before calculating new position. For RTHMT this issue must be resolved by other function. Often it can occur that a new position for the actuator is calculated before the actuator is actually at the last position. The ideal position control function should be such that whenever a new position is calculated the old position is overwritten, and if the actuator is not at last position the new position is now the new actuator set position. There is no need for verification between. Whenever the new position is calculated the signal is sent directly without waiting for confirmation from the drive regarding last position. Initial functions used in TwinCat for motion control was not suited for RTHMT. When set position is reached by the actuator it waits for 30 ms until next set position is implemented. The position the actuator tried to follow was a harmonic sine curve with period on 5 s. Which is representable for model testing in ocean basin. Each point within the actuator path showed 30 ms delay, and the drive actual path was not smooth and oscillation to reach each new point. The error was negligible between set position and actual position. During testing the actual position of drive showed a stepwise path on a smooth set point sine curve. The functions used, calculated intermediate positions and adjust the velocity during its path. This functions is very accurate with little error in the position, but for RTHMT is more advantage to have speed than very accurate position. An small error in position for the actuator is less important than speed. RIFLEX is running on 100 Hz or even faster which will not work with position

control as mention above. Different position control functions in TwinCat was tested and same delay and not smooth path was observed. By skipping inbuilt functions and by controlling direct to drive the results was more suited for RTHMT. Initial test showed a delay on 7 ms between drive actual position and set position, and the path of the actuator was smooth. Each new set point had a smooth path and there was no sign for acceleration and deceleration for each time step with set position as behavior for inbuilt TwinCat move functions, that showed stepwise path.

6.2 PLC program for RTHMT

The RTHMT program in TwinCat is divided into 7 parts. This is done in order to have better overview of all operations in the program. The program 7 parts contains following: Drive commands for left drive, drive commands for right drive, environmental forcing, surge force, reading of surge position, wave generator and main program connection all parts. A flow chart of data communication between different parts of the PLC program is shown in figure 6.4. Each part of PLC program is described later in this section.

6.2.1 Main program

In main program the variables from Java program is read, and surge position is sent from PLC to Java. All scaling of full scale values from RIFLEX is also scaled in this program before it is processed further. RIFLEX read full scale values, so the surge displacement is converted to full scale before sent. The surge force from RIFLEX is scaled to model scale before sent to surge force program.

6.2.2 Drive commands

The drive commands program convert position to correct type and enable position control. It also contain safety parameters which is a define available range of motion. In drive commands program variables such as actual position, actual velocity and control position value is linked to drive from

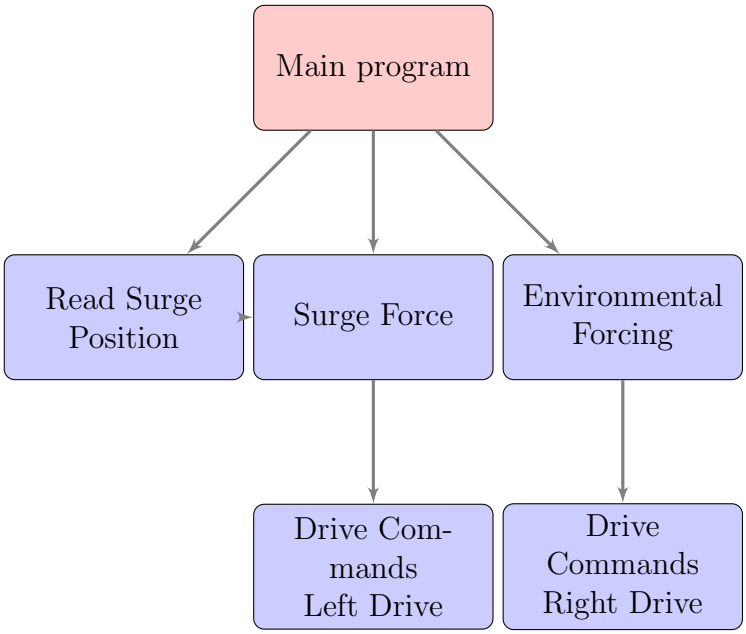

Figure 6.4: Flow chart of communication within PLC program

PLC program. For enabling position control for the drive a boolean variable have to be manually enabled in TwinCat while running in order for control bits to be sent to drive to enable position control. If the calculated motor position based on RIFLEX force is larger than defined range of motion this bits is disabled by a if function which turn off position control immediately. Initially on a RTHMT the position control is turned on. The drive is set to move to the position where it was placed during last restart which. This position is at a defined pretension position which the drive is placed before start of test. A boolean variable have to be enabled for enabling RTHMT. Then the position based on RIFLEX and spring stiffness calculate a motor position. The drive command program is the same for both drives. The only difference is the motor position calculation which is based on another program.

6.2.3 Read surge position

The "ReadSurgePos" program convert the incremental bits signal into a value in meter. Since the encoder is incremental and uses a 16 bit signal. The position signal will behave as a sawtooth function with a period on 2^{16} bit. A if function is used for converting position in a signed variable. Instead of a unsigned variable which is the actual value from the linked variable form the incremental encoder. The incremental encoder have a resolution on 10 00 bits per mm. Position of the carriage is converted to meter and further read in the surge force program. Read surge position program has another useful functionality. The surge position can be set in the program by enabling a another variable that is programmable. This functionality was useful during pullout test for defining restoring force characteristics in RIFLEX for the model. The surge position was then possible to increase slowly for each time step without moving the physical model.

6.2.4 Surge Force

The surge force reads the surge position and the actual drive position from both drives and calculate the elongation of the springs. Both drive position signal is also converted into meter from it bits signal form its incremental signal. This encoder behaves the same as the middle carriage encoder in read surge program. The surge force from main program is linked into this program and calculate the difference between spring force from linear springs and RIFLEX surge force. The force from the force rings is also used in this program based on the linked variable from HBM amplifier on the EtherCat bus. The force from rings is only used for calibration of elongation of spring.

6.2.5 Environmental forcing

The environmental forcing program calculate input for motor position on the environmental drive. This calculation can be a simple sine curve, or read a predefined time series. The environmental forcing has no communication with other programs than drive command program. A boolean variable have to enabled in order for start "hydrodynamic loading" on the system, else

the value of the motor position is 0. In main program there environmental forcing is enabled for running each cycle.

6.2.6 Time step

TwinCat is run with variable time step initially. However the PLC program need to have small time step due to drive control consideration. Therefore all time steps is not set equal to the same value in all programs. It is even possible to set the time step as low as 50 μs in TwinCat, but however noise, instability and varying time step occurred from TwinCat due to limitation on hardware was reached, therefore slower time step was preferred and set to 1 ms for each cycle in TwinCat. When RIFLEX and Java program had same time step equal to 100 Hz, every 10th value for surge position a new value was updated for the surge force. The time step was observed to be constant from RIFLEX and Java program in TwinCat.

In RIFLEX it is possible to scale the time to model scale. This was done by acceleration the time according to Froude law by 5.5 times faster with model scale on λ=30. Now the time step in RIFLEX was shorter, but however limitation on the java program was reached. Java program or communication between RIFLEX and Java program was limiting the calculated surge force. Therefore the time step in java program was increased to 0.008, and now the results was now more stable, and only few values in TwinCat was equal to the last value. Last value equal the previous value for surge force occur if a new value is not yet calculated or sent to TwinCat. If not a new value is available, TwinCat set the previous value equal to this time step value. The difference between HLA time step used in Java program and Riflex is due to the scaling of time step done in SIMA, therefore the time step could be decreased slightly in Java program to match the Riflex time step, according λ=30.

The signal which is unprocessed is shown in figure 6.5. As seen in figure the noise is very high frequent and need a low pass filtering. The high frequencies that is shown need to be filtered out and a low-frequency processed signal showing the sum surge force is need for efficient control for the drive. This pullout restoring characteristics is based on a very simplified RIFLEX model as mention in 4.3. The restoring characteristics used later in RTHMT is more smooth and didn't need filtering.

Table 6.1: Main dimensions Åsgard B.

TwinCat Time step [s]	RIFLEX Time step [s]	Frequency
0.001	0.001	100 Hz
0.001	0.008	125 Hz
0.001	0.015	66.67 Hz
0.001	0.02	50 Hz
0.001	0.03	30 Hz

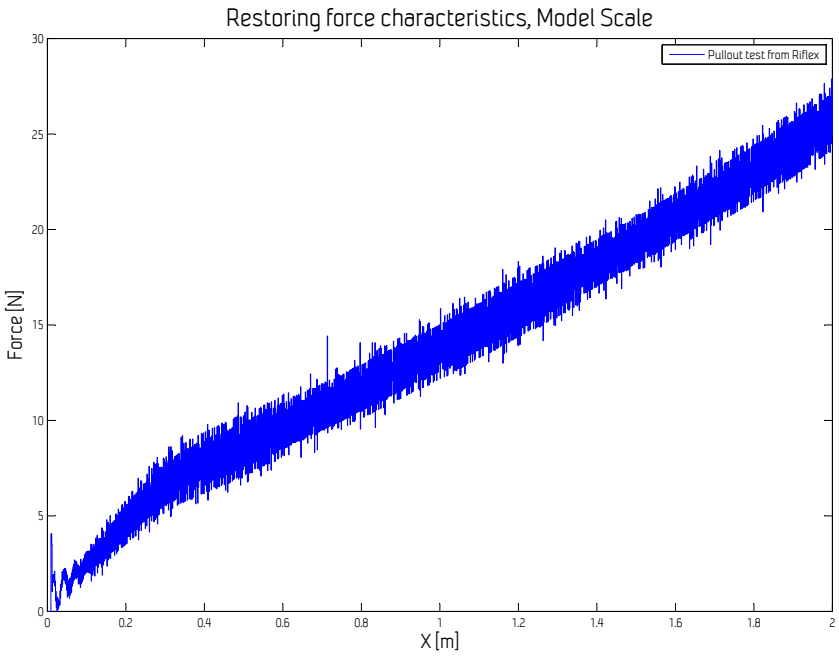

Figure 6.5: Pullout test with no filtering

6.2.7 Filtering

The force rings used have an analog Bessel filter with a sampling frequency on 100 Hz and cut of frequency on 20 Hz. This could however be studied more, but for calibration with the spring stiffness and spring offset filtering

it was suited. The filtering was performed from the amplifier, but however it is also possible to filter the signal in TwinCat. In TwinCat a digital filter can be used if the the coefficients in the transfer function is calculated, and can easily be implemented. For the rest of the signals there is no filtering because it was no significant noise.

6.2.8 Coordinate system

In RIFLEX and on test setup same coordinate system is used, but the test setup displacements is scaled. If the actuator move to left seen from front of test setup this is in positive direction. Same directions is used in RIFLEX. This notation is used in the thesis when commenting left or right drive.

6.3 Beckhoff test model

From Beckhoff a simplified model with two rotating actuator and same servo drive as used in the main test setup was borrowed. The rotating actuators was isolated from each other and had full freedom of movement in rotation. The rotating actuator was quite useful during testing, and was failsafe compared to linear main setup. Since the actuators had only rotational DOF and not linear DOF as the RTHMT setup. An error in the code or other fault during testing didn't cause any problems on the Beckhoff model. The main test setup model, will if any error in code or other factors cause large amplitude and can destroy equipment if it moved fast with large force. There is a mechanical and an software safety mechanism, but it was still valuable to Hardware in the loop (HIL) testing and on a setup with a peak force less than 1400 N. Issue regarding initialization of RIFLEX with drive occurred. For first time step in RIFLEX the drive have to sudden move a point different to standstill position. This may cause large displacement and large gain. This issue can be resolved by having a ramp function until drive has reached actual position. The Beckhoff actuator had a phase difference on its actuators when harmonic motion with period of 2 seconds and displacement on 10 cm in rotational direction of the discs. The phase difference on this actuators was to large for use of RTHMT. The Beckhoff model was very valuable for

studying tuning of the controller for the drive which was applied later on the tuning of the controller for linear drives.

6.4 Safety mechanism

Three main mechanism:

- Mechanical end stopper
- Magnetic end stopper switch
- Software limitation on displacement
- Emergency switch

The mechanical end stopper is a fixed stopper at the end of linear carriage system. The stopper is fitted with a piston for retardation over 3 cm. The magnetic stopper is connected to the servo drive and react on metal passing the stopper. The actuator wagon is fitted with a steel metal plate for use with the magnetic switch. If the magnet stopper senses metal the commando is sent directly to the servo drive to turn torque off. Each actuator is given range of displacement and if this range is breached the magnetic stopper will turn off torque. In software slightly shorter range of displacement is also defined. At the end of the control system code there is a if condition that will override results from RIFLEX and if any error in the code. The last safety mechanism is a emergency switch for use by the operator. This safety mechanism will turn off both servo drives and is doubled redundancy. The switch is connected to a separate safety card slot in the actuator. There is a safety switch at each end of the carriage system.

6.5 Control algorithm and actuator dynamics

For optimal control of the actuator it is needed to have a suitable control algorithm to achieve the synchronization of the stiffness from the numerical software and the stiffness from the test. As the decomposed mooring system (Cao & Tahchiev, 2013) mention a proportional integral derivative (PID) controller is the most widely used in feedback control design.

In the hybrid setup method as mention in chapter 5. The PID-controller will calculate an “error” between the force value which is given from the numerical software and the measured value. The controller attempts to minimize the error by adjusting the process control inputs. The PID-controller

is often considered very useful in the absence of knowledge of the underlying process. By tuning the three parameters in the PID-controller algorithm the control can provide the desired requirements. In the response of the actuator three response effects should be examine before tuning the PID-controller. Response can be describe in terms of responsiveness of the controller to an error, overshoot of the desired set point, and the oscillation around the set point. The block diagram of a PID-controller is in figure 6.6. In a PID-controller the system must also check for stability which is not guaranteed.

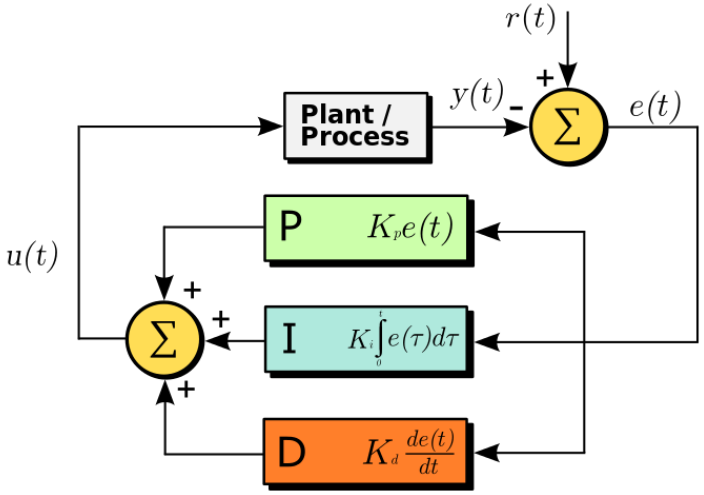

Figure 6.6: Block diagram of a PID-controller with a feedback loop(Balchen *et al.*, 2003)

The desired output which is the force can be defined by following PID-algorithm:

$$u(t) = K_P e(t) + K_i \int_0^t e(\tau)d\tau + K_d \frac{d}{dt} e(t) \tag{6.1}$$

In equation 6.1 the term $K_P e(t)$ is the proportional gain parameter. The larger gain will lead to faster response, but to high gain can make the system unstable. In AHTM time-delays is very important, and time-delays is one of the success criteria for a working real-time hybrid system. The term

$K_i \int_0^t e(\tau)d\tau$ is the integral term. This therm is proportional both to the magnitude of the error and to the duration of the error. The last term remaining is the derivative term $K_d \frac{d}{dt} e(t)$. The derivative is calculated by determining the slope of the error over time and multiplying this by the derivative gain K_d. Derivative term will predict the behavior and can thus improve settling time and stability of the system. In tuning of the derivative term, care must be taken due to the inherent sensitivity to measurements noise from sensors. Increasing the K_d will decrease overshoot, and slow down transient response.

Early testing had problems with high frequency oscillation of the actuators while doing commutation tuning with drive and position encoder. The oscillation had very high frequency and results in error in TwinCat or large amplitude for drift off. Tuning was required for the K_P parameter. The gain was to large and the system had become very unstable. The K_P parameter was reduced down to half which was 199.9 A/(m/s) in the velocity control unit for the drive. During testing of the inbuilt TwinCat function for motion the K_V parameter was tuned and increased for hopefully get faster velocity and less lag on the trajectory calculated position. This value was set to 4 from original value of 1. This had very little effect and results was mostly 'screaming" noise from actuator due to large responsiveness. This parameter was tuned in the position control unit. This test was also tested with the set point generator codes but it result in almost no change so original values was kept.

A simple test of a step response was performed and by logging actual drive position and set position the parameters that need tuning was obvious. The drive had no overshoot and was very damped. Tuning of the controller is performed with little or no basis on the TwinCat parameters. TwinCat uses three controller units which controls the drive. The position-, velocity-, and current controller unit is in this order put in series. Each unit has it own parameters for tuning. In the position controller the K_V parameter was set as high as possible. For more advanced tuning this parameter can be set to two constants one for moving and one for holding the position. A low value can be useful while moving, but for velocity near zero the value could be high. In the velocity controller unit the K_P factor was reduced so natural harmonics of the system was avoided which occurs when this value was high. This value introduced damping. For RTHMT little rise time and damping is important, but however damping will introduce delay.

Chapter 7

RTHMT applications

RTHMT testing can be divided into top parts one physical part and one numerical simulation part. Both parts are in real-time. The numerical simulation part can implement a wide range of applications. Some of them are mention below. Main core area is testing floaters with mooring and riser systems in ultra deep water, where ocean basin limits are exceed. The use of actuators in all 6-DOF a model of other applications can also introduce a forcing in real-time. The idea of still using springs with linear stiffness and correct natural period in each motion will reduce the need for external interference. By introducing other applications and increasing external forcing from actuators the accuracy may decrease. The decrease may be due to inaccuracy and time delays for the increased external forcing. A complete replacement of mooring system by actuators will be unlikely.

In report by MARINTEK (Sauder, 2014) many potential applications have been mentioned such as:

- Drilling operations with simulation of dynamic loading of drilling equipment on floater.
- Offshore wave energy with real-time control of latching mechanism.
- Offshore floating wind turbine testing.
- Aquaculture model test performed at larger scale. Truncations of mooring required today require lower depth.

- Short-sea or deep-sea shipping with implementation of sloshing or ore liquefaction on the vessel.
- Machinery studies with simulation of hydrodynamic loads on propeller/shaft.

7.1 Arctic operations

Drilling operation in the arctic will be effected by ice loads which is not possible to model without using actuators in todays ocean basin at NTNU. As long as these loads can be predicted they can be implemented. By implementing hydrodynamic loads with ice loads on the environmental actuator arctic operation can be analyzed. In a RTHMT in ocean basin it is mainly actuators for implementing correct mooring line dynamics. To introduce ice loads new actuators needs to be installed or implementation as mention above on the environmental actuator. Implementing ice loads on the mooring line dynamic actuators will not be accurate, and is best suited to installed or implemented in environmental loading actuators.

7.2 Viscoelasticity

As mention in section 2.3.2 the synthetic fiber material have a viscoelasticity behavior. This behavior can be implemented in a theoretical mooring line characteristics. It is also possible to change the behavior on the fly while doing testing if the overall stiffness is within same force range. Care must be taken into account when using Froude scaling and deformation rate is changing with time due to viscoelasticity. This effect cab be taken into account in Riflex.

7.3 Seafloor friction of moorings

The mooring lines for a catenary setup should only impose a horizontal load on an anchor. There exist other types as well for taut mooring system but they are not drag depended. The lower segment of a mooring line usually

have large weight in water pr unit length compared to the other segments of the mooring lines. At touch down point for the mooring and to the anchor, the mooring interact with the seafloor. Due to varying response the mooring, the touch down point varies in time. For the segment laying on the seafloor it will impose seafloor friction on this mooring line segment. If the floater is exposed to varying directional load on mooring it can also be exposed to varying directional friction loads, which will introduce larger seafloor friction. This effect is most significant for large responses and extreme loads, and is recommended to account for in a coupled analysis in recommended practice in DNV (DNV, 2010b). In RTHMT it is possible to account for this effect at real-time and not in the numerical calculation after the model test. This can be accounted for in RIFLEX or with use of a simplified method. In the proposed setup in chapter 5 this effect can be accounted.

7.4 Riser

Use of risers in model test have not been frequently used, but would be easily implemented in an RTHMT. Riser can be taken into account in the numerical calculations after model test with PHMT. The riser will only be modeled in the numerical software, or a stiffness characteristics and damping can be calculated and implemented in the controller. In the time domain software many risers can be easily implemented, and the dynamics related will be added to the mooring line dynamic force resultants. Then effects regarding riser and hull effects will be accounted for in numerical software only. It is also possible to visualize the riser in RTHMT. For riser the flow around riser is important and Reynolds number is important to capture similar effects in full scale and model scale. In RIFLEX the riser will be modeled in full scale, and most effects will be taken into account within the software limits.

7.5 Line breakage

RTHMT has the ability to simulate line breakage. By changing the spring and the parameters in the numerical code a line breakage can be easily model in RTHMT. For checking a line breakage with todays setup in ocean basin

divers need to unhook mooring lines and this is time consuming.The linear springs used in the horizontal plane can be scaled little down. So that the linear springs does not need be replaced, with softer spring in order to simulate a line breakage. The actuator will then until line breakage represent the mooring line stiffness until breakage. For many platforms which have many mooring lines it may be also possible to just change parameters in the numerical real times software to implement a line breakage. For the proposed system line breakage have to be simulated differently. Since this setup has only two mooring lines. A line breakage can be simulated with loss of capacity in one of the mooring with proposed setup. The hole line can not break. After the storm in January 2011 a few floater in the Northsea had line breakage. This was also the main subject at the yearly Tekna DP and Mooring of offshore installations conference. This subject is very relevant on the basis of the latests incidents. Those line breakage incidents happened at a storm which was only a storm with 2 years return period. After this incidents effort is made in the industry of how to understand this incidents.

Chapter 8

Results

The RTHMT, test setup that was built performed complete tests with all equipment and functionality. However the friction was not as low as it was supposed to be. The system was highly damped as later discussed. Due to the difference in damping, the RTHMT response was not compared with only RIFLEX simulation. This can be done in further development if the there is less significant damping contribution on the test setup, or a damping model is implemented in the RTHMT program for compensation. During design and with contact with supplier the carriage system was believed to have less friction such that the damping in RIFLEX model was governing, and damping from carriage system was small. Still with damping, correct tension forces is calculated from RIFLEX. Validation from the responses in RTHMT test setup could have been compared with a PHMT model test, and a pure RIFLEX time domain analysis. RIFLEX could have used the described displacements from model test as input for the analysis, and the environmental loads can be calculated from the RIFLEX model and used for environmental loading on the RTHMT test setup. With this comparative study the result can not be compared directly. Since RIFLEX model need to be through tuned for the model test.

8.0.1 Time delay on drive

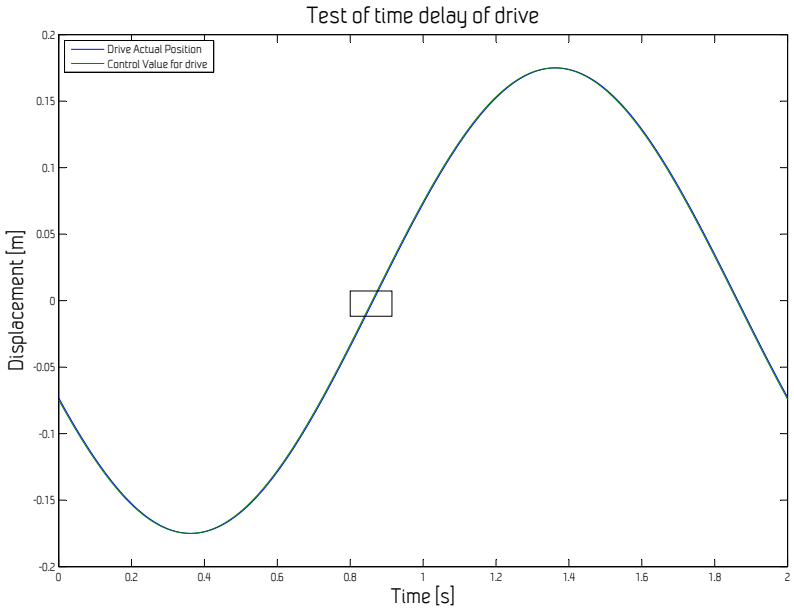

Figure 8.1: Test of time delay for drive

A simple sine generator was used for input signal to drive. In figure 8.1 the actual drive position and the set point for the drive is shown. The test was performed with a sine curve with a period on 2 sec. From figure 8.2, the time delay is around 3 ms, between actual position and set point of drive, and it is constant along the path of sine curve. The sine curve has a period of 2 sec, which is low and on the limit for the tuning of controller of the drive. Nevertheless, the drive could handle faster harmonic oscillation with assumed same performance or even better with a proper tuned controller. The drive uses 3 ms before a desired set position is reached for each time step while ongoing a harmonic path for the drive.

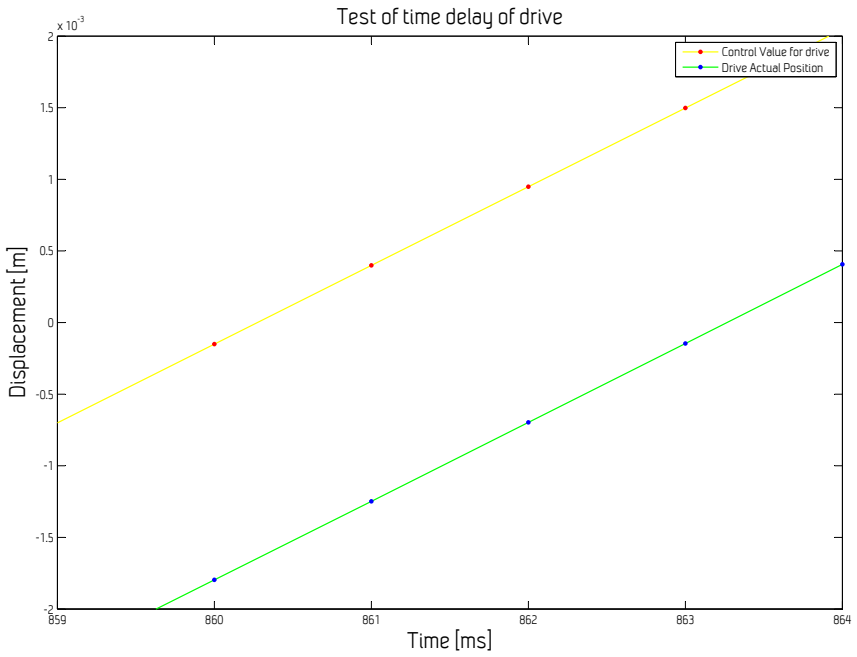

Figure 8.2: Test of time delay for drive

A magnified view of figure 8.1 is seen in figure 8.2. This is for continuous motion with no significant change in velocity or direction. A ramp step function with different directions and large amplitudes have larger delay. If the amplitude was set to 10 cm the time delay would be quite different. A simple test with a ramp step with 600 000 bit displacement which is 6 cm showed a delay on 31 ms before 90 % of the set value was reached. For this test, the motor had a constant position and no velocity or change, other than a few bit oscillation around the set point before initiation of the ramp step.

8.0.2 Mooring line stiffness

The mooring line characteristic was determine from a pullout test. The result is shown in figure 8.3. This test was performed by EMT with RIFLEX and TwinCat and no motion of the physical model. The surge position was

programmed with large time steps and results was logged in TwinCat. The restoring characteristics is shown in figure 8.3. From the figure both the elastic and geometrical stiffness can be seen, but however this is restoring characteristic, and not single mooring line dynamic. Restoring characteristic is based on two mooring line contributing by each stiffness contribution. For small displacement the geometric stiffness is governing. For large displacement the elastic stiffness is governing and is linear when the mooring line is more or less straight. Similarities of this can be seen in figure 8.3.

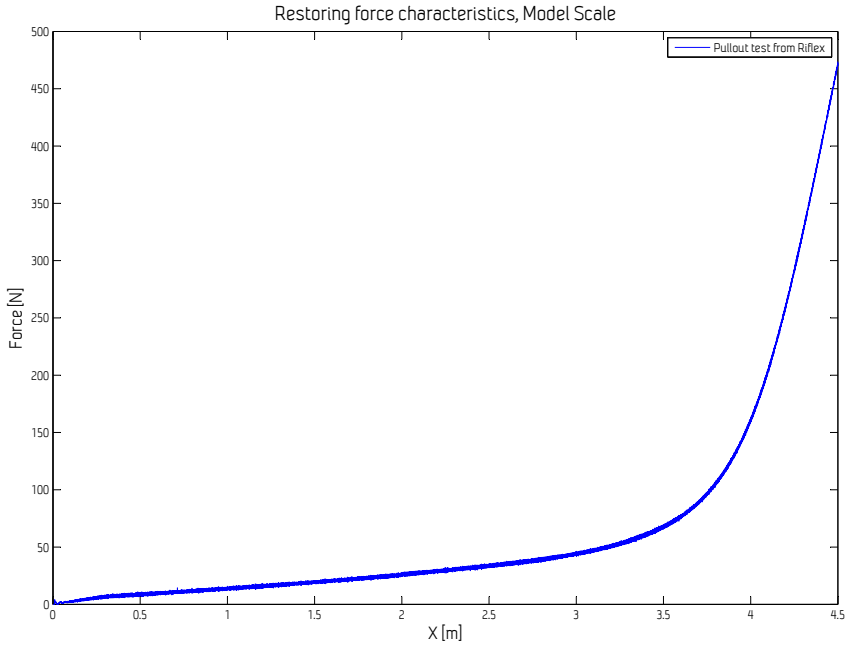

Figure 8.3: Mooring line characteristic after pullout test

8.1 Damping in carriage system

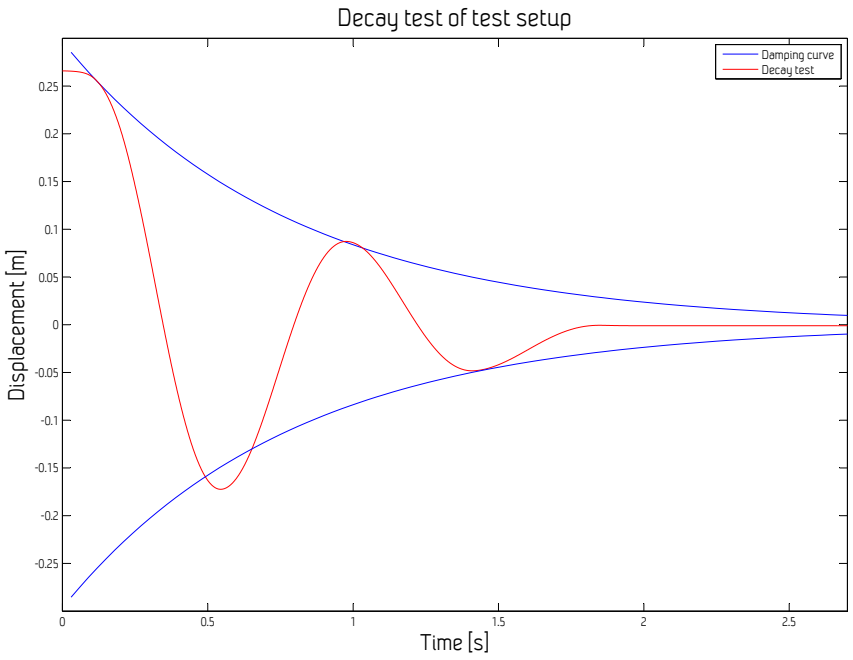

Figure 8.4: Decay test of carriage system

A decay test was performed in order to document the friction, and to comment the deviation from model test in water. Damping of the test setup is presented in figure 8.4, while a model test with damping from water is presented in figure 8.5. The carriage with attached linear springs was pulled out to 0.25 m from its equilibrium position and released. After first oscillation the amplitude reduced significant, and after only three periods it is back to equilibrium position. The decay test is not far from being critical damped, with so few oscillations. The comparison with a similar model test of a spar-platform show that damping level is quite significant different. As seen from the decay test results from RTHMT test will be influenced by the large damping difference, and this is also the reason why environmental loading of the drive was not so successful. A prescribed time series of hydrodynamic

loading from SIMA, did not lead to same displacement of the model. The model did not also behave as supposed due to the forcing. The motion was damped out and response frequencies was quite different. The loading was scaled down to low responses, due to low mass of the system. Small loading amplitudes didn't give any response of mass. The irregular loading was programmed according to spring stiffness for forcing. The carriage system was then moved by hand given different WF forcing. When the mass was moved by hand the calculated force from force rings and calculations based on force from spring force showed agreement with only small differences. Most time series in this report is based on WF loading by hand. Therefor the focus was rather on the time delays, and documenting the suitability from the data communication and system itself, instead of validation of the responses.

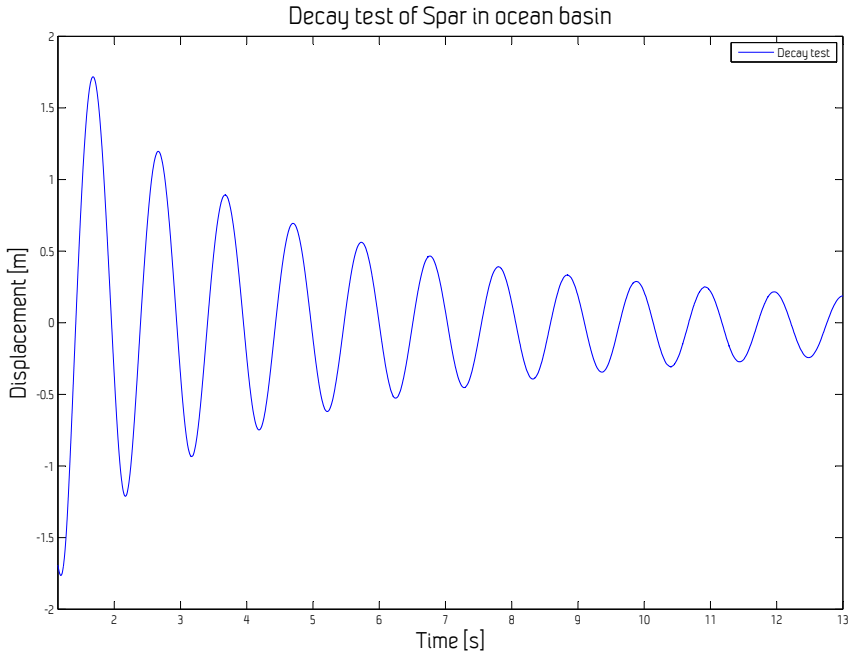

Figure 8.5: Decay test of floater in water in model scale

For the RTHMT test setup oscillation over two periods before equilibrium is reached at rest, but for the model test many oscillations occur before rest.

The ratio between relative damping and amplitude is much lower for model test, than RTHMT test. Both actuators used in RTHMT used position control, and will not be influenced by any friction when they are moving. However, the control algorithms use the elongation of the springs as input for each time step. The coulomb friction on the carriage system will introduce a delay. This can be seen on the decay test. During all decay test of the RTHMT setup equilibrium position differed around 1-2 cm. In full scale this difference is quite large. The Froude scale used for displacement is $\lambda = 30$.

8.1.1 Time delay between TwinCat and Drive

The controller was tuned to a stable setup, with rather more damping than overshoot and instability. The rise time is important, but the increased rise time introduced less damping. The velocity gain parameter introduced damping for the drive and this parameter was set such that noise and high frequent oscillation around set point disappear. This was the issue when the rise time was low. Rise time is defined as the time until the value of 90% of the set point is reached. The delay for the drive was 50 ms with the tuning parameters used in RTHMT tests. When a large step response was performed from rest. Based on drive specification this can be reduced, but due to lack of support from supplier on controller functionality and documentation on software, this was not further studied.

As mention in RTHMT for earthquake application the delays from communication and controller are usually small (Carrion & Billie F. Spencer, 2007). This can be seen by a 3 ms delay on a sinus curve between set point and actual position of drive. A delay on 50 ms on a large displacement (6 cm)for a step response seen as a fast response. For this system as well the delay by communication and controller is small. However, the step response did not use HLA or java program for communication and the step response was defined in TwinCat only. For RTHMT the response will not have to force the model with so large magnitude on so short time. The time delay was also seen for a sine curve path to be constant, but however during RTHMT it was seen as varying. The variation was small and close to constant, but this is believed to be the a results of very short time step in the analysis and in java code. Sometimes during RTHMT, if another program is run in background the signal between TwinCat and RIFLEX could sometimes show noise.

8.1.2 Transient response

An issue that arises during, RTHMT testing was the response on the floater model on the carriage system. The springs are stiff, and the drive will have force control based on the spring elongation. A small change in the stiff springs had an immediate influence on the carriage position. The lack of large mass and inertia on the carriage introduced rapid displacement on the carriage which cause on the other hand large forces in RIFLEX. This transient behavior cause instability in the test and maximum displacement of the drive was reached, and then the drive was turned off, due to emergency procedures defining maximum range of motion. Rapid displacement of the vessel in RIFLEX cause large force peaks, and this was immediate sent to the drive. The drive had then to elongate the spring for a large distance, which cause again rapid displacement of the floater. This instability occurred when the displacement of the carriage system was rapid. When the instability was reached the system maximum displacement was reached within seconds for the drive and test was stopped. This issue can be solved by introducing larger mass on the carriage, due to spring stiffness this mass have to be large in order to have enough inertia. According to Froude law the mass should be 3247 kg when using same scaling for displacement and force which is used. The maximum mass the carriage system can carry is around 70kg, but as it is built now there is not ability to place mass in that magnitude on the carriage. The mass is increased to a maximum of what the system as it is can carry, without problems.

The mass was increased to 15 kg for the vessel in the actual test setup. The actual mass should be 3247 kg table 5.1. The inertia on the system was now increased so it was possible to perform a RTHMT without transient and instability due to rapid responsiveness on the carriage mass position when the restoring force for a small displacement was received from RIFLEX. However the decay curve for a 15 kg mass on the carriage was the same. Initially the increase of mass was assumed to not be proportional with the friction force. The friction coefficients is given in table 8.1.

Table 8.1: Friction on carriage with mass of 15 kg

	Force [N]	Coefficient [-]
Static	2.81	0.19
Kinetic	3.40	0.023

8.2 Friction

Based on the friction of the system a damping model can be implemented in RTHMT. This model can take into account the friction on the environmental loading and restoring forces. The two test performed to document the friction given in this section is however very basic and more test is needed for design of a damping model. Most important the damping distribution must be separated. This can be difficult, but for this setup the dry friction is governing. Friction can also be seen on the time series when comparing force measured in force rings and displacement measured.

8.2.1 Static friction

The static friction was determine by pulling the carriage system with 15 kg mass until a displacement occurred. The static friction coefficient is shown in table 8.1.

8.2.2 Kinetic friction

The kinetic friction was determine by pulling the carriage wagon with constant speed. The carriage wagon was pulled by hand. The wagon was pulled by a force ring attached to the wagon. In figure 8.6 the displacement and force is shown. The force ring as seen is very sensitive and the velocity was difficult to keep at constant speed. An average is performed in order to determine the constant force needed. The constant force is 3.4 N with the 15 kg mass. The velocity was approximately 0.15 m/s during towing. The kinetic friction coefficient is determine to be 0.023. From the figure 8.6 there is some noise regarding force fluctuation, but the fluctuation is constant if it

is averaged. This related to the constant damping called Coulomb damping in section 5.2.4.

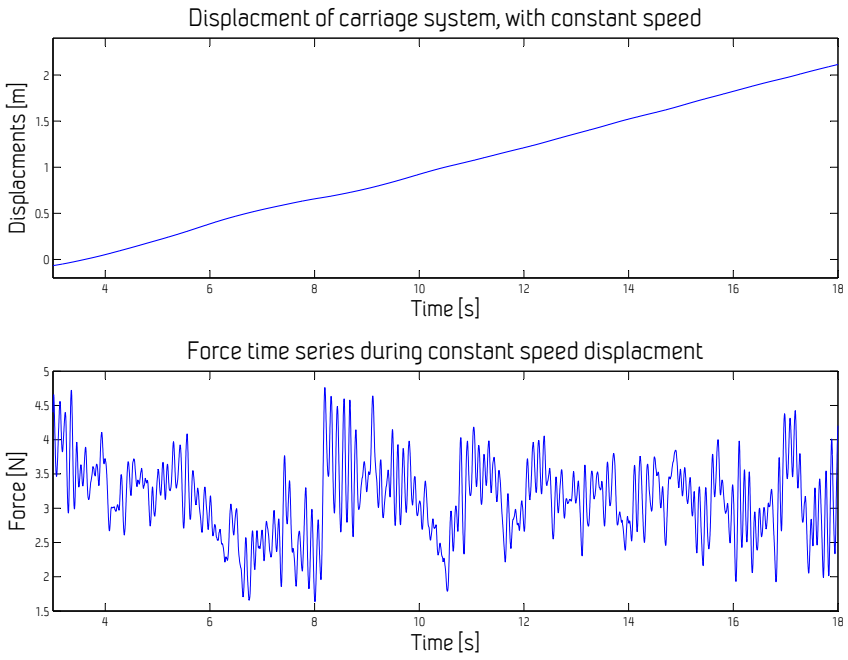

Figure 8.6: Kinetic friction

8.2.3 Time series from RTHMT test

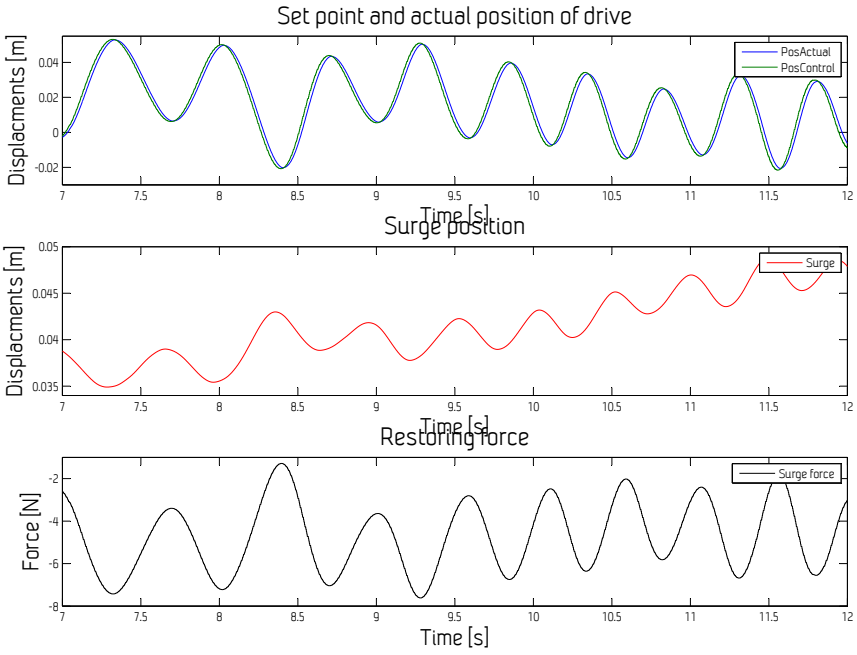

Figure 8.7: Subplot time series during RTHMT

During RTHMT many parameters was logged in TwinCat. For the logging TwinCat uses the same frequency as the cycle frequency for PLC program. During all test this was 1 ms. In figure 8.7 drive command position, actual drive position, surge position of carriage wagon and surge restoring force is shown. This results was performed with a short test with small displacements. The time delay for the drive is easy to seen and is around 30 ms and is constant as seen in graph. When the set position is sent to drive it takes 30 ms before the drive is at the actual position. This test can document that time delay on drive is constant around 30 ms.

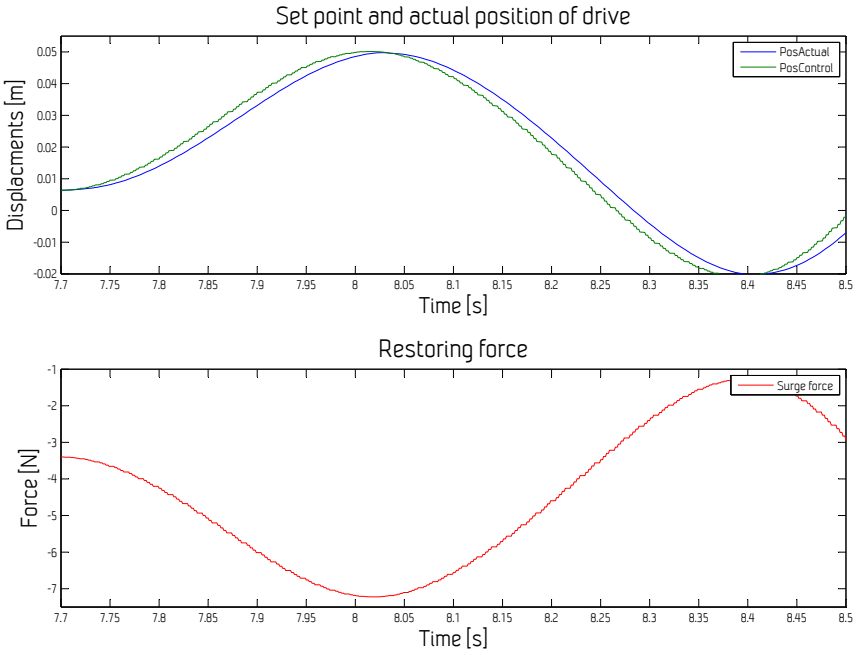

Figure 8.8: Time series during RTHMT

If more narrow view of the time series is studied time delay can be even further examine. In figure 8.8 narrow view of the time series is shown. It is seen that the surge force curve is not smooth and have a stepwise path. This is due to the RIFLEX or communication between RIFLEX until it is read in TwinCat. However earlier RTHMT didn't see this behavior when using similar communication (Garlid, 2010). So it is assumed to be RIFLEX which cause this behavior, since the setup used in this thesis uses faster communication setup than given in (Garlid, 2010). The stepwise path of the surge force curve have a locally harmonic path. The steps of the path is repeating it self. Then the time delay is also stepwise constant for this communication and program part. According to conclusion of earthquake test the time delay for communication and controller are generally small for RTHMT (Carrion & Billie F. Spencer, 2007). In the test performed it is rather opposite. Since test without use of RIFLEX and data communication showed that the time delay was around 3 ms for a sine path signal sent to

the drive. In the test performed the set position of the drive is following an irregular path, with more rapid accelerations than the sine path. The difference between regular and irregular path should lead to a larger time delay for the drive, but not as large as seen in figure 8.7. The periodicity of the surge force signal is unknown. The surge position sent to RIFLEX have been checked and is smooth, but however this signal was written to a file in the java program, and if delays occur during HLA communication this is unknown. The same periodicity of the surge restoring force and set point for drive is seen, this may reject the hypothesis that time delay is due to java program or HLA communication since the surge position signal follow a smooth path in TwinCat. This signal is sent to the java program, but output from java program based on RIFLEX calculation is a stepwise surge force, that has same periodicity with the set point for the drive. The periodicity may lead to a conclusion that RIFLEX is causing the delay. The delay is on average 4 equal values after each other until a new value is received. Varying between 3 ms and 6 ms delay with average 4 ms delay. The time delay given in (Garlid, 2010) was also around 4-5 time steps, but however the time steps used in this thesis is smaller than the compared results.

8.3 Stiffness forces of the model

As seen in figure 8.9 a time series linear spring force, RIFLEX surge force, and actuator forcing is given. The actuator forcing is based on the difference between the RIFLEX surge force and the actuator forcing. Based on 8.3 it can bee seen that the linear spring force is larger the restoring characteristics. Therefor the actuator have to introduce softer spring system on the model. Then the actuator needs to decrease the spring elongation until correct sum forces from both springs is achieved.

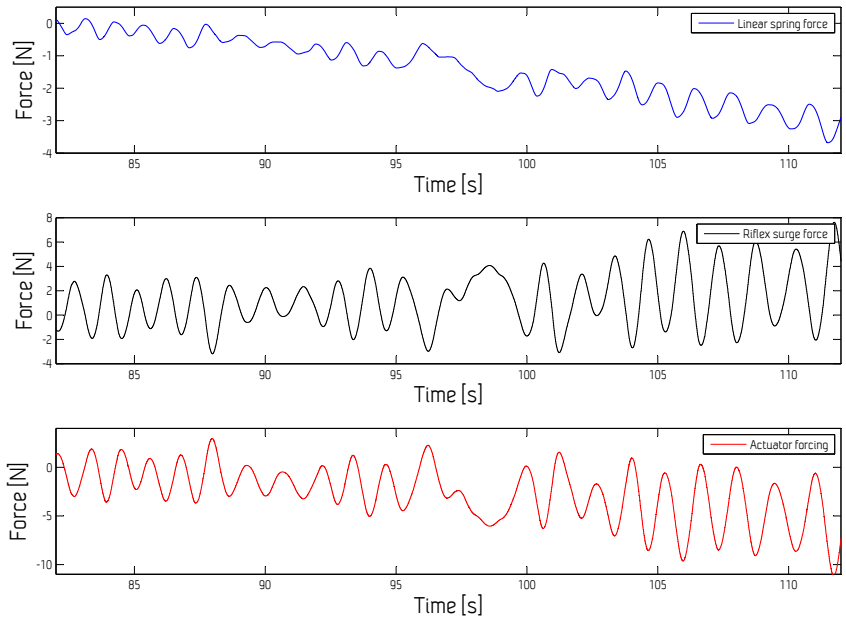

Figure 8.9: Forcing parameters for model

Chapter 9

Concluding remarks

A new framework for simulating deep-water moored platform have been tested for SDOF motion. However, limitation with the test setup comparing realistic responses of a floating offshore structure was not achieved. This was due to damping issues and simplified scaling. The system setup communication with non-linear finite element model for slender structures and automation control was successful. The issues raised was mainly due to the simplification made on the design of the setup, and will be taken care of if a test with a model in water is performed. If the test setup proposed is used on a model in water, that is scaled by using Froude law, many issues regarding inertia could be solved. Also if the linear springs used fits with the natural period, similarities in dynamics would be achieved. Based on the time delays and responsiveness the system, reliable responses of a floater should be achieved, if Froude scaling is used and a model is placed in water.

The proposed architecture and methodology of RTHMT is an alternative to the PHTM and ultra scale model testing. This method simplifies the forcing magnitude when it has linear springs attached, and not rely only on the forcing to represent mooring lines, compared to ATLAS system and the decomposed system. Complexity is reduced when the number of actuators is reduced, and when forcing the model directly, instead of forcing the truncated mooring line at the end in multiple directions. The RTHMT test procedure will give more accurate drag forces on the mooring lines, and the induced damping in the horizontal motion than PHTM experiments. Possibility to change parameters on the fly for mooring and riser while doing model test,

which is not possible with PHTM. The RTHMT method have the ability to implement important effects such as LF resonant motions and other effects which will increase when expanding into deep water. RTHMT can be an important and suitable test method when limitations in laboratories are met regarding water depth. Earthquake engineering RTHMT is verified and recognized as a reliable testing method. RTHMT can simulate line breakage and seafloor friction and this can be changed during test in real-time.

With proper tuning of the controller of drive, it should also be possible to achieve better performance and responsiveness of the drives. The setup presented is suited for a SDOF motion, and same procedure can be used for sway as for surge.

The time delay results shows that RIFLEX is introducing time delays in the system, and also the drives, but this contribution is constant and is not significant in comparison with RIFLEX delay. The RIFLEX delay is small and during RTHMT the system is assumed to present accurate and realistic responses.

Chapter 10

Future research

The work presented in this project is in the early phase of developing RTHMT for deep-water moored structures. During the work, several interesting and important aspect have arised and needs further study before the RTHMT can be used in industry model tests at MARINTEK. Following subject should be considered for further development of RTHMT:

- Perform testing with the test setup with a model in water.
- Use force control instead of position control on the drives.
- Try two degree of freedom by duplicating drive setup and place a model in water.
- Use QTM position sensor for the model instead of incremental encoder.
- Verify mooring tension of model in water with only RIFLEX analysis with prescribed displacement.
- Testing of actuator dynamics
- Sensitivity studies on influence of DOF need for RTHMT.
- Verification and divergence check
- Study on comparison with numerical time integration used in RIFLEX with LSTR solvers.

Next step in developing RTHMT the test equipment and actuators should be connected to a ultra scale model in water. Then the damping issue with large coulomb friction is taken care of, also the mass could be increased be Froude scaled. The actuator setup on the rig could be the same for a ultra scale model test in water. By flipping the hole setup upside down and place a model in water the test setup can be easily modified. If the model is not used with wave machine, the environmental actuator will still be useful. If the model have a wave machine, one spring end needs to be fixed. The actuator need an arm for connecting the spring, and give space for the model to be underneath the floating model. The mass of the model can also be significant increased, to have proper inertia. Proper scaling regarding Froude law is now also possible, but an ultra scale model should be used, since the electric cabinet is not built for large forces, and fuses will not withstand large force amplitudes if a larger model is to be used which can lead to large forcing.

Both drives used position control in this thesis. Force control is possible as told by the supplier, but this was not easy to implement, with the servo drives used. With a different servo drive the iron-less actuators can be more easily force controlled with a controller in the servo for this application. Force control need proper tuning of drives and a programmed algorithm using speed, acceleration, position and current as input. Using force control will give flexibility and is applicable in a variety of tests in the model basin, and not only for RTHMT.

Two degree of freedom test could be easily setup by duplicating the motor test setup. This test should be done in water, and with a wave machine. Modification can be done by splitting the test setup in two parts, if a wave machine is not available. Then one end of the spring need to be fixed and the other spring needs to attached to the actuator.

The QTM position sensor with EMT is tested in ocean basin in beginning of June 2014. The QTM system have possibility of using 400Hz sampling frequency, but not yet tested. The QTM can also use EtherCat for position signal. Results from EMT of a FPSO could be useful for further study on RIFLEX model.

A sensitivity study with influence of DOF's needed in RTHMT should be performed. It may be that only a few DOF's need RTHMT and the other DOF's can use traditional mooring lines. The sensitivity study depend much on the scope of model test, and most important is the system of the floater.

The test setup proposed have to be checked and assessed during the development. Since this is a new field of development, effort must be made in order to verify results, and to show that the results are reliable. One way of doing this is to replace mooring line actuator with a nonlinear spring and check if the system behave in same way in RTHMT test and RIFLEX. The nonlinear spring can be modeled as a an equivalent progressive spring by the use of a series of linear coil springs, where each spring is stopped successively at certain elongations. This spring will be stepwise nonlinear. This is a very useful way of checking the time history between the two setups and compare. Then it is possible to check if the solutions over time will diverge or be similar. The RIFLEX model will introduce larger force due to rapid change of the mooring line positions which will give large tension forces, which is not the same for a nonlinear spring based on the restoring force characteristics. The restoring force characteristics doesn't take into account accelerations and dynamic behavior. Nevertheless, for slow motions with large harmonic oscillation period, a test with non-linear spring based on restoring characteristics could still be useful.

Perform a study on the use of Newmark - β compared with L-stable real-time 3 order (LSRT3) numerical methods could check the feasibility and if there the simulation time compared with RIFLEX. In earthquake engineering LSRT3 is widely used and recognized (Bursi *et al.*, 2011), also for a wind turbine example LSRT3 was recommended (Chabaud, 1999). No such study has been performed in this thesis.

References

Aage, Christian, Bernitsas, M.M., Choi, H.S., Crudu, L., Hirata, K., Incecik, A., Kinoshita, T., & Moxnes, S. 1999. *Report of the ITTC Specialist Committee on Deep Water Mooring*. The Society of Naval Architects of Korea and The Chinese Society of Naval Architects and Marine Engineers.

Baarholm, R., Stansberg, C. T., Fylling, I., Lee, M. Y., & Ma, W. *Pages 2229–2238 of: A robust procedure for ultra deepwater model testing*. 17th 2007 International Offshore and Polar Engineering Conference, ISOPE 2007.

Balchen, Jens G., Andresen, Trond, & Foss, Bjarne A. 2003. *Reguleringsteknikk*. Institutt for teknisk kybernetikk.

Buchner, B., Wichers, J. E. W., & de Wilde, J. J. 1999. Features of the state-of-the-art deepwater offshore basin. *Proceedings of the Annual Offshore Technology Conference*, **2**.

Bursi, O. S., Jia, C., Vulcan, L., Neild, S. A., & Wagg, D. J. 2011. Rosenbrock-based algorithms and subcycling strategies for real-time nonlinear substructure testing. *Earthquake Engineering and Structural Dynamics*.

Cao, Yusong, & Tahchiev, Galin. 2013. A study on an active hybrid decomposed mooring system for model testing in in ocean basin for offshore platforms. *Proceedings of the of the ASME 2013 32nd International Conference on Ocean, Offshore and Arctic Engineering*.

Carrion, Juan E., & Billie F. Spencer, Jr. 2007. *Model-based Strategies for*

Real-time Hybrid Testing. The Newmark Structural Engineering Laboratory.

Chabaud, V., & Skjetne, R. 2013. Real-Time Hybrid Testing for Marine Structures: Challenges and Strategies. *In: Proc. Int. Conf. Ocean, Offshore and Arctic Eng.*, vol. 32.

Chabaud, Valentin. 1999 (14.11.2011). *MA8404 - Project,Numerical integrators for real-time hybrid testing*. Report. NTNU.

Chakrabarti, Subrata K. 1994. *Offshore Structure Modeling*. Vol. Advanced Series on Ocean Engineering ; V. 9 (Book 9). World Scientific Publishing Company, Incorporated.

Dahl, Kristian. 2010. *Hybrid model testing of deep-water moored structures by active control of simulated line forces.* M.Phil. thesis, Norwegian University of Science and Technology.

DNV. 2010a. DNV-OS-E301 Position mooring. *Offshore standard, Høvik*.

DNV. 2010b. RP-C205, Enviromental conditions and enviromental loads. *Recommended practice Det Norske Veritas*.

Faltinsen, Odd M. 1989. *Sea loads on ships and offshore structures*. Marinteknisk senter.

Fryer, D., Watts, S., & Evans, M. 2001. Experiment methods for non-linear hydrodynamic response to waves. 20th International Conference on Offshore Mechanics and Arctic Engineering; Offshore Technology, vol. 1.

Fylling, Ivar J. 2005a. *MIMOSA NLPQL*. MARINTEK Report 570002.06.01.

Fylling, Ivar J. 2005b. *MOORPOT-Trunc - A program for truncation of mooring and risers.* Report.

Fylling, Ivar J., & Sødahl, Nils. 1995. *RIFLEX: general description*. Vol. STF70 A95217. Trondheim: SINTEF, Konstruksjonsteknikk/FCB. Undertittel på omslaget: Flexible riser system analysis program.

Garlid, Stian. 2010. *Hybrid Testing of Deep Water Moored Structures*. M.Phil. thesis, Norwegian University of Science and Technology.

Greco, Marilena. 2012. *TMR 4215: Sea Loads, Lecture Notes*. Tech. rept. NTNU.

Halkyard, John. 2013. *OT 5204: Mooring and Risers, Lecture Notes.* Tech. rept. National University of Singapore.

Hansen, Vigleik L., Wang, Lihua, Sodahl, Nils, DNV, & Ward, E. G. 2004. Guidelines on Coupled Analyses of Deepwater Floating Systems. *Offshore Technology Conference, May 2004, Houston, Texas.*

Horiuchi, T., Inoue, M., Konno, T., & Namita, Y. 1999. Real-time hybrid experimental system with actuator delay compensation and its application to a piping system with energy absorber. *Earthquake Engineering and Structural Dynamics*, **28**(10), 1121–1141.

ITTC. 2008. ITTC – Recommended Procedures and Guidelines:Testing and Extrapolation Methods, Loads and Responses, Ocean Engineering,Stationary Floating Systems Hybrid, Mooring Simulation, Model Test Experiments. *International towing tank conference*, 9.

Kassen, Karl E., Lie, Halvor, & Mo, Knut. 2012. *MIMOSA User Documentation.* Report.

Kendon, T. E., Oritsland, O., Baarholm, R. J., Karlsen, S. I., Stansberg, C. T., Rossi, R. R., Barreira, R. A., Matos, V. L. F., & Sales Jr, J. S. *Pages 277–290 of: Ultra-deepwater model testing of a semisubmersible and hybrid verification.* 27th International Conference on Offshore Mechanics and Arctic Engineering, OMAE 2008, vol. 4.

Kendon, Timothy. 2014. *Åsgard B Semi-submersible sponsons analysis.* Report.

Langen, Ivar, & Sigbjörnsson, Ragnar. 1999. *Dynamisk analyse av konstruksjoner.* [s.n.].

Lehn, Erik. 2012. *The Fine Art of Model Testing.* Report. MARINTEK.

Lie, Halvor, Stansberg, Carl Trygve, Øritsland, Ola, & Ormberg, Harald. 2000. Deepstar 4401C: Overview of Hydrodynamic Verification of Deepwater Floating Production Systems. *MARINTEK internal project.*

Ormberg, H., Larsen, & K. 1998. Coupled analysis of floater motion and mooring dynamics for a turret-moored ship. *Applied Ocean Research*, **20**.

Sauder, Thomas. 2011 (17.11.2011). *Extended model testing - Status and way forward*. Report. MARINTEK.

Sauder, Thomas. 2014. *Real-Time Hybrid Model Testing*. Report.

Stansberg, C. T., Oritsland, O., & Kleiven, G. VERIDEEP: reliable methods for laboratory verification of mooring and stationkeeping in deep water. vol. 2.

Stansberg, C. T., Ormberg, H., & Oritsland, O. 2002. Challenges in deep water experiments: Hybrid approach. *Journal of Offshore Mechanics and Arctic Engineering*.

Stansberg, C. T., Karlsen, S.I., Ward, E.G., Wichers, J.E.W., & Irani, M.B. 2004. *In: Model Testing for Ultradeep Waters*. Offshore Technology Conference, 3 May-6 May 2004, Houston, Texas.

Stansberg, C.T., Øritsland, Ola, Yttervik, Rune, & Ormberg, Harald. 1999 (08.04.1999). *Deep water model test methods, Recommendations and Guidelines on Hybrid Testing with Experience from Case Studies*. Report. MARINTEK.

Storflor, Fredrik Moen. 2013. *Hybrid testing of deep water moored structures.* Report.

Zhang, H. M., Yang, J. M., & Xiao, L. F. 2007. *Hybrid model testing technique for deep-sea platforms based on equivalent water depth truncation.*

Appendices

Appendix A

Process of building of test setup

During building of the test setup problems with the equipment occurred. Most of the equipment was bought from the same supplier (Beckhoff), except position encoders (Reinshaw). During sales process all equipment was told to work together in TwinCat. During assembly and testing many problems arise in software control system.

Main problems occurred was as following:

- Equipment was not tested together before and implementation in TwinCat was not yet developed.
- Wrong encoder bit signal from position sensors
- Commutation error for the drive during initiation of drive.

The position controllers that was supposed to "plug and play" did not work properly and after 2 weeks with telephone and online meetings the encoders was sent to Beckhoff headquarter in Germany for testing. The bit puls signal from encoder was not as it was documented from supplier Reinshaw, and also functionality in TwinCat was not able to read this bit signal pulse. The encoder was then sent back to Reinshaw office in Slovakia for update of the controller. After this update the controller was sent to the Beckhoff for further software development and testing before encoder was sent back to NTNU. In the mean time position encoders was bought on Ebay for still be able to test setup and drives. In mean time Beckhoff had developed a new firmware for the servo drives and updated motor drive parameters to

work properly. After new position encoders arrived problems occurred with reading signal and use this for motor feedback. Support was given by Beckhoff to solve this problem. Main issue was to adjust the commutation of the drive. For controlling the magnetic field by the drive the incremental position sensor is used. Every start up the commutation need to be adjusted. Absolute position encoders need only to be adjusted once and will not be affected by restart such as the incremental position encoders. Fault in the commutation caused high frequency oscillations and drift off by the drive. This issue was solved by tuning help of the controller and adjusting parameters of the position signal and friday before eastern both actuators was able to read position signal and simple position command could be sent to drive, but however still errors occur for the controller of the drive and further tuning of drives is needed. The absolute position encoders was received by supplier after firmware update. According to Beckhoff the encoder was now ready for use. But however after the encoders was received from Reinshaw with firmware updates the encoders still doesn't work. After some tuning on parameters the encoders was turned on and communication was established. Still the position was not read by servo drive. The signal was possible to read right after restart, but with a slightly displacement of the encoder the position data was invalid. After testing with an external power drive for the encoders the encoder worked. The power supply had to deliver 5.1 V in order for the encoder to work. The encoder needs 5 V to work. The fault could be due to two solutions voltage drop in the cable which is less than 4 m. Or the servo drive doesn't deliver enough power. The voltage drop is according to supplier 0.45 V per 10 m of cable. Most likely the servo drive is causing this issue. A new firmware for the servo drive was decided to build, with possibilities for changing output voltage for feedback encoders. Still Reinshaw and Beckhoff haven't solved the absolute encoders, and further contact with supplier regarding this issue was not prioritized.

Appendix B

Riflex model

The view of the mooring system layout is shown in Fig. B.1.

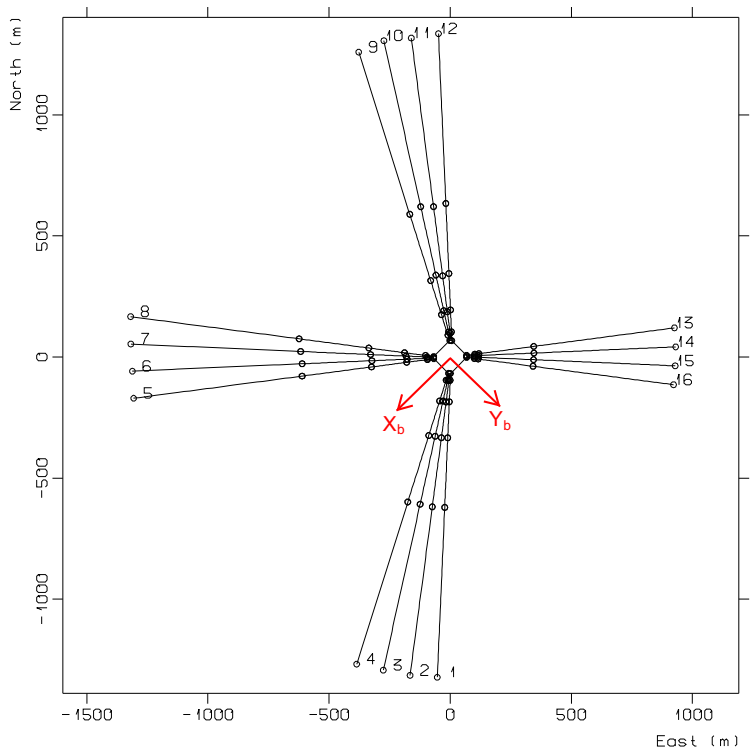

Figure B.1: Overview of the mooring system (Kendon, 2014)

Table B.1: Main dimension Åsgard B.

Parameter	Unit	Value
Draught	m	25
Length pontoons	m	102
Breadth pontoons	m	96
Height pontoons	m	8.96
Corner Column Diameter	m	19.2
Inner Column Diameter	m	12
Total Displacement	10^3 kg	84848
Vertical Component riser	10^3 kg	2382
Vertical Component mooring	10^3 kg	2412

Table B.2: Fairlead and anchor coordinates of the as-built system.

Line no.	Heading	Horizontal distance from fairlead	Anchors Northing	Anchors Easting	Fairleads X_b	Fairleads Y_b
1	182.5	1255.40	-1322.01	-53.11	46.78	49.12
2	187.5	1256.20	-1314.13	-165.36	49.55	47.58
3	192.5	1253.90	-1292.69	-275.88	51.62	45.27
4	197.5	1258.70	-1267.74	-385.97	52.87	42.31
5	262.5	1249.90	-170.36	-1306.56	52.73	-42.53
6	267.5	1244.40	-58.51	-1311.76	51.46	-45.48
7	272.5	1250.50	53.41	-1318.00	49.37	-47.77
8	277.5	1262.00	166.64	-1319.00	46.58	-49.29
9	342.5	1248.40	1258.36	-377.57	-46.36	-49.44
10	347.5	1266.80	1305.43	-273.31	-49.16	-47.93
11	352.5	1258.70	1316.47	-160.33	-51.26	-45.66
12	357.5	1268.60	1334.76	-48.38	-52.56	-42.72
13	82.5	865.90	120.24	925.85	-52.73	42.53
14	87.5	863.10	41.87	930.83	-51.46	45.48
15	92.5	861.10	-36.43	928.97	-49.37	47.77
16	97.5	861.80	-114.40	922.22	-46.58	49.29

Table B.3: Mooring line dimension

	Segment	Length [m]	d [m]
Bottom chain	1	700	0.142
Connection plate	2	1.5	0.2
Bottom chain	3	300	0.142
Connection plate	4	1.5	0.2
Mooring line wire	5	180	0.156
Connection plate	6	1.5	0.2
Connection chain	7	120	0.142
Connection plate	8	1.5	0.2
Platform chain	9	40	0.142

Table B.4: Weight and drag coefficients

	Weight in water [kN/m]	Drag coefficients Cd_n	Cd_l
Bottom chain	3.4453	2.7	1.3
Connection plate	13.0549	2.6	0.1
Bottom chain	3.4453	2.7	1.3
Connection plate	13.0549	2.6	0.1
Mooring line wire	0.9173	1.33	0.1
Connection plate	13.0659	3.1	1.5
Connection chain	3.4621	3.4	1.6
Connection plate	13.0659	3.1	1.5
Platform chain	3.6623	4.4	2.1

Table B.5: Pretension of mooring lines

Line no.	Pretension [kN]
1	2300
2	2300
3	2350
4	2350
5	2100
6	2100
7	2100
8	2100
9	2300
10	2300
11	2300
12	2300
13	2300
14	2300
15	2300
16	2300

The bottom friction was modeled by a coefficient of 0.6.

Appendix C

TwinCat program

C.1 Main program

```
PROGRAM Main
VAR
    DoubleFromJava , HLATime , LRealFromPLC : LREAL ;
    scaling : BOOL := TRUE ;
    scaleForce : LREAL := 34 ; //34 during EMT and RHTMT
END_VAR
```

```
//Scaling of parameters in Riflex
IF scaling = TRUE THEN
    LRealFromPLC := FromPlc * scaleDisp ;
    FromJava := DoubleFromJava / ( EXPT ( scaleForce , 3 ) ) ;
    scopeForce := FromJava ;
    scopeSurge := LRealFromPLC ;
ELSE
    LRealFromPLC := FromPlc ;
    FromJava := DoubleFromJava ;
    scopeForce := - FromJava ;
    scopeSurge := LRealFromPLC ;
END_IF

DriveCommandsLeft ( ) ;
ReadSurgePos ( ) ;
SurgeForce ( ) ;
Enviromentalforcing ( ) ;

TestRunSine ( ) ;
DriveCommandsRight ( ) ;
```

C.2 Program for left drive

```
PROGRAM DriveCommandsLeft
VAR
    //Drive 1
    wCtrlWord1 AT %Q* : UINT ;
    diPosControlValue1 AT %Q* : DINT ;
    wStatusWord1 AT %I* : UINT ;
    diVelActualValue1 AT %I* : DINT ;
    diCorrVelocity1 : DINT ;
    diGotoPosition1 : DINT ;
    diPosActualValue1 AT %I* : DINT ;

    wCtrlValue1 : UINT ;
    w1Bit13 : UINT := 2#0010_0000_0000_0000 ;
    w1Bit14 : UINT := 2#0100_0000_0000_0000 ;
    w1Bit15 : UINT := 2#1000_0000_0000_0000 ;
    bDrive2On1 : BOOL := FALSE ;            // Controlword bit 15
    bDrive2Enable1 : BOOL := FALSE ;        // Controlword bit 14
    bDrive2RstHalt1 : BOOL := FALSE ;           // Controlword bit 13

    //Emegency parameters
    MaxlimitLeftDrive : LREAL := 4000000 ;
    MinlimitLeftDrive : LREAL := - 4000000 ;

    //Sine Curve
    fVal : LREAL ;
    temp : LREAL ;
    fAmp : LREAL := 0 ;
    fPeriod : LREAL := 30 ;
    diTime : DINT ;

    runRHTMT : BOOL := FALSE ;
    startRHTMT : BOOL := FALSE ;
    PosDrive1 : DINT ;
END_VAR
```

```
//Drive1 commands left drive
PosDrive1 := diPosActualValue1 ;

wCtrlValue1 := 0 ;
IF bDrive2RstHalt1 THEN
    wCtrlValue1 := w1Bit13 ;
END_IF
IF bDrive2Enable1 THEN
    wCtrlValue1 := wCtrlValue1 OR w1Bit14 ;
END_IF
IF bDrive2On1 THEN
    wCtrlValue1 := wCtrlValue1 OR w1Bit15 ;
END_IF
wCtrlWord1 := wCtrlValue1 ;

diTime := diTime + 1 ;
IF diTime > 1000000 THEN
    diTime := 0 ;
END_IF

diCorrVelocity1 := SHR ( diVelActualValue1 , 12 ) ;
// Modify velocity to 20 bits

fVal := fAmp * SIN ( 6.28 * 0.001 * DINT_TO_REAL ( diTime ) / fPeriod ) ;
```

C.3 Program for left drive

```
        // Pos in mm, loop time is 1 ms
24
25      IF wStatusWord1.3 THEN        //Bit 3 : Drive is following target pos
26              IF runRHTMT THEN
27                  diGotoPosition1 := REAL_TO_DINT (motorpos1);   //RHTMT calc
28              ELSE
29                  diGotoPosition1 := REAL_TO_DINT (fVal);   //Test sine curve
30              END_IF
31          diPosControlValue1 := diGotoPosition1;
        // Send Target position command
32      END_IF
33
34
35      //Emergency check  Turn off position controll
36      IF startRHTMT  THEN
37          IF motorpos1 > MaxlimitLeftDrive OR motorpos1 < MinlimitLeftDrive
        THEN
38              bDrive2On1 := FALSE;
39              bDrive2Enable1 := FALSE;
40              bDrive2RstHalt1 := FALSE;
41          END_IF
42
43      END_IF
44
```

C.4 Program for right drive

```
PROGRAM DriveCommandsRight
VAR
    //Drive 1
    wCtrlWord2 AT %Q* : UINT;
    diPosControlValue2 AT %Q* : DINT;
    wStatusWord2 AT %I* : UINT;
    diVelActualValue2 AT %I* : DINT;
    diGotoPosition2, diCorrVelocity2 : DINT;
    diPosActualValue2  AT %I* : DINT;

    wCtrlValue2 : UINT;
    w2Bit13 : UINT := 2#0010_0000_0000_0000;
    w2Bit14 : UINT := 2#0100_0000_0000_0000;
    w2Bit15 : UINT := 2#1000_0000_0000_0000;
    bDrive2On2 : BOOL := FALSE;           // Controlword bit 15
    bDrive2Enable2 : BOOL := FALSE;       // Controlword bit 14
    bDrive2RstHalt2 : BOOL := FALSE;          // Controlword bit 13

    //Emegency parameters
    MaxlimitRightDrive : LREAL := 3500000;
    MinlimitRightDrive : LREAL := -3500000;
END_VAR
```

```
//Drive1 commands left drive
wCtrlValue2 := 0;
IF bDrive2RstHalt2 THEN
    wCtrlValue2 := w2Bit13;
END_IF
IF bDrive2Enable2 THEN
    wCtrlValue2 := wCtrlValue2 OR w2Bit14;
END_IF
IF bDrive2On2 THEN
    wCtrlValue2 := wCtrlValue2 OR w2Bit15;
END_IF
wCtrlWord2 := wCtrlValue2;

IF wStatusWord2.3 THEN            //Bit 3 : Drive is following target pos
    diGotoPosition2 := REAL_TO_DINT(motorpos2);
    diPosControlValue2 := diGotoPosition2;
// Send Target position command
END_IF
diCorrVelocity2 := SHR (diVelActualValue2, 12);
// Modify velocity to 20 bits

//Emergency check Turn off position controll
IF motorpos2 > MaxlimitRightDrive OR motorpos2 < MinlimitRightDrive THEN
    bDrive2On2 := FALSE;          // Controlword bit 15
    bDrive2Enable2 := FALSE;      // Controlword bit 14
    bDrive2RstHalt2 := FALSE;         // Controlword bit 13
END_IF
```

C.5 Program for read surge position

```
PROGRAM ReadSurgePos
VAR
LM10    AT %I* : UDINT ;
Surge , temp , temp2 ,  fVal :  LREAL ;
diTime : UDINT ;
fValue  : LREAL := 0 ;
fAmp  : LREAL := 0.5 ;
fPeriod : LREAL := 80 ;
GOGO : BOOL ;

//Rampfactor
teller : LREAL ;
rampstep : UDINT := 10000 ;
EMT : BOOL := TRUE ;
PULLOUT , zero : BOOL ;

END_VAR
```

```
//SurgePos converstion to meter [m]
temp := UDINT_TO_LREAL ( LM10 ) ;
temp2 := EXPT ( 2 , 32 ) - 1000000 ;

IF temp > temp2 THEN
    SurgePosLM10 := ( EXPT ( 2 , 32 ) - temp ) * EXPT ( 10 , - 6 ) ;
ELSE
    SurgePosLM10 := - temp * EXPT ( 10 , - 6 ) ;
END_IF

IF PULLOUT = TRUE THEN
    Surgepos :=  Surgepos + 0.001 ;
    FromPLC := Surgepos ;
END_IF

IF EMT = TRUE THEN
    Surgepos := SurgePosLM10 ;
    FromPLC := Surgepos ;
END_IF

IF zero = TRUE THEN
    Surgepos := fValue ;
    FromPLC := Surgepos ;
END_IF

IF diTime > 1000000 THEN
    diTime := 0 ;
END_IF


    diTime := diTime + 1 ;
    //Rampfactor
IF diTime < rampstep THEN
        teller := teller + 1 ;
        rampfactor :=  ( teller + 1 ) / ( rampstep ) ;
END_IF
```

C.6 Program for surge force

```
PROGRAM SurgeForce
VAR
//[m]
Force , x1 , x2 , Fx1 , Fx2 , SumForce , temp , dx , SumKraft , dF , scopeDiff ,
motorpoScaled : LREAL ;
springstiff : LREAL := 95.8 ;
springstiff1 : LREAL := 60 ;
springstiff2 : LREAL := 60 ;
springOffset1 : LREAL := 0.312 ;
springOffset2 : LREAL := 0.355 ;

//Kraftringer
    VenstreKraftring , HoyreKraftring AT %I* : REAL ;
END_VAR
```

```
//Force and spring calulations
x1 := ( - 0.5 * PosDrive1 * EXPT ( 10 , - 7 ) + Surgepos ) ;
x2 := ( 0.5 * PosDrive1 * EXPT ( 10 , - 7 ) - Surgepos ) ;

Fx1 := springstiff1 * ( x1 + springOffset1 ) ;
Fx2 := springstiff2 * ( x2 + springOffset2 ) ;

dF := Fx1 - Fx2 ;

scopeDiff := FromJava - dF ;
SumForce := Fx2 - Fx1 ;   //Check forces from each actuator
SumKraft := HoyreKraftring - VenstreKraftring ;

dx := - ( FromJava - SumForce ) / springstiff ;
//Input from Riflex, uses same direction as test setup   [m]

motorpos1 := ( 0.5 * PosDrive1 * EXPT ( 10 , - 7 ) + dx ) * EXPT ( 10 , 7 ) ;
//diPosActualValue 1mm =20 000bit
motorpoScaled := LREAL_TO_DINT ( motorpos1 ) ;
```

C.7 Program for environmental forcing

```
1  PROGRAM Enviromentalforcing
2  VAR
3      fAmp : LREAL := 3000000 ;
4      diTime : DINT ;
5      fPeriod : LREAL := 5 ;
6      fVal : LREAL ;
7      TurnOnWaves : BOOL ;
8  END_VAR
9
```

```
1  IF TurnOnWaves = TRUE THEN
2  diTime := diTime + 1 ;
3  fVal := fAmp * SIN ( 6.28 * 0.001 * DINT_TO_REAL ( diTime ) / fPeriod ) ;
   // Pos in mm, loop time is 1 ms
4  END_IF
5
6
```

C.8 Declaration of global values in PLC

```
1   VAR_GLOBAL
2   motorpos2 , Surgepos ,  rampfactor ,  scopeSurge , FromPlc ,  scopeForce ,
    FromJava , SurgePosLM10 , motorpos1  : LREAL ;
3   scaleDisp   :  LREAL := 30 ;  //Input to Riflex should be fullscale
4   PosDrive1  :  DINT ;
5   END_VAR
6
```

Appendix D

Java program

D.1 Explanation of java program

. The code consist of eight methods and each method contain a certain operation. The class SIMO import 15 packages.The new packages used compared to earlier worke done (Garlid, 2010) is following: java.nio.Bytebuffer
java.nio.ByteOrder
de.beckhoff.jni.Convert
de.beckhoff.jni.JNIByteBuffer
de.beckhoff.jni.tcads.AmsAddr
de.beckhoff.jni.tcads.AdsCallDllFunction

java.nio packages are used for converting from byte to a double variable. The Beckhoff packages are used for Automation Device Specification (ADS) communication. The ADS describes a device-independent and fieldbus-independent interface governing the type of access to ADS devices. In TwinCat only the PLC is using the ADS, but it is also possible for modules such monitoring to be connected to ADS directly. For communication by ADS all data variables is converted to byte. First each variable is converted to byte and then converted back to a double variable after the value byte memory is read, similar conversion for writing to a variable.

D.2 Java code

```
//HlaToTwinCat.java

package no.marintek.hla.case_one;

import static java.lang.Math.*;
import java.net.*;
import java.nio.ByteBuffer;
import java.nio.ByteOrder;
import static marintek.hla.AttributeType.i_CHAR;
import static marintek.hla.AttributeType.i_DOUBLE;
import static marintek.hla.AttributeType.i_INT;
import marintek.hla.app.HLAApp;
import marintek.hla.app.HLAException;
import java.io.File;
import java.io.FileNotFoundException;
import java.io.FileOutputStream;
import java.io.PrintStream;
import java.util.Scanner;
import java.io.IOException;
import de.beckhoff.jni.Convert;
import de.beckhoff.jni.JNIByteBuffer;
import de.beckhoff.jni.tcads.AmsAddr;
import de.beckhoff.jni.tcads.AdsCallDllFunction;

public class FakeSimo extends HLAApp {
    private static final double DT = 0.008;
    private static final double RAMP_STEPS = 1000;

    // class handles
    private int ch_body;
```

```
private int ch_force;
// attribute handles - MOP.Body
private int hPos;
private int hVel;
private int hAcc;
private int hPosEst;
private int hVelEst;
// attribute handles - MOP.ExternalForce
private int ah_iInfoFor;
private int ah_dInfoFor;
private int ah_cInfoFor;
private int ah_force;
private int ah_attackPoint;
// object handles
private int[] oh_forces;
private int oh_body;
// attribute handles - MOP.ExternalForce
private String[] on_forces;
private int[][]  oah_iInfosFor;
private double[][] oah_dInfosFor;
private char[][] oah_cInfosFor;
private double[][] oah_forces;
private double[][] oah_attackPoints;
// attribute handles - MOP.Body
private double[] myBodyPos;
private double[] myBodyVel;
private double[] myBodyAcc;
private double[] myBodyPosEst;
private double[] myBodyVelEst;

//Variabler brukt Til TwinCat I/O
long err;
```

```
AmsAddr addr;
int hdl1BuffToInt;
int hdl2BuffToInt;
int hdl3BuffToInt;
JNIByteBuffer data1Buff;
JNIByteBuffer data2Buff;
JNIByteBuffer data3Buff;
Double PositionSurge;
Double SumSurgeForce;
double temp;

PrintStream logFileH = null;
private DatagramSocket serverSocket = null;
public FakeSimo(double dt) {
    super("127.0.0.1", "HLATask1", "externalHLAfederate", dt);
}
@Override
protected void publishAndSubscribeObjects() throws HLAException
    {
    // Informing the RTI what objects is subscribed to and what
        objects will be published.
    ch_body = helper.getClassHandle("MOP.Body");
    ch_force = helper.getClassHandle("MOP.ExternalForce");

    hPos = helper.getClassAttributeHandle(ch_body, "position");
    hVel = helper.getClassAttributeHandle(ch_body, "velocity");
    hAcc = helper.getClassAttributeHandle(ch_body,
        "acceleration");
    hPosEst = helper.getClassAttributeHandle(ch_body,
        "est_position");
    hVelEst = helper.getClassAttributeHandle(ch_body,
        "est_velocity");
```

```
        ah_iInfoFor = helper.getClassAttributeHandle(ch_force,
            "iInfo");
        ah_dInfoFor = helper.getClassAttributeHandle(ch_force,
            "dInfo");
        ah_cInfoFor = helper.getClassAttributeHandle(ch_force,
            "cInfo");
        ah_force    = helper.getClassAttributeHandle(ch_force,
            "force");
        ah_attackPoint = helper.getClassAttributeHandle(ch_force,
            "attackPoint");

        helper.publishClassAttributes(ch_body, new int [] {hPos,
            hVel, hAcc, hPosEst, hVelEst}, new int[] {i_DOUBLE,
            i_DOUBLE, i_DOUBLE, i_DOUBLE, i_DOUBLE});
        helper.subscribeClassAttributes(ch_force, new int[]
            {ah_iInfoFor, ah_dInfoFor, ah_cInfoFor, ah_attackPoint,
            ah_force}, new int[] {i_INT, i_DOUBLE, i_CHAR, i_DOUBLE,
            i_DOUBLE});
    }

    @Override
    protected void registerObjects() throws HLAException {
        // Registering objects that is published by this code
        oh_body = helper.registerObject("supportVessel", ch_body);
        helper.initializeObjectAttributes(oh_body, new int []
            {hPos, hVel, hAcc, hPosEst, hVelEst}, new int[] {6, 6,
            6, 6, 6});
    }

    @Override
    protected void initializeObjects() throws HLAException {
```

```
// Initializing objects that is published by this code
myBodyPos = helper.getDoubleAttribute(oh_body, hPos);
myBodyVel = helper.getDoubleAttribute(oh_body, hVel);
myBodyAcc = helper.getDoubleAttribute(oh_body, hAcc);
myBodyPosEst = helper.getDoubleAttribute(oh_body, hPos);
myBodyVelEst = helper.getDoubleAttribute(oh_body, hVel);

for(int i = 0; i < 6; i++) {
    myBodyPos[i] = 0.0;
    myBodyVel[i] = 0.0;
    myBodyAcc[i] = 0.0;
    myBodyPosEst[i] = 0.0;
    myBodyVelEst[i] = 0.0;
}
helper.attributeUpdated(oh_body, hPos);
helper.attributeUpdated(oh_body, hVel);
helper.attributeUpdated(oh_body, hAcc);
helper.attributeUpdated(oh_body, hPosEst);
helper.attributeUpdated(oh_body, hVelEst);
helper.sendObjectUpdates(oh_body);

try {
    logFileH = new
        PrintStream("logSurgDispForceAndTime3.dat");

} catch (FileNotFoundException e) {
    System.out.println("Error in logger initialization.");
    e.printStackTrace();
}
addr = new AmsAddr();
// Handledefinisjon for LREAL plc to double java
```

```
JNIByteBuffer handle1Buff = new JNIByteBuffer(Integer.SIZE
    / Byte.SIZE);
JNIByteBuffer symbol1Buff = new
    JNIByteBuffer(Convert.StringToByteArr("MAIN.LRealFromPLC",true));
    //Posisjon i surge for flyter
data1Buff = new JNIByteBuffer(Double.SIZE / Byte.SIZE);

//  Handledefinisjon for Double i java til LREAL PLC
JNIByteBuffer handle2Buff = new JNIByteBuffer(Integer.SIZE
    / Byte.SIZE);
JNIByteBuffer symbol2Buff = new
    JNIByteBuffer(Convert.StringToByteArr("MAIN.DoubleFromJava",true));
    // Sum surge force for flyter
data2Buff = new JNIByteBuffer(Double.SIZE / Byte.SIZE);

// Handledefinisjon for Double JAVA til LREAL PLC
JNIByteBuffer handle3Buff = new JNIByteBuffer(Integer.SIZE
    / Byte.SIZE);
JNIByteBuffer symbol3Buff = new
    JNIByteBuffer(Convert.StringToByteArr("MAIN.HLATime",true));
    //Posisjon i surge for flyter
data3Buff = new JNIByteBuffer(Double.SIZE / Byte.SIZE);

// Open communication
AdsCallDllFunction.adsPortOpen();
AdsCallDllFunction.getLocalAddress(addr);
addr.setPort(851);

// Get handle by symbol name for Double (LREAL)
AdsCallDllFunction.adsSyncReadWriteReq(addr,
                                    AdsCallDllFunction.ADSIGRP_SYM_HNDBYNAME,
                                    0x0,
```

```
                                handle1Buff.getUsedBytesCount(),
                                handle1Buff,
                                symbol1Buff.getUsedBytesCount(),
                                symbol1Buff);


    // Handle: byte[] to int
    hdl1BuffToInt =
        Convert.ByteArrToInt(handle1Buff.getByteArray());

    // Get handle by symbol name for Float (REAL)
    AdsCallDllFunction.adsSyncReadWriteReq(addr,
                                AdsCallDllFunction.ADSIGRP_SYM_HNDBYNAME,
                                0x0,
                                handle2Buff.getUsedBytesCount(),
                                handle2Buff,
                                symbol2Buff.getUsedBytesCount(),
                                symbol2Buff);

    // Handle: byte[] to int
    hdl2BuffToInt =
        Convert.ByteArrToInt(handle2Buff.getByteArray());

    AdsCallDllFunction.adsSyncReadWriteReq(addr,
                                AdsCallDllFunction.ADSIGRP_SYM_HNDBYNAME,
                                0x0,
                                handle3Buff.getUsedBytesCount(),
                                handle3Buff,
                                symbol3Buff.getUsedBytesCount(),
                                symbol3Buff);

    // Handle: byte[] to int
```

```
        hdl3BuffToInt =
            Convert.ByteArrToInt(handle3Buff.getByteArray());
    }

    @Override
    protected void discoverObjects() throws HLAException {
        // Discovering objects that are subscribed to
        oh_forces = helper.getObjects(ch_force);
        int nfor = oh_forces.length;

        on_forces = new String[nfor];
        oah_iInfosFor = new int[nfor][];
        oah_dInfosFor = new double[nfor][];
        oah_cInfosFor = new char[nfor][];
        oah_forces = new double[nfor][];
        oah_attackPoints = new double[nfor][];

        for(int ifor = 0; ifor < oh_forces.length; ifor++) {
            on_forces[ifor] = helper.getObjectName(oh_forces[ifor]);
            oah_iInfosFor[ifor] =
                helper.getIntegerAttribute(oh_forces[ifor],
                ah_iInfoFor);
            oah_dInfosFor[ifor] =
                helper.getDoubleAttribute(oh_forces[ifor],
                ah_dInfoFor);
            oah_cInfosFor[ifor] =
                helper.getCharacterAttribute(oh_forces[ifor],
                ah_cInfoFor);
            oah_forces[ifor]  =
                ambassador.getDoubleAttribute(oh_forces[ifor],
                ah_force);
```

```
            oah_attackPoints[ifor] =
                ambassador.getDoubleAttribute(oh_forces[ifor],
                ah_attackPoint);
        }
    }
    @Override
    protected void doTimeStepWork(int istep, double timeNow, double
        timeNext)
            throws HLAException {
            double t=timeNow;

        SumSurgeForce=oah_forces[0][0]+oah_forces[1][0];

         // Read value by handle (Double)
        err = AdsCallDllFunction.adsSyncReadReq(addr,
                                        AdsCallDllFunction.ADSIGRP_SYM_VALBYHND,
                                        hdl1BuffToInt,
                                        data1Buff.getUsedBytesCount(),
                                            // <- Antall bytes som
                                            skal leses fra PLC
                                        data1Buff);

        // Write struct to PLC
        err = AdsCallDllFunction.adsSyncWriteReq(addr,
                                        AdsCallDllFunction.ADSIGRP_SYM_VALBYHND,
                                        hdl2BuffToInt,
                                        data2Buff.getUsedBytesCount(),
                                        data2Buff);

        err = AdsCallDllFunction.adsSyncWriteReq(addr,
                                        AdsCallDllFunction.ADSIGRP_SYM_VALBYHND,
                                        hdl3BuffToInt,
```

```
                                        data3Buff.getUsedBytesCount(),
                                            // <- Antall bytes som
                                            skal leses fra PLC
                                        data3Buff);

            // Lese en LREAL fra PLC til en Double i Java
            ByteBuffer bb =
                ByteBuffer.wrap(data1Buff.getByteArray()).order(ByteOrder.LITTLE_ENDI
            PositionSurge = bb.getDouble();

            ByteBuffer bb1 =
                ByteBuffer.wrap(data2Buff.getByteArray()).order(ByteOrder.LITTLE_ENDI
                bb1.putDouble(SumSurgeForce);

            ByteBuffer bb2 =
                ByteBuffer.wrap(data3Buff.getByteArray()).order(ByteOrder.LITTLE_ENDI
                bb2.putDouble(timeNow);

        logFileH.printf(" %f %f   %f  \n",
            PositionSurge,-SumSurgeForce/Math.pow(34,3), timeNow);
        System.out.printf("%f %f  %f  \n",
            PositionSurge,-SumSurgeForce/Math.pow(34,3), timeNow);

        myBodyPos[0] = PositionSurge;
        myBodyPos[1] = 0;
        myBodyPos[2] = 0;
        myBodyPos[3] = 0;
        myBodyPos[4] = 0;
        myBodyPos[5] = 0;

        myBodyVel[0] = 0;
        myBodyVel[1] = 0;
```

```
        myBodyVel[2] = 0;
        myBodyVel[3] = 0;
        myBodyVel[4] = 0;
        myBodyVel[5] = 0;

        myBodyAcc[0] = 0;
        myBodyAcc[1] = 0;
        myBodyAcc[2] = 0;
        myBodyAcc[3] = 0;
        myBodyAcc[4] = 0;
        myBodyAcc[5] = 0;

        // Sending updated position and velocity data to the RTI
        helper.attributeUpdated(oh_body, hPos);
        helper.attributeUpdated(oh_body, hVel);
        helper.attributeUpdated(oh_body, hAcc);
        helper.attributeUpdated(oh_body, hPosEst);
        helper.attributeUpdated(oh_body, hVelEst);
        helper.sendObjectUpdates(oh_body, timeNext);

        }
    @Override
    protected void finishSimulation() throws HLAException {
    logFileH.close();
    }

    /**
     * @param args
     */
    public static void main(String[] args) {

        FakeSimo app = new FakeSimo(DT);
```

```
        app.runSimulation(false);
    }
}
```

Appendix E

Startup procedure for RTHMT

Since the drives are running on incremental encoders and not absolute care is needed in order to startup and run tests. All position encoders are incremental, and at every restart the position is zeroed. Same position is used for the drives and carriage system at every startup. The position differ within 1-2 cm at every startup. Therefore the spring specification and offsets is calibrated at every startup. Force transducer is used for calibration of spring offset in elongation and for spring stiffness. The actuators also need to calibrate the commutations settings for drive controller at every restart.

Following procedure must be performed for testing RTHMT of the SDOF test arrangement:

Place both actuator wagon to each fixed position along.
Turn on power supply for electrical cabinet for the test arrangment.
Start TwinCat and login for real-time streaming.
Start HLA task in SIMA.
Compile and run Java program.
Remove each spring form each actuator.
Perform commutation tuning for both drives.

Make sure motorpos input is set to zero, and RTHMT boolean variable is set to false (default).
Place the drives close to counter value of 0 ±2-6000 bit is no problem.
Set bDriveOn, bDriveEnable, bDriveRstHalt to true for both drives, no hands on carriage system.
When actuators is on position control attach springs again.
Calibrate spring offset and stiffness based on scope in TwinCat by comparing with force rings.
When no further motion of mass carriage is needed set startRTHMT to true.
Monitor the GL.scopeDx value and make sure, no large dx value for drive position is needed.
As long as dx value is small, set runRTHMT to true, makes sure no obstacles or hands is on the carriage system.
No RTHMT should be running, next is then to turn on waves. This is done by set TurnOnWaves to true, check amplitude. diTime should be set to zero when an amplitude is set, else a sudden step response will occur. Last turn on record and monitor variable that is wanted.

Appendix F

Content of attached memory stick

This appendix describes the attached content.

Pictures: Folder containing pictures of the built test setup.

JavaProgram: Contain program code for the java program. By typing ./compileAndRun in terminal the java program compiled and run. All used libraries is attached in the folder.

SIMA: Containing the input files as well as the RIFLEX task, and HLA task. RTHMT.stask contains the HLA workspace. For running HLA task the newest SIMA version is needed with implementation of the newest HLA updates. SIMA academic version doesn't contain functionality per June 2014.

TwinCat: Contains the complete TwinCat workspace with all programs, and also all used variables for discussion in this thesis is added to monitoring in TwinCat.

EnvironmentalTimeseries: The environmental time series used for testing is written to a file. The time series is not scaled.